



AUSTRALIA

University of Southern Queensland
Faculty of Health, Engineering and Sciences

**SIMULATION AND EXPERIMENTAL INVESTIGATIONS
ON TRIBOLOGICAL CHARACTERISTICS OF
KENAF/THERMOSET COMPOSITES**

A Dissertation Submitted by

CHIN CHEE WEN

006 10 359 03

For the Award of

Doctor of Philosophy

2013

Principle Supervisor: Dr. B.F. Yousif

Principle Supervisor: Dr. H. Ku f

ABSTRACT

Over the current decade, the use of natural fibres as an alternative to synthetic fibres such as glass and carbon has been growing due to the environmental and economic advantages of natural fibres. In this study, the mechanical and tribological performance of epoxy composites based on kenaf fibres was evaluated. The interfacial adhesion between the kenaf fibres and the epoxy matrix was studied and the effect of NaOH treatment was considered. The tensile and flexural properties of the untreated and treated kenaf fibre reinforced epoxy (KFRE) were determined, and their fracture behaviour was examined using scanning electron microscopy (SEM). For the tribological experiments, the adhesive wear and frictional experiments were performed considering three different orientations of the fibres with respect to the sliding of the counterface. Different operating parameters were considered, such as applied loads (5–200 N), sliding distances (0–5 km) and sliding velocity (0–3.5m/s) under dry/wet contact conditions. The prediction of the frictional performance of the composites was modelled using artificial neural networks (ANN) considering different configurations. Furthermore, the effects of sand particle size, applied load and kenaf fibre orientation on the three-body abrasion (3B-A) wear behaviour of epoxy composites subjected to high stress were investigated. ABAQUS software was used to develop the 3B-A model aiming to assist in understanding the damage features on the composite surfaces, considering different particle angles, pressures, and fibre orientations.

The results revealed that treating the kenaf fibre with 6 per cent NaOH contributed to the high interfacial adhesion of the fibre with the matrix, which resulted in significant improvements to the mechanical properties of the epoxy composites. The wear and frictional performance of the composites was significantly affected by the fibre orientation rather than the operating parameters under all the conditions tested. When the kenaf fibres were oriented in N-O, the wear and frictional performance of the composite was much better than in the other orientations and NE for both adhesive and abrasive wear loadings. The wear mechanisms of the composite tested in N-O were predominately micro-cracks under dry adhesive wear and polishing mechanisms under wet conditions. The presence of water at the interface helped to remove debris from the interface and cooled the contacted surface, which lowered the interaction between the asperities at the contact interface and led to a low friction coefficient. The ANN approach was found to be a useful tool to predict the friction coefficient. However, selection of training and learning functions was key in controlling the error and the prediction performance of the model. The numerical results were found to be in strong agreement with the experimental findings, where the most pronounced factor affecting the wear behaviour of the composite was the fibre orientation.

LIST OF PUBLICATIONS

1. **Chin, C.** and B. Yousif. Adhesive and frictional behaviour of polymeric composites based on kenaf fibre. In: Proceedings of the 2nd International Conference on Advanced Tribology (ICAT 2008) 2008. National University of Singapore.
2. **Chin, C.** and B. Yousif, Potential of kenaf fibres as reinforcement for tribological applications. *Wear*, 2009. 267(9): pp. 1550–1557.
3. **Chin, C.** and F. Yousif, Influence of particle size, applied load, and fibre orientation on 3B-A wear and frictional behaviour of epoxy composite based on kenaf fibres. *Proceedings of the Institution of Mechanical Engineers, Part J: Journal of Engineering Tribology*, 2010. 224(5): pp. 481–489.
4. **Chin, C.** and B. Yousif, Tribological behaviour of KFRE composite. *International Journal of Modern Physics B*, 2010. 24(28): pp. 5589–5599.
5. Yousif, B., **C. Chin** et al., Flexural properties of treated and untreated kenaf-epoxy composites. Volume 40, September 2012, Pages 378–385, *Materials & Design*, 2012.
6. Yousif, B. and **C. Chin**, Epoxy composite based on kenaf fibres for tribological applications under wet contact conditions. *Surface Review and Letters*, 2012. 19(05).
7. **Chin, C.**, B. Yousif, and H. Ku. Prediction of friction coefficient of KFRE composites considering large experimental data. In preparation; to be submitted to *Wear*.

CERTIFICATION OF DISSERTATION

I certify that the ideas, designs and experimental work, results, analyses and conclusions set out in this dissertation are entirely my own effort, except where otherwise indicated and acknowledged.

I further certify that the work is original and has not been previously submitted for assessment in any other course or institution, except where specifically stated.

CHIN CHEE WEN

006 10 359 03

Signature of Candidate

Date

ENDORSEMENT

Signature of Principle Supervisor

Date

Signature of Associate Supervisor

Date

ACKNOWLEDGEMENTS

I would like to express my most sincere appreciation to my PhD project supervisors Dr. B.F. Yousif and Dr. Harry Ku for all their support, encouragement, valuable input and guidance provided at every stage of this thesis. I would also like to extend my gratitude toward the entire departmental and technical staff for their assistance and support in using the facilities and materials for conducting the experimental work.

In addition, I wish to express my deepest appreciation to my family, Mrs Yeo Chin Moey, Jing Ee and Jing Wei for their constant support throughout this study. I would like to extend my appreciation to my friends for their encouragement. My gratitude and special thanks go to Abdullah Shalwan and K.C. Ming for their support and encouragement for all this time.

My particular appreciation is also extended to the University of Southern Queensland for financial support during this study.

TABLE OF CONTENT

ABSTRACT.....	i
LIST OF PUBLICATIONS	iii
CERTIFICATION OF DISSERTATION.....	iv
ACKNOWLEDGEMENTS	v
TABLE OF CONTENT	vi
LIST OF TABLES	x
LIST OF FIGURES	xi
CHAPTER 1: INTRODUCTION.....	1
1.1 INTRODUCTION	1
1.2 OBJECTIVES	3
1.3 PROJECT SIGNIFICANCE AND CONTRIBUTIONS	4
1.4 ORGANISATION OF THE THESIS	5
CHAPTER 2: LITERATURE REVIEW.....	8
2.1 INTRODUCTION	8
2.2 NATURAL FIBRES AS REINFORCEMENTS	8
2.2.1 Interfacial Adhesion of Natural Fibres	10
2.2.2 Fibre Orientation in Composites.....	12
2.3 TRIBOLOGY IN MATERIAL SELECTION AND DESIGN	14
2.3.1 Tribology of Fibre-Polymer Composites	15
2.3.2 Natural Fibres as Reinforcement for Tribo-Polymeric Composites	18
2.3.2.1 Dry Adhesive Wear.....	21
2.3.2.2 Wet Adhesive Wear	23
2.3.2.3 Three-Body Abrasive Wear	24
2.4 ARTIFICIAL NEURAL NETWORKS IN TRIBOLOGY.....	27

2.5 SUMMARY	29
CHAPTER 3: METHODOLOGY AND MATERIAL PROPERTIES	30
3.1 INTRODUCTION	30
3.2 MATERIAL SELECTION AND PREPARATION	30
3.2.1 Kenaf Fibre Selection and Preparation	31
3.2.2 Epoxy Composite Preparation	33
3.2.2.1 Interfacial Adhesion Sample Preparation.....	34
3.2.2.2 Sample Preparation for The Tensile, Flexural and Tribological Experiments.....	35
3.3 MECHANICAL PROPERTIES OF THE COMPOSITES.....	38
3.3.1 Interfacial Adhesion and Tensile Properties	38
3.3.2 Flexural Properties	41
3.4 TRIBOLOGICAL EXPERIMENTS.....	45
3.4.1 Dry/Wet Adhesive Wear Experiments.....	45
3.4.2 Three-Body Abrasion Tests	50
3.5 DEVELOPMENT OF THE ARTIFICIAL NEURAL NETWORK MODEL.....	54
3.5.1 The Optimum Learning Rule and Transfer Function.....	54
3.5.2 Optimum Number of Neurons	57
CHAPTER 4: ADHESIVE WEAR AND FRICTIONAL BEHAVIOUR OF THE COMPOSITES	60
4.1 INTRODUCTION	60
4.2 DRY ADHESIVE WEAR AND FRICTIONAL BEHAVIOUR	61
4.2.1 Dry Adhesive Wear Behaviour	61
4.2.1.1 Wear Behaviour Under Different Sliding Distances.....	61
4.2.1.2 Dry Adhesive Wear At Different Applied Loads	63
4.2.1.3 Dry Adhesive Wear At Different Sliding Velocities	64

4.2.2 Dry Adhesive Frictional Behaviour of the Composites	66
4.3 DISCUSSION AND SURFACE OBSERVATIONS	70
4.3.1 Dry Adhesive Wear Behaviour in the Published Literature.....	77
4.4 WET ADHESIVE WEAR AND FRICTIONAL BEHAVIOUR	80
4.4.1 Wear Behaviour Under Wet Contact Conditions.....	80
4.4.2 Frictional Behaviour Under Wet Contact Conditions.....	83
4.4.3 Surface Observation of Worn Surfaces Subjected to Wet Adhesive Wear ..	85
4.5 ARTIFICIAL NEURAL NETWORK RESULTS	88
4.5.1 Comparison of the Experimental and ANN Results	88
4.5.2 Verification of the ANN Model	92
4.5.3 Prediction of the Friction Coefficient Using Artificial Neural Networks.....	93
4.6 SUMMARY	94
CHAPTER 5 THREE-BODY ABRASION BEHAVIOUR OF THE EPOXY COMPOSITE	95
5.1 INTRODUCTION	95
5.2 WEAR BEHAVIOUR OF THE COMPOSITE UNDER THREE-BODY ABRASION	95
5.2.1 Three-Body Abrasive Behaviour at Different Sliding Distances.....	96
5.2.2 Three-Body Abrasion Behaviour at Different Applied Loads.....	99
5.3 FRICTION RESULTS OF THE COMPOSITE UNDER THREE-BODY ABRASION	102
5.3.1 Three-Body Abrasion Frictional Behaviour at Different Sliding Distances	102
5.3.2 Influence of Particle Size and Applied Load on Three-Body Abrasion Frictional Behaviour	104
5.4 DISCUSSION OF THE THREE-BODY ABRASION RESULTS	106
5.4.1 Rolling and/or Sliding of Particles.....	106

5.4.1.1 Morphology of The Sand Particles After The Tests	108
5.4.2 Worn Surface of the Composites after the Three-Body Abrasion Tests	111
5.4.2.1 Observations on KFRE at AP-O	111
5.4.2.2 Observations on KFRE at P-O	115
5.4.2.3 Observations on KFRE at N-O	117
5.5 SIMULATION OF THE DAMAGE MECHANISM TO THE COMPOSITE SURFACE.....	119
5.5.1 Results of the Simulation	122
5.6 COMPARISON WITH PREVIOUS STUDIES	127
5.7 SUMMARY	129
CHAPTER 6: CONCLUSIONS AND RECOMMENDATIONS	130
6.1 CONCLUSIONS.....	130
6.2 RECOMMENDATIONS FOR FUTURE WORK	133
REFERENCES.....	134
APPENDIX A: ARTIFICIAL NEURAL NETWORKS DEVELOPMENT STEPS	154
A.1 MATLAB WORKSPACE AND TOOLBOX	154
A1.1 Input Data.....	154
A.2 MATLAB SCRIPT	161
APPENDIX B : SAMPLE OF ABAQUS SIMULATION RESULTS.....	164
B.1 KFRE In the Anti-Parallel Orientation.....	164
B.2 KFRE In The Parallel Orientation.....	166

LIST OF TABLES

Table 3. 1 Mechanical Properties of the prepared composite	41
Table 4. 1 Typical values of the standard deviation of Ws. and friction coefficient .	60
Table 4. 2 Specific Wear Rate And Friction Coefficient of Some Previous Studies.	79
Table 5. 1 3B-A wear results of KFRE (in N-O), UT-OPRP and T-OPRP composites at 50 rpm rotational speed.	128

LIST OF FIGURES

Fig. 1. 1	Layout of the thesis.....	7
Fig. 2. 1	Number of publication on natural fibre as reinforcements from 2002-2012. *the data extracted from www.sciencedirect.com on the 30-5-2013, the keyword was natural fibre, reinforcement and polymers.....	10
Fig. 3. 1	Untreated kenaf fibres (a) photo of the raw fibre, (b) Micrograph of cleaned fibres	32
Fig. 3. 2	Micrographs of the treated kenaf fibres	33
Fig. 3. 3	SEM micrographs on the cross-section of kenaf fibre-reinforced epoxy composite: a) Pure composite , b) Untreated kenaf fibre, c) Treated kenaf fibres	34
Fig. 3. 4	Schematic drawing describing the single fibre pull-out test (SFTP)	35
Fig. 3. 5	Specimen geometry and dimensions for tensile and flexural tests	37
Fig. 3. 6	Micrographs of the pull-out samples for treated and untreated kenaf fibres embedded inside epoxy matrix.	3940
Fig. 3. 7	Bar charts of flexural properties of untreated KFRE and treated KFRE	42
Fig. 3. 8	SEM micrographs of untreated KFRE after test.....	43
Fig. 3. 9	SEM micrographs of treated KFRE after test.....	44
Fig. 3. 10	Fibre orientations with respect to the sliding direction.....	45
Fig. 3. 11	Block-On-Disc machine working under dry contact condition	46
Fig. 3. 12	Sample of the roughness profile of the composite surface in different orientations	48
Fig. 3. 13	Block On-Disc (BOD) Tribological machine operated under wet contact conditions	49
Fig. 3. 14	Calibration chart for measuring interface temperature	50
Fig. 3. 15	Three-body abrasive set-up.....	51
Fig. 3. 16	Micrographs of three different sizes of sand particles before the tests.....	52
Fig. 3. 17	Artificial Neural Network configuration for prediction of the friction coefficient	53

Fig. 3. 18 Transfer function and learning rules vs. errors percentage of ANN models	56
Fig. 3. 19 Number of neurons vs. errors percentage of ANN models.....	57
Fig. 3. 20 Flow chart represents the procedure of developing and selection of suitable ANN model configuration	59
Fig. 4. 1 Specific wear rate versus sliding distance at 50N applied load.....	60
Fig. 4. 2 Specific wear rate versus applied load after 3.36km sliding distance	64
Fig. 4. 3 Specific wear rate versus sliding velocity at 50N applied load.	66
Fig. 4. 4 Sample of the frictional collected data showing the coefficient versus sliding distance of KFRE at N-O at sliding velocity of 2.8 m/s.....	67
Fig. 4. 5 Friction coefficient versus applied load for NE and KFRE under different orientations.....	69
Fig. 4. 6 Film transfer behaviour of epoxy against stainless steel	69
Fig. 4. 7 Interface temperature versus applied load.	70
Fig. 4. 8 Proposed wear mechanism of the KFRE composite in three different orientations.....	72
Fig. 4. 9 Worn surface of the KFRE composite tested in N-O at different operating parameters.	74
Fig. 4. 10 Worn surface of the KFRE composite tested in P-O at different operating parameters.	75
Fig. 4. 11 Worn surface of the NE at different operating parameters.....	75
Fig. 4. 12 Counterface roughness after tests: before and after cleaning.	76
Fig. 4. 13 Composite roughness after tests.	77
Fig. 4. 14 Roughness of the worn surface of the composite and NE after the tests at 2.8m/s sliding velocity, 50N applied load after 3.36 km sliding distance ...	78
Fig. 4. 15 Specific wear rate (Ws) results of the epoxy composites at different sliding distances at 2.8 m/s sliding velocity and 100 N applied load.....	81
Fig. 4. 16 Adhesive wear behaviour under wet and dry contact conditions	81
Fig. 4. 17 Specific wear rate (Ws) results of the epoxy composites at different applied loads	83
Fig. 4. 18 Average of friction coefficient of the epoxy composites at different sliding distances at 150N applied load and sliding velocity of 2.8 m/s	84

Fig. 4. 19 Micrographs of KFRE worn surface at AP-O after 30km sliding distance.	87
Fig. 4. 20 Micrographs of KFRE worn surface at P-O after 30km sliding distance..	87
Fig. 4. 21 Micrographs of KFRE worn surface at N-O after 30km sliding distance.	87
Fig. 4. 22 Experimental and modelling of friction coefficient of KFRE composite at different applied load at 2.8m/s sliding velocity.	91
Fig. 4. 23 Correlation between the experimental and ANN friction coefficient.....	92
Fig. 4. 24 Prediction results of KFRE friction coefficient at different orientations...	93
Fig. 5. 1 Wear rate against sliding distance under different particle sizes and applied load of 20 N.	97
Fig. 5. 2 Schematic drawing showing the contact and the number of particles in the interface at short and long sliding distances.	98
Fig. 5. 3 Wear rate vs. applied load with different particle sizes after 0.18 km sliding distance	100
Fig. 5. 4 Wear rate of the materials with different particle sizes under 5 N and 20 N applied loads after 0.18 km sliding distance.....	101
Fig. 5. 5 Friction coefficient vs. sliding distance at different particle sizes at applied load of 20 N.	103
Fig. 5. 6 Averages of friction coefficient associated with maximum and minimum values at different applied load and particle sizes	105
Fig. 5. 7 Proposed particle movement on the composite surface for fibres in three different orientations.....	107
Fig. 5. 8 Micrographs of three different sizes of sand particles after the test at 20N applied force.....	110
Fig. 5. 9 SEM micrographics of KFRE composite tested in AP-O at different conditions against particle size 370-390 μm	112
Fig. 5. 10 SEM micrographics of KFRE composite tested in AP-O at different conditions against particle size 650-750 μm	114
Fig. 5. 11 SEM micrographics of KFRE composite tested in AP-O at different conditions against particle size 1200-1400 μm	114
Fig. 5. 12 SEM micrographics of KFRE composite tested in P-O at different conditions against particles in size of 370-390 μm	116

Fig. 5. 13 SEM micrographics of KFRE composite tested in P-O at different conditions against particles in size of 1200-1400 μm	116
Fig. 5. 14 SEM micrographics of KFRE composite tested in N-O at different conditions against particle size of 370-390 μm	118
Fig. 5. 15 SEM micrographics of KFRE composite tested in N-O at different conditions against particle size of 650-750 μm	118
Fig. 5. 16 SEM micrographics of KFRE composite tested in N-O at different conditions against particle size of 1200-1400 μm	119
Fig. 5. 17 Attack angle, θ of sand particle.....	120
Fig. 5. 18 Boundary condition for a) Normal Orientation b) Parallel Orientation...	120
Fig. 5. 19 Stress distribution in the composite.....	124
Fig. 5. 20 Maximum stress vs. attacked angle at different pressures and composite orientations	126
Fig. 5. 21 Stress distribution on the composite surface in N-O, fibre, bonding area, and the resinous regions.	127

CHAPTER 1: INTRODUCTION

1.1 INTRODUCTION

The tribological performance of materials is one of the essential considerations in material selection and component design. Currently, there is tremendous interest in using polymeric composites for tribological applications, such as bearings, gears and bushes. However, growing environmental awareness has aroused an interest in research into, and the development of, biodegradable high performance materials. Over the last few years, natural fibres have become a promising alternative reinforcement fibre to replace the synthetic fibres currently used in polymeric composites (Azwa et al. 2013; Shalwan & Yousif 2013; Heitzmann et al. 2013). Natural fibres have several advantages over synthetic fibres, such as being renewable, environmentally friendly, low cost, lightweight, flexible in their usage, naturally recyclable and biodegradable. Natural fibres such as jute, linen, banana, bamboo, sugarcane, coir and oil palm have been used as reinforcements in different types of polymers for different applications. Due to this interest and the benefits of using bio-reinforcements, numerous studies have attempted to evaluate the influence of these new reinforcement materials on composite performance under different loading conditions. In recent years, kenaf fibres have attracted both academic researchers and industries, since promising results have been obtained using kenaf fibres in different applications (Asumani, Reid & Paskaramoorthy 2012; Amel et al. 2013; Meon et al. 2012). Industrial applications for kenaf-polymer composites are growing for automobile, housing, packaging and electronic products (Nishimura et al. 2012). With regard to the properties and performance of these newly developed

natural fibre-polymer composites, the majority of the existing research studies have been conducted on the mechanical performance of these composites. However, it is well known that the majority of these components are subjected to tribological loading, which may be the main reason for component failure. In other words, less attention has been paid to the tribological behaviour of these new composites (Yousif 2013b; Davim 2013a). The tribological performance of polymers and their composites are generally dependent on operating and test conditions. Over the past few years, several studies have been initiated in order to investigate the effects of jute, linen, sugarcane and cotton fibres on the wear performances of polymeric composites (Chand & Dwivedi 2006a; El-Tayeb 2009; Nirmal et al. 2012; Yousif 2009), but the potential of other natural fibres remains to be explored. This has been the motivation for this research study, which aims to conduct a comprehensive investigation of the effect of kenaf fibres on the tribo-characteristics of epoxy composites. A closed compressed mould was used to fabricate kenaf reinforced epoxy composites (KFRE). Two KFRE composites were developed, based on untreated or treated (with 6 per cent NaOH) kenaf fibres. In addition, neat epoxy (NE) was prepared to investigate the effect of each fibre on tribo-performance. The tribological performance of the selected materials was primarily evaluated in adhesive and abrasive wear modes. The composites were tested under three principal orientations according to the orientation of the fibres in the matrix relative to the sliding direction of the counterface; i.e., parallel (P-O), anti-parallel (AP-O) and normal (N-O). The adhesive wear tests were conducted under wet and dry contact conditions using the block-on-disc (BOD) technique against smooth stainless steel at various sliding distances (0–14 km), sliding velocities (1.1–7.8 m/s) and applied

loads (30–100 N). The abrasive wear characteristics were evaluated in three-body abrasion (3B-A) wear modes at either of two rotational speeds (50 and 100 rpm) and for applied loads of between 5 and 25 N. The 3B-A wear tests were performed against different sizes of sand particles with a flow rate of 4.5 g/s, under high stress conditions.

The morphology of the worn surfaces of the composites was examined by scanning electron microscopy (SEM) in order to categorise the wear failure mechanisms. In addition, frictional forces and interface temperatures were recorded during the tests. The results of wear (i.e., specific wear rate, wear rate and weight loss), friction coefficients and interface temperatures were presented as functions of the operating parameters. The experimental results revealed many important issues that should largely contribute to tribological science.

1.2 OBJECTIVES

The main objectives of this study are to:

- Develop new environmentally friendly polymeric composites based on natural fibres. This can be achieved by developing epoxy composites based on attractive natural fibres, such as kenaf fibre.
- Study the mechanical properties of KFRE composites and the influence of NaOH treatment on the interfacial adhesion of the kenaf fibre with the epoxy matrix.

- Evaluate the adhesive wear and frictional characteristics of the natural fibre composites under dry/wet contact conditions when subjected to adhesive wear load and categorise the wear mechanisms of the composites.
- To study the 3B-A wear performance of the selected material and explore the effects of the natural fibre on the tribo-performance of the composites.
- To develop a friction coefficient prediction model using the artificial neural network (ANN) approach considering different operating parameters and output using different training and learning functions to gain the optimum performance.

1.3 PROJECT SIGNIFICANCE AND CONTRIBUTIONS

The impact of the project will be felt in different aspects: economic, environmental, industrial and scientific. Some of the significant aspects of the project are:

1. Natural fibres are becoming superior alternatives to synthetic fibres as reinforcements for polymeric composites due to their advantages over synthetic fibres. Replacing synthetic fibres with natural fibres as a biodegradable reinforcement is a significant approach to reducing the impact of synthetic polymeric composites on the environment.
2. In the recent decade, applications based on natural fibre reinforced polymeric composites have been found for numerous products that may be exposed to tribological loading during their service. For example, sugarcane, jute, coir, date palm fibre reinforced different types of resins such as epoxy and polyester have been developed for mechanical and civil components. The outcomes of this study will contribute significantly to our knowledge of these

materials and assist both industrial and basic researchers in understanding them.

3. Development of a new predictive modelling system based on ANN theory is a new approach in tribology and mechanical science. The significance of this is to overcome a major issue in tribological experiments: the number of experiments required to evaluate the tribological performance of materials can be significantly reduced by predictive modelling.
4. The findings of this study have been published in 6 articles in high-standard international journals, which will assist researchers working in the field of natural fibres, mechanical properties and the tribological characteristics of polymer composites.

1.4 ORGANISATION OF THE THESIS

The thesis contains six chapters. Chapter 1 presents a brief introduction to the importance of natural fibres as a reinforcing material for polymeric composites, as well as their benefits to the environment. Additionally, this chapter identifies on-going work with respect to tribological investigations of polymer composites based on untreated and treated natural fibres. Further, it summarises the objectives of this study and presents a brief overview of the research efforts and the findings. Chapter 2 introduces the history of natural fibre reinforced polymer composites and their applications. It presents the relevant background information that has been recently reported for tribo-polymeric composites. It discusses recent issues in adhesive and abrasive wear of synthetic and natural polymeric composites. The merits, limitations and arguments for the effect of natural and synthetic reinforcement on the

tribological performance of polymeric composites under various wear modes and conditions are presented. Chapter 3 describes the material fabrication processes, as well as mechanical, pull-out, and tribological test procedures. The development of ANN models and approaches are given. Further, mechanical and pull-out results are presented and discussed in this chapter. Chapter 4 presents the results and findings of the tests conducted in dry and wet adhesive wear mode experiments. The results of frictional prediction using the ANN model are presented in this chapter as well. At the end of the chapter, a summary of the results is given in order to present conclusions on the effect of kenaf fibres on the tribo-performance of the epoxy under dry/wet contact conditions. The 3B-A results are presented and discussed in Chapter 5. Chapter 6 concludes the findings of this thesis, and gives recommendations for future work.

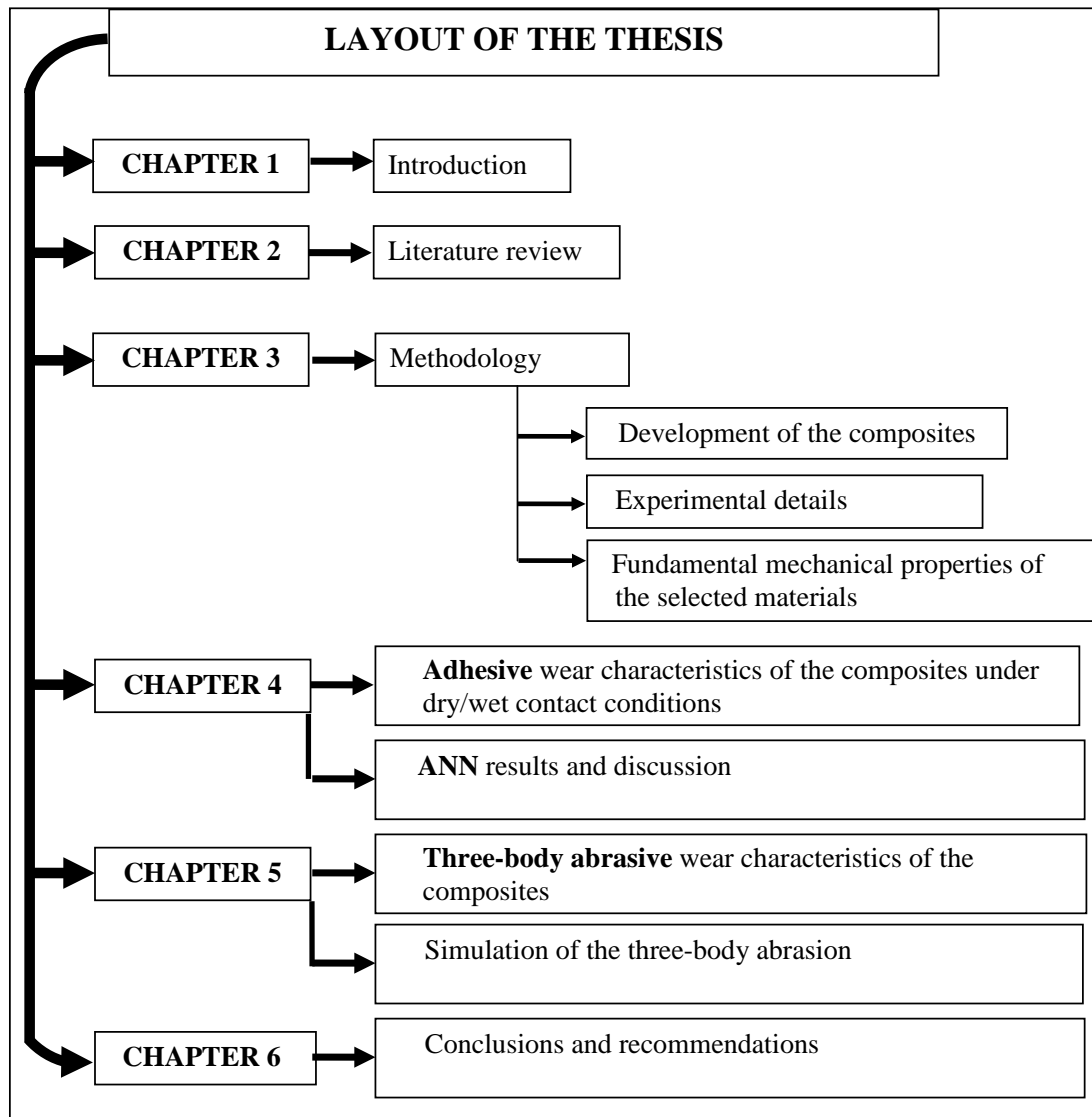


Figure 1.1 Layout of the thesis

CHAPTER 2: LITERATURE REVIEW

2.1 INTRODUCTION

In this chapter, a literature review covering the most recent related research work is presented. This review includes studies on the tribological performance of fibre-polymer composites, the influence of operating parameters and fibre orientation on performance, natural fibres as reinforcements for mechanical and tribological applications and ANNs in the tribology field.

2.2 NATURAL FIBRES AS REINFORCEMENTS

Increasing pressure from environmental activists, the necessity for the preservation of natural resources and the stringency of laws passed by developing countries has led to the invention and development of natural materials with a focus on renewable raw materials. As a result of this, natural fibres are drawing considerable attention as substitutes for synthetic fibres. Until this year, there has been a steady increase in papers reporting on natural fibre properties and their utilisation in applications across different sectors. Based on the database, www.sciencedirect.com, there is rapidly increasing interest in the research field of natural fibres as reinforcements (**Figure 2.1**).

Applications for natural fibres are expanding in many sectors, such as automobiles, furniture, packing and construction. Natural fibres have several advantages over

synthetic fibres, including their low cost, low weight and good relative mechanical properties. They also cause less damage to processing equipment, provide an improved surface finish to moulded parts of composites and are abundant and renewable resources.

Currently, plant fibres such as sisal, jute, coir and flax are the most common materials used as reinforcements and fillers for polymer composites, owing to their enhancement of the mechanical properties of polymers. These fibres improve the tensile, impact and flexural properties of composites, as recently reported by Velmurugan and Manikandan (2007), Sapuan et al. (2006), Haque et al. (2009), Rosa et al. (2009) and Saha et al. (2010). Despite the advantages of using natural fibres as reinforcements, they have several limitations, including low fire resistance, low moisture resistance, variety in the quality of the fibres and poor interfacial adhesion with synthetic fibres (Shalwan & Yousif 2013; Alsaeed, Yousif & Ku 2013). Vilay et al. (2008) reported that the mechanical properties of natural fibre reinforced composites are highly dependent on the interfacial adhesion between the fibres and the polymer matrix and the quality of the fibre itself. Natural fibres tend to have strong polarity and are hydrophilic, while polymers exhibit hydrophobicity. In other words, there is a significant compatibility problem between natural fibres and synthetic matrices, which can result in weakness in the fibre-matrix adhesion.

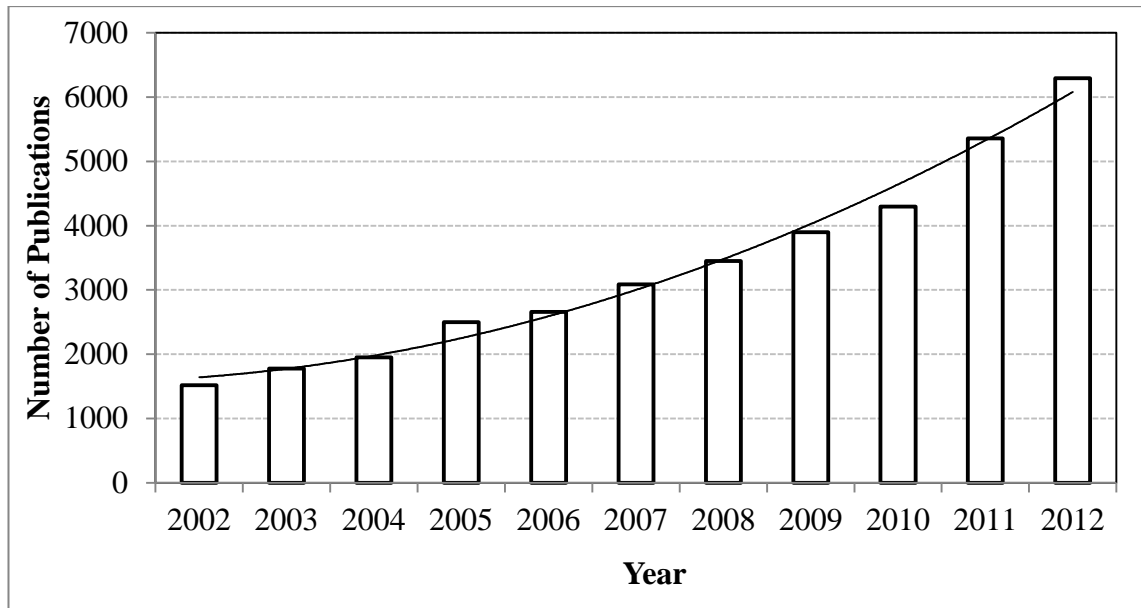


Figure 2.1 Number of publications on natural fibres as reinforcements, 2002–2012

*Data extracted from www.sciencedirect.com on 30 May 2013, using the keywords natural fibre, reinforcement and polymers.

2.2.1 Interfacial Adhesion of Natural Fibres

Surface modification of natural fibres by means of certain treatments is one of the largest areas of recent research aiming to improve compatibility and interfacial bond strength in fibre reinforced composites. Chemical treatments, such as alkali treatment, have been reported to enhance fibre-matrix adhesion by increasing the surface roughness of the fibres, stripping them of impurities and disrupting the moisture absorption process by coating the OH groups in the fibres (Cantero et al. 2003; Edeerozey et al. 2007; Haque et al. 2009; Rokbi et al. 2011; Rosa et al. 2009; Saha et al. 2010; Torres & Cubillas 2005; Chai et al. 2010). Many investigations have focused on the treatment of fibres to improve their bonding with a resin matrix. Vilay et al. (2008) investigated the effect of fibre surface treatment (NaOH) and fibre loading (0–20 vol per cent) on the flexural properties of bagasse fibre reinforced

unsaturated polyester composites. At different fibre volume fractions, NaOH-treated fibre composites showed better flexural strength and modulus (an increase of approximately 11 per cent and 20 per cent, respectively) compared to untreated fibre composites. These findings were attributed to the improved fibre-matrix interaction as a result of the modification of the fibre surface by the alkali treatment. Rokbi et al. (2011) studied the effect of concentration (1–10 per cent) and time (24 h and 48 h) of alkali treatment on the flexural properties of alfa (*Stipa tenacissima L.*)-polyester composites (40 wt per cent, randomly oriented fibres). The flexural test results showed that alkali treatment of alfa fibres improved the quality of the fibre-matrix interface. Both the NaOH concentration and the duration of treatment had a significant effect on the flexural properties of alfa fibre reinforced composites. For fibres treated with 10 per cent NaOH for 24 h, the flexural strength and flexural modulus were improved by 60 per cent and 62 per cent respectively, compared to the untreated fibre composites. Islam and colleagues (2010) investigated the flexural properties of coir polypropylene composites under different treatment conditions with a hydroxybenzene diazonium salt. The addition of both untreated and treated coir fibres increased the flexural properties of the composites compared to the neat polypropylene. A significant improvement in the flexural strength and modulus has also been observed for composites based on chemically treated coir compared to those of untreated coir. This was attributed to better wetting of the treated coir fibres with the polypropylene matrix and to improved interfacial bonding between the filler and the matrix. Mysamy and Rajendran (2011) studied the flexural properties of alkali-treated agave fibre reinforced epoxy composite (TCEC) and untreated agave fibre reinforced epoxy composite (UTCEC). The TCEC sample was considered to

have 15 per cent higher flexural strength than the UTCEC sample. These results showed that alkali treatment increased the area of contact between the core of the fibres and the matrix, which led to better fibre-matrix interaction.

2.2.2 Fibre Orientation in Composites

In polymeric composites based on natural fibres, the shape of the composite and its surface appearance are determined by the matrix, while the fibres act as carriers of load and stress (stiffness and strength) when the composite is subjected to load (Pickering 2008; Brahim & Cheik 2007; Ku et al. 2011; Jacob, Thomas & Varughese 2004). Therefore, the orientation of the fibres has a significant effect and plays an important role in enhancing the mechanical properties of these composites (Jacob, Thomas & Varughese 2004; Brahim & Cheikh 2007; Ku et al. 2011; Fu & Lauke 1996; Tungjitpornkull & Sombatsompop 2009; Herrera-Franco & Valadez-Gonzalez 2004). Brahim and Cheikh (2007) studied the influence of fibre orientation on the mechanical properties of alfa-polyester composites with a 45 per cent fibre volume fraction. All specimens were made from unidirectional alfa fibres and tested at different orientation angles (α): 0°, 10°, 30°, 45° and 90°. The percentage reduction of tensile strength (σ) with the change of angle from 0° (longitudinal specimens) to 45° was 78 per cent and 88 per cent at 90° (transverse direction), respectively. Jacob, Thomas and Varughese (2004) investigated the relationship between the mechanical properties of sisal/oil palm/natural rubber composites with different orientation angles: 0° (the longitudinal orientation), 30°, 45°, 60° and 90° (the transverse orientation). Maximum tensile strength of the composite was observed at the

longitudinal fibre orientation, where the fibres were arranged parallel to the direction of the load, while minimum tensile strength was observed with transversely oriented fibres queued perpendicular to the direction of the load. Increasing the angle of orientation of the fibres decreased the tensile strength of the composite.

Kenaf fibres have advantageous characteristics compared to other natural fibres; long fibre length, small diameter and high interfacial adhesion to matrix (Aziz & Ansell 2004). Kenaf has a long history of cultivation in certain countries, including India, Bangladesh, Thailand, parts of Africa, Malaysia and southeast Europe. The fibre from this plant has been mainly used in rope, twine, coarse cloth and paper. Nowadays, there is a demand for kenaf fibre as a reinforcement material for polymers (Nishino et al. 2003). However, the utility of kenaf fibres in polymeric composites, especially under mechanical loading conditions, has not been comprehensively assessed. This motivates the current study examining the possibility of using kenaf fibres as a reinforcement for tribological applications.

2.3 TRIBOLOGY IN MATERIAL SELECTION AND DESIGN

Tribology is an important branch of the mechanical engineering sector (Nosonovsky & Bhushan 2012; Davim 2013b). The principle interest of tribology is the deterioration of surfaces as a result of friction and wear. Friction and wear are the most common problems encountered in industrial engineering and machine elements, and necessitate the replacement of components and assemblies in engineering (Unal, Mimaroglu & Arda 2006). Therefore, an understanding of the tribological behaviour of polymers is essential in polymer science and engineering (Brostow et al. 2003). From the economic point of view, it has been reported that an increase in economic loss in the United States (US) is due to wear and friction; the reduction of wear and friction in machines could save resources equivalent to \$40 billion per year (Holmberg, Andersson & Erdemir 2012). Consequently, attention has recently been directed to the design of machine components (Yousif 2013b). Adhesive and abrasive wear are the fundamental wear modes that occur in machines (Davim 2013b). Therefore, the study of the adhesive and abrasive wear characteristics of newly developed polymeric composites is crucial. Over the current decade, this has directed many tribologist researchers to concentrate on the adhesive and abrasive wear behaviour of polymeric composites (Singh, Yousif & Rilling 2011).

It is well known by many researchers that tribology is response of the materials to the interaction between the asperities and to simulate it, this should go under several assumptions which make it far from the reality, (Chang et al. 2013; Li 2012; Martínez et al. 2012; Strickland et al. 2012).

2.3.1 Tribology of Fibre-Polymer Composites

Since the 1960s, synthetic fibres have become the main resources for fibre-polymer composites and their usage has increased dramatically (Jawaid & Abdul Khalil 2011). Fibre reinforced polymer composites are currently widely used due to their superior properties, low density and cost. Numerous applications for polymeric composites are found in many of the components used in the automotive and aerospace industries; for example, seals, bushes and cams (Bhushan 1999).

In general, the adhesive wear behaviour of neat polymers is subject to many issues, such as high material removal, high friction coefficients, and stick/slip behaviour (Sharma, Rao & Bijwi 2009, Sharma; Bijwi & Mitschang 2011; Suresha et al. 2010; Chang & Friedrich 2010). The most common technique used to enhance the dry adhesive wear characteristics of polymers is to introduce synthetic fibres such as carbon (Sharma, Rao & Bijwi 2009; Sharma, Bijwi & Mitschang 2011; Chang & Friedrich 2010) or glass (Suresha et al. 2010; Yousif & El-Tayeb 2010). These studies have shown that the presence of synthetic fibres in different thermoplastic and thermoset polymer composites may improve some of the tribological characteristics of the polymer and worsen others. Several factors control the performance of synthetic fibre-polymer composites: operating parameters, contact conditions (dry or wet), interfacial adhesion of the fibre with the matrix, film transfer characteristics and the counterface surface properties. For instance, Sharma, Bijwi and Mitschang (2011) studied the effect of carbon fabric on the wear and frictional behaviour of PEEK composite subjected to dry adhesive wear loadings. Their study

showed that the interfacial adhesion of the carbon fibres with the PEEK matrix is the most important parameter affecting the friction and wear behaviour of these composites. An approximately 20–25 per cent improvement was achieved when the carbon fibres had been treated chemically; the interfacial adhesion of the fibre with the matrix was enhanced by chemical treatment. During the rubbing process, the high interfacial adhesion of the treated carbon fibre with the PEEK matrix prevented the pull-out and delamination of fibres in the rubbing surfaces. This was the main reason for the high performance of the treated carbon fibre-PEEK compared to the untreated carbon fibre. Similar findings have been reported when carbon fabric was used to reinforce a polythiersulphone composite (Sharma & Bijwe 2011).

Suresha et al. (2010) investigated the wear and frictional behaviour of vinylester composites reinforced with either carbon or glass woven fibres. Interestingly, both types of synthetic fibres managed to reduce the wear rate of the neat polymer. However, due to the brittleness of the glass fibres, high levels of damage were found in the composites based on glass fibres. In spite of that, there was no major difference on the influence of both synthetic fibres on the frictional behaviour of the neat polymer. These authors studied the tribological performance of the composites in one direction, where the fibre mats were oriented perpendicular to the applied force and parallel to the counterface. In this orientation, the fibre matrix did not provide much support to the matrix region on the contact surfaces. Therefore, high levels of damage could be observed on the composite surfaces.

To study the influence of fibre orientation in the rubbing area on wear removal Sharma, Rao and Bijwi (2009) tested a carbon fibre-polyetherimide composite in different orientation (0–75°). However, in this study the fibres were parallel to the counterface in all the tested orientations. In other words, the ends of the fibres were not exposed to the rubbing process. In this study, the fibre orientation had a significant effect on the wear performance of the composite. When the fibres were parallel to the counterface and the shear force, a low wear rate was observed. Meanwhile, other orientations showed a higher wear rate compared to the 0° fibre orientation. This was primarily due to the debonding and shear forces acting on the surface of the composite. At the 90° orientation, the fibres were exposed to a high shear loading that was associated with thermo-mechanical loadings. Both effects deteriorated the surface of the composites.

Chang and Friedrich (2010) introduced carbon in the form of nanoparticles into epoxy composites. The presence of the nanoparticles in the interface region generated a thin film on the counterface, which led to high wear removal in the running-in period, followed by high reduction. However, the nanoparticles greatly enhanced the friction behaviour (a significant reduction in the value of the friction coefficient); this was due to the smooth film transfer on the counterface.

The adhesive wear and frictional performance of polyester composites have been studied by El-Tayeb and Yousif (2007) using chopped and woven glass fibres. In

both of these studies, glass fibres greatly enhanced the wear performance of the polyester, reducing the wear rate by around 20–40 per cent depending on the operating parameters. Applied load, sliding velocity, and fibre orientations were the most important parameters controlling the wear and the frictional behaviour of the composites. At severe conditions (high applied loads with a sliding velocity), deterioration was observed on the surface of the composites. In other words, a softening process took place on the resinous regions, which led to pull-out, detachment and breakage in the fibrous region. Less damage was observed when the ends of the fibres were exposed to the rubbing surface, which assisted in carrying the load out of the resinous area and resisting the shear loading. However, a high friction coefficient was observed, especially at high interface temperatures, due to the stick/slip behaviour of the composites under these conditions.

2.3.2 Natural Fibres as Reinforcement for Tribo-Polymeric Composites

Over the last decade, many researchers have studied the tribological performance of polymer composites reinforced with synthetic fibres. Recently, there has been growing concern over the increasing rate of depletion of petroleum resources, which has led to the enactment of new environmental regulations. This has pushed material designers to find substitutes for synthetic fibres that are compatible with the environment. Recently, natural fibres have been found to be a good alternative to synthetic fibres. This has been reported by many researchers (Towo & Ansell 2008). Natural fibres have numerous advantages over synthetics ones: they are obtained from abundantly available renewable resources, they are non-toxic, biodegradable,

low cost, flexible in usage, have high specific strength and a low density. These advantages, together with the current environmental issues, make natural fibres more attractive as reinforcement materials for polymer composites. In mechanical engineering, a number of researchers have attempted to study the influence of natural fibres on the mechanical properties of composites. However, the introduction of natural fibres as reinforcement in tribo-polymeric composites has not been comprehensively studied. Thus, there is a lack of understanding of the impact of natural fibres on the tribological performance of polymeric composites. A literature search revealed that some studies have been conducted in the adhesive and abrasive wear modes to examine the tribological performance of bamboo (Chand et al. 2007). The effect of fibre orientation on the 3B-A wear behaviour of bamboo in the abrasive mode with varying grit size has been investigated by Chand and Dwivedi (2006). Since the current research study focuses on the adhesive and 3B-A wear of composites, the next sections will examine these areas.

It has been mentioned previously that the tribo-behaviour of polymeric composites is subject to many factors, including contact conditions (Yousif & El-Tayeb 2008d; Bijwe, Awtade & Ghosh 2006; Liu et al. 2006; Borruto, Crivellone & Marani 1998; Yamamoto & Hashimoto 2004; Jia et al. 2005), operating parameters (Yamamoto & Hashimoto 2004; Yousif & El-Tayeb 2007d) and fibre orientation. In the previous section, the influence of the operating parameters on the adhesive wear behaviour of the composites was addressed. The contact conditions (wet/dry) have an equally important role in influencing the tribo-performance of polymeric composites. Several

published studies have reported that the tribo-performance of polymeric composites such as PA, UHMWPE (Bijwe, Awtade & Ghosh 2006), and epoxy (Liu et al. 2006) were improved under wet contact conditions compared to dry conditions. This was due to the use of water, which served as a cleaner/polisher by removing wear debris from the rubbing area and helped to absorb the heat generated by friction. However, the wear and frictional properties of other composites, such as particle erosion in polyphenylene sulphide (PPS) and PEEK, were worsened under wet contact conditions (Borruto, Crivellone & Marani 1998). This was due to the reduction in the hardness of the surface layer of the composite. Further, the wear mechanism could be transferred from adhesive to abrasive, due to the absence of film transfer on the counterface, allowing the removed debris and fibres at the interface to attack both surfaces (Liu et al. 2006).

In recent publications, Danaelan & Yousif (2008), Yousif & El-Tayeb (2007c, 2008d) and Chauhan, Kumar and Singh (2010) have studied the influence of water as a lubricant on the adhesive wear performance of polyester and vinylester composites based on glass fibres. In these studies, the results were compared to findings under dry contact conditions. In general, the trend of the results under wet contact conditions was almost opposite to those under dry contact conditions. For example, under dry contact conditions, an increase in the applied load increased the friction and wear of the composites, while under wet contact conditions the opposite occurred. Significantly, the surfaces of the composites were highly damaged under wet contact conditions in spite of the low material removal. The reduction of thermal

loading in the presence of water assisted in reducing the softening process of the resinous regions. However, it can be concluded that debris in the contact area acted as a third body, contributing to the high levels of delamination, bending and breakage of the synthetic fibres. This was considered to be due to the fact that glass fibres are brittle materials.

2.3.2.1 Dry Adhesive Wear

With regard to the use of natural fibres as reinforcement for tribological applications in polymeric composites, few studies have investigated polyester composites reinforced with oil palm, jute or sugarcane (Yousif & El-Tayeb 2007b, 2008c; El-Tayeb 2008; Chand & Dwivedi 2006b). These fibres have poor interfacial adhesion with polyester. The wear and frictional properties of jute fibre reinforced polyester composites are determined by the interfacial adhesion of the fibres with the matrix. Ochi (2008) reported that treated jute fibres gave better abrasive wear resistance than untreated fibres. In other words, stronger interfacial adhesion between the fibres and the matrix results in better wear performance.

Yousif and El-Tayeb (2010b) studied the potential use of betelnut fibres to reinforce polyester composites for adhesive wear applications. In this study, the poor interfacial adhesion of the natural fibre led to high micro- and macro-crack propagation on the composite surfaces at the interface. However, the ends of the fibres resisted the shear force and managed to protect the polyester region. The large

diameter of this fibre was considered to be the main reason for the micro- and macro-crack propagation on the rubbing surfaces. The use of fine fibres like kenaf may result in better performance of polyester composites. Moreover, the presence of the waxy layer on the betelnut fibres prevented the resin from entering the fibre during the curing process, and hence the fibres were empty, resulting in a highly porous composite. Yousif (2009) has reported similar findings when polyester was reinforced with coir fibres. NaOH-treated coir fibres enhanced the interfacial adhesion of the fibre with the matrix and reduced the porosity of the composites. However, some fibre debris was transferred onto the counterface, which roughened the surface at high applied loads and speeds and led to high friction coefficient (>0.9). Sabeel Ahmed et al. (2012) tried to overcome this issue by introducing additives such as SiC or Al₂O₃ to the epoxy matrix with jute fibres. The presence of these additives significantly deteriorated the composite surface where the decomposition process occurred during the rubbing process. This is mainly due to the brittle behaviour of these additives and the poor interaction between the additives and the matrix.

With regards to the possibility of using kenaf fibres as reinforcements for tribological applications, there are recent works have been attempted to used the kenaf fibre for thermoplastic materials as reported by (Singh et al., 2011a), (Singh et al., 2011b, Narish et al., 2011). In those three articles, the polyurethane resin was reinforced with kenaf fibre and tested under dry and wet adhesive wear condition under different operating conditions. It is well known that the elasticity of the polyurethane is very high and reinforcing it with kenaf could not present a good result in term of mechanical

properties. In those works, the mechanical properties are not conducted. Further to this, the interfacial adhesion of the fibre with the matrix seems to be good, however, due to the high elasticity of the resin, the SEM observation showed pull out mechanism of the fibre during the dry and/or wet adhesive wear loadings. Besides that, the applications of the polyurethane for tribological is very limited since such resin is commonly used for shock absorbing components, i.e. they are subjected to impact loading. On the other hand, thermosets such as epoxy are very commonly used materials for different applications such as bearings, slidings, pumps, brake pads and etc, i.e. there is lack of understanding on the influence of the kenaf fibres on the thermoset composites. Based on this, there is a need to comprehensibly understand the mechanical and tribological application of the kenaf fibres for thermoset composites.

2.3.2.2 Wet Adhesive Wear

It is believed that the use of natural fibres in composites could result in better wear and frictional performance compared to glass-polymer composites under the same conditions. This has been investigated in recent studies such as those by Yousif and El-Tayeb (2008b, 2010c) and Nirmal et al. (2010a). These studies showed that oil palm and betelnut fibre-polyester composites exhibited higher wear and frictional performance under wet contact conditions compared to dry conditions. In addition, the damage on the surfaces appeared to be much less than that observed in glass-polyester composites under the same conditions. This is due to the low abrasiveness of these natural fibres. However, debonding of the fibres was noticed at high applied

loads (200N). Improving the interfacial adhesion of natural fibres may play an important role in maintaining the wear performance of these composites under severe conditions. Moreover, introducing kenaf fibres to thermosets (e.g., epoxy) may result in much better wear and frictional performance compared to that achieved by other natural or synthetic fibre-thermoset composites due to the high interfacial adhesion of kenaf fibres. This motivates the current research study.

2.3.2.3 Three-Body Abrasive Wear

The effects of jute, sugarcane, oil palm, coir and bamboo fibres on polymeric composites have been investigated either in adhesive or multi-pass abrasion wear modes (Chin & Yousif 2009; Yousif & El-Tayeb 2007b; El-Tayeb 2008; Chand & Dwivedi 2006b; Shibata, Cao & Fukumoto 2006; Xue et al. 2009; Yousif 2009; El-Sayed et al. 1995; Hashmi, Dwivedi & Chand 2007). In practical applications, 3B-A is far more prevalent than other types of wear modes (Shipway & Ngao 2003). Hence, 3B-A wear has recently gained the attention of many researchers (Cenna et al. 2000, 2001, 2003; Suresha et al. 2007; Harsha, Tewari & Venkatraman 2003; Chand, Naik & Neogi 2000; Harsha & Tewari 2002, 2003). Moreover, 3B-A has become a major problem in agricultural machines and mining components (Suresha et al. 2007).

3B-A modes are divided into high and low stresses. In both modes, the tested sample is pressed against a rotating or sliding counterface. During the tests, particles flow into the rubbing area. High stress occurs when the particles fracture during the rubbing process. Meanwhile, at low stress, there is no damage to the particles.

Experimentally, the type of counterface material can determine the type of the 3B-A mode; high stress occurs in the case of a metal counterface and low stress in the case of rubber. Many attempts have been made to understand the tribological behaviour of various polymeric composites under low stress conditions (Shipway & Ngao 2003; Cenna et al. 2000, 2001, 2003; Suresha et al. 2007; Harsha, Tewari & Venkatraman 2003, Chand, Naik & Neogi 2000, Harsha & Tewari 2002, 2003). In general, these studies have revealed that the predominant wear mechanisms are matrix failure, pitting, cracking and grooving. The presence of glass fibres on the composite surface protects the composite, leading to lower wear rates compared to those of the neat polymers. However, carbon fibres provide poorer support for PEEK composites compared to glass fibres. Abrasive media affect the wear behaviour of composites, with the wear properties of a UHMPE-glass composite being enhanced by glass fibres when the abrasive medium was coal, but worsened in a mineral medium (Cenna et al. 2001). This was due to the reduction of the size of the soft particles during the test, which led to transition of the 3B-A wear mode into a two-body abrasion (2B-A) mode. Yousif (2010) studied the wear behaviour of a glass-polyester composite considering different orientations of fibres with respect to the sliding direction. In this study, parallel orientation of fibres resulted in better wear performance compared to the other orientations tested. In this orientation, the fibre mats are parallel to the sliding direction and the applied force, and become an obstacle to the sand particles during the rubbing process. In addition, continued exposure of the glass fibres at the interface protected the resinous regions leading to less material being removed from the composite surface. Similar findings have been

reported by Siddhartha and Gupta (2012) when glass-epoxy composites were tested under low stress 3B-A conditions.

With regard to the 3B-A wear behaviour of polymeric composites based on natural fibres, polyester composites based on oil palm or betelnut fibres have been studied by Yousif and El-Tayeb (2008c) and Chai et al. (2010). In these studies, high stress techniques were used, where the composites were subjected to rubbing against a stainless steel counterface in the presence of SiC particles at the interface. This is a more realistic test than the low stress 3B-A test. In the case of the oil palm fibre-polyester composite, treatment of the fibres with 6 per cent NaOH significantly enhanced the wear performance of the composite, especially under severe conditions of high load and speed. With untreated fibres, the surface of the composite was weak and did not resist the impact energy from the sand and the counterface, which led to high levels of debonding, breakage and pull-out of fibres. Treating the fibres strengthened the composite surface, which was then able to carry the impact load. Moreover, the low porosity of composites based on treated fibres also contributes to the better wear performance of the treated composites. The betelnut fibre-polyester composite was tested in a reciprocating machine in which the steel counterface moved linearly. As a result of the large diameter of the betelnut fibres, micro- and macro-cracks were the dominant wear mechanism under high stress abrasive loading. Thus, it can be suggested that the use of fine fibres, such as kenaf, may provide better support to the composite surface under high stress conditions.

2.4 ARTIFICIAL NEURAL NETWORKS IN TRIBOLOGY

To comprehensively understand the frictional behaviour of one material against another, several experimental sets need to be established at different operating parameters (Senatore et al. 2011). This is limited by the two materials tested. Due to the time and expensive equipment needed to conduct such experiments, numerical modelling has been proposed by many researchers as an alternative approach. Numerical simulations have been found to be a useful tool to study various parameters and advanced issues in tribological loadings. However, the most recent works by Solar et al. (2011) and Myshkin, Petrokovets and Kovalev (2005) have found a number of limitations and issues associated with modelling tribological pairs, such as the simulation time needed, the level of complicity and the error percentages. In addition, each developed model is applicable to a unique tribological application; there is no universal simulation model to predict the frictional behaviour of all materials. Myshkin, Petrokovets and Kovalev (2005) state, '*it appears important to study the structural changes*'. In other words, simulation modelling cannot predict the changes in contact surfaces. This is particularly relevant for polymers and polymeric composites (Solar et al. 2011; Myshkin, Petrokovets & Kovalev 2005). In summary, experimental investigations are necessary to understand the frictional property of a material. On the other hand, it is possible to reduce the number of experiments needed by introducing intelligent modelling, such as ANNs. Based on the discussion in the previous sections, it is evident that the tribological properties of polymeric composites are strongly influenced by many operating parameters and contact conditions (Yousif & El-Tayeb 2007d, 2007e, 2008d), which require numerous experimental investigations. The ANN prediction method has been

used for several applications, including wear (LiuJie, Davim & Cardoso 2007; Nasir et al. 2010) and friction (Zhang, Friedrich & Velten 2002; Jiang, Zhang & Friedrich 2007). ANNs have proven to be a successful tool for predicting certain tribological properties (Nasir et al. 2010). ANNs are a mathematical model inspired by the biological nervous system, and this technology has been used to solve complex scientific and engineering problems. The significance of this technology is that ANN models can be trained, based on experimental or real life data, to recognise solutions. Certain elements that control the ANN system performance are the training function, input data and number of hidden layers (Nasir et al. 2010).

ANN technology has been used successfully to predict the wear behaviour of A365/SiC metal matrix composites (MMC) (Rashed & Mahmoud 2009). In this study, wear performance was influenced by SiC particle size, SiC weight percentage, applied pressure and testing temperature. It has been shown that considerable cost and time can be saved by using ANN technology to predict outcomes. In another study, ANN was applied to predict solid PPS (Suresh, Harsha & Ghosh 2009). A three-layer neural network was optimised to perform the prediction task, which led to an acceptable range. ANNs have also been used for frictional material performance prediction by Aleksendric and Duboka (2006). In this study, 15 different ANN models, trained with five different algorithms, were tested. The results demonstrated the incredible prediction capability of ANN technology, even with a large number of input parameters. Similar findings have been reported for the prediction of

temperature sensitivity of frictional material or fading performance (Aleksendrić & Duboka 2007).

2.5 SUMMARY

Growing environmental awareness has aroused an interest in research into, and development of, biodegradable high performance materials. This makes natural fibres promising candidates for bio-reinforcements for polymeric composites. However, there is no clear direction for the application of these fibres in industry, since little technical data is currently available. Further, comprehensive study is required to establish adequate fundamental knowledge of this reinforcement. Most of the components designed from these composites are subjected to tribological loading. Since there is a lack of understanding of the tribological behaviour of natural fibre-polymer composites, there is a corresponding need to study the tribological behaviour of these materials under different operating parameters and conditions, as their performances are dependent on these factors. A comprehensive tribological evaluation of these newly developed composites is an essential point to be considered when designing a component and/or allocating an application.

CHAPTER 3: METHODOLOGY AND MATERIAL PROPERTIES

3.1 INTRODUCTION

In this chapter, the selection of the natural fibre and synthetic resin are addressed. The preparation and fabrication of the mechanical and tribological samples are explained, and the details of the experimental procedure and set-ups are given. Fundamental interfacial adhesion and the tensile and flexural properties of the prepared NE and its composites are discussed.

3.2 MATERIAL SELECTION AND PREPARATION

Currently, there is considerable interest in using natural fibres as reinforcements in numerous applications. One of the best-known natural fibres is kenaf, which is traditionally grown for the production of twine, rope and sackcloth (Nishimura et al. 2012). In recent years there has been a high demand for, and interest in, the use of kenaf fibres for composites, due to their good mechanical properties. Kenaf fibre has thus found its way into industrial applications in a range of domains, including automotive, housing, packaging and electrical products (Amel et al. 2013; Shin et al. 2012). In the light of this, kenaf fibre was selected as the reinforcement in the current study.

Liquid epoxy (DER 331), a liquid reaction product of epichlorohydrin and disponol A, was used as the resin in this study. It is widely used for general purposes and is recognised as used in a standard form. It is suitable for applications such as casting

and tooling, composites and automotive parts. The curing agent used for this epoxy was JOINTMINE 905-3S, a low viscosity aliphatic amine for room temperature curing. It has good wetting properties and impact resistance.

3.2.1 Kenaf Fibre Selection and Preparation

Raw kenaf fibres were supplied by the Malaysian Agricultural Research and Development Institute. The fibres had been well extracted, since they did not contain much dirt (Figure 3.1a). However, they were soaked in warm water for three hours until the fibres become yellow to indicate the cleaning process completed and then cleaned with fresh water. To extract the undesired substances, the fibres were combed and then dried for 24 hours in an oven at 40 °C. The oven contained a fan to aid the drying process. A micrograph of the cleaned fibres is shown in Figure 3.1b. Other natural fibres have a waxy outer layer that covers their inner structure. This has been noted with oil palm (Shinoj et al. 2011), coir (Saw, Sarkhel & Choudhury 2011; Tran et al. 2011), and banana fibres (Merlini, Soldi & Barra 2011). NaOH treatment was necessary to clean these natural fibres. For the current study, a preliminary investigation was performed to determine the interfacial adhesion of the fibre before treatment, which showed that kenaf fibres exhibit good interfacial adhesion with epoxy resin without treatment. However, the high volume fraction of the fibres in the matrix may deteriorate the bonding regions. Therefore, it is recommended to treat the fibres to ensure better bonding condition of the fibre in the composites during the loading. Despite this, treatments were performed on a portion of the cleaned fibres

and an evaluation of the interfacial adhesion and the tensile and flexural properties of the kenaf-epoxy composites was conducted with both treated and untreated fibres.

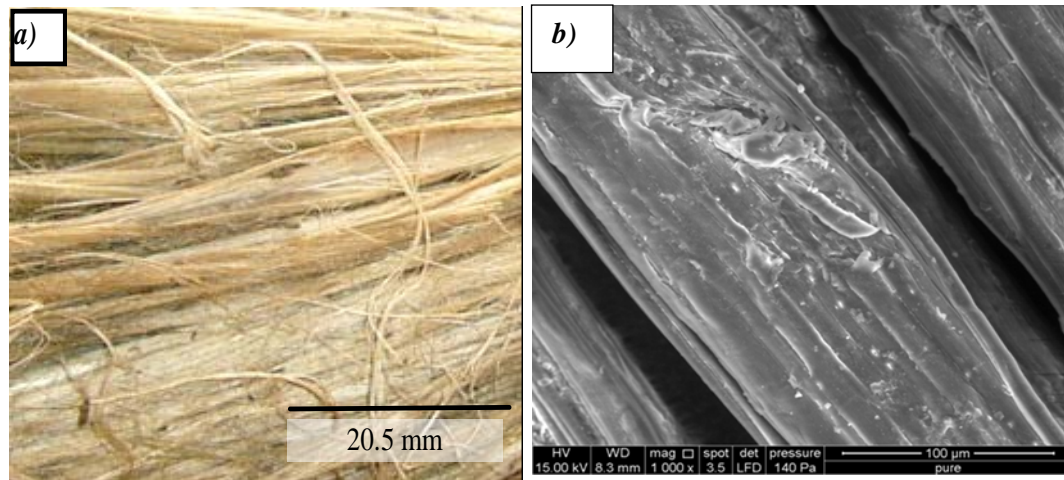


Figure 3.1 Untreated kenaf fibres: (a) Photo of the raw fibre; (b) Micrograph of cleaned fibres

In the treatment process, a portion of the cleaned kenaf fibres were cut into an average length of 100 mm. A NaOH solution was prepared with a 6 weight per cent concentration. The selected fibres were immersed in this aqueous NaOH solution for 24 hours at room temperature. After treatment, the fibres were washed with tap water and then dried for 24 hours in an oven at a temperature of 40 °C.

Samples of the micrographs of the treated kenaf fibres are shown in **Figure 3.2**. Comparing **Figure 3.1b** and **Figure 3.2**, it was evident that the NaOH treatment had thoroughly cleaned the surfaces of the fibres, the inner bundles of the fibres were exposed and any undesired substances had been removed. This may result in better

interfacial adhesion of the kenaf fibres and the epoxy matrix, a hypothesis that was tested and will be discussed in Section 3.3.

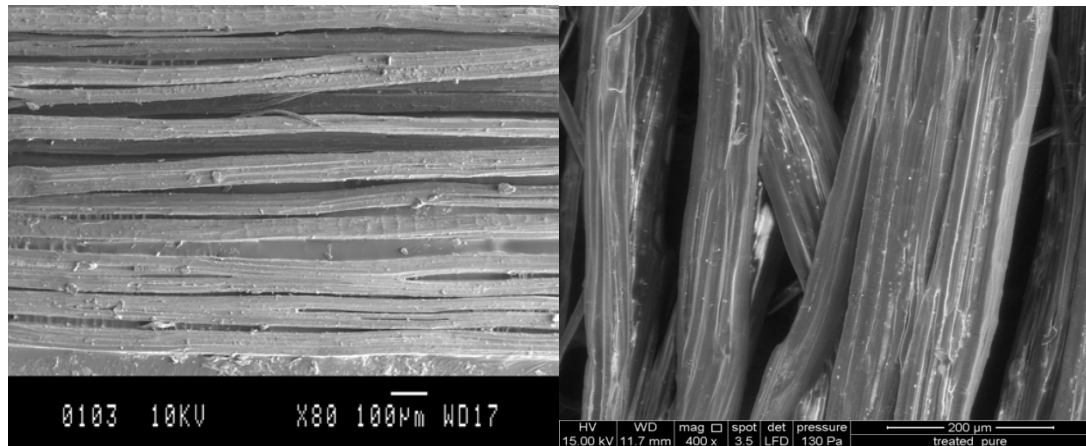


Figure 3.2 Micrographs of the treated kenaf fibres

3.2.2 Epoxy Composite Preparation

The fabrication process was the same for the mechanical and tribological samples, except for the dimension of the sample, which was controlled by the mould used in the fabrication process. The epoxy resin and the hardener were uniformly mixed at a 2:1 ratio using an electric stirrer and then poured into the desired mould. The mould was placed in a vacuum chamber (MCP 004PLC) at a pressure of 0.5 bar to remove any air bubbles trapped in between the fibres. The vacuum extracted blocks were kept for curing at room temperature for 24 hours. The volume fraction of the fibre in the matrix was controlled to be approximately 48 per cent vol. A sample of the prepared composite is shown in **Figure 3.3, a–c**. Comparing **Figure 3.3 b** and **c** clearly shows that the NaOH treatment enhanced the bonding regions of the fibre with the matrix.

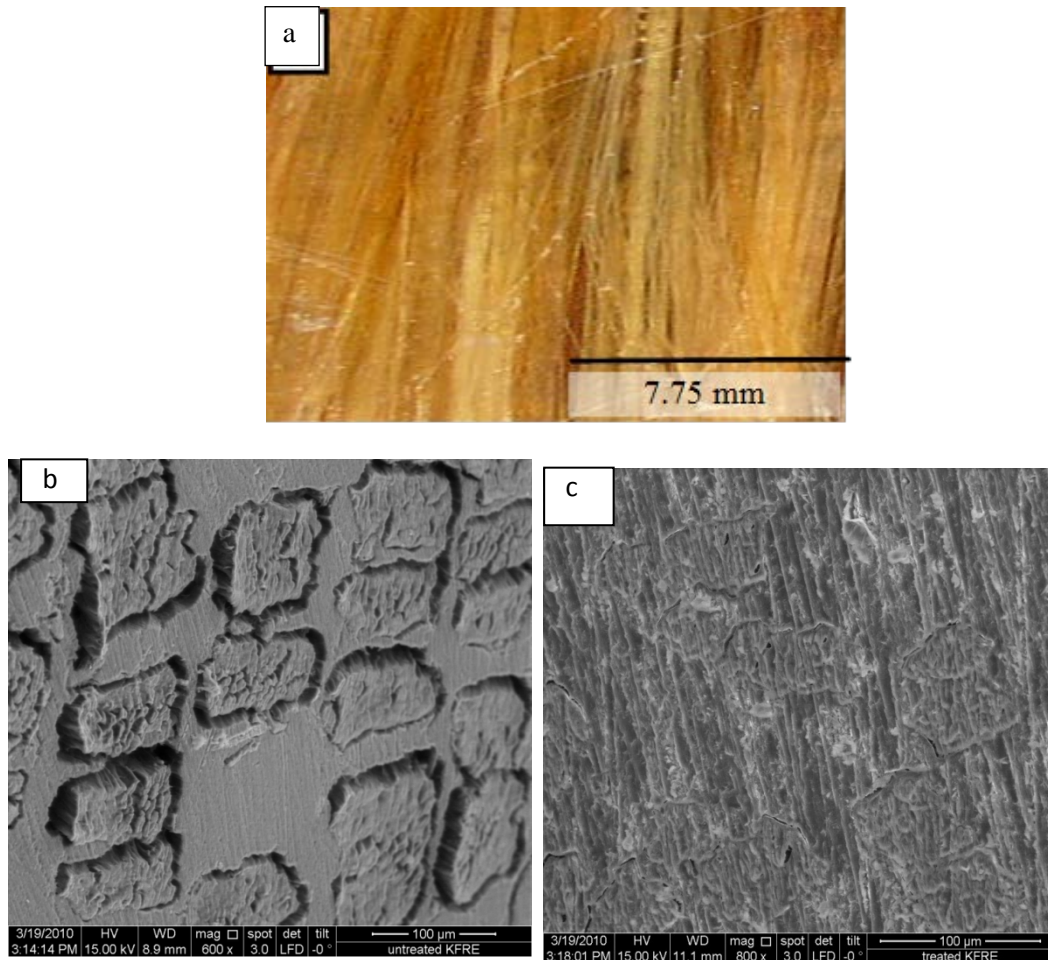


Figure 3.3 SEM micrographs of cross-sections of KFRE composites: a) Photo of the composite; b) Untreated kenaf fibre; c) Treated kenaf fibres

3.2.2.1 Interfacial Adhesion Sample Preparation

For studying the interfacial adhesion characteristics of kenaf fibres with the epoxy matrix, a single fibre pull-out test was performed, which is shown schematically in **Figure 3.4**. The samples were prepared based on the ASTM STP 1290 (Piggott et al. 1996). For the preparation of the test samples, a metal mould with dimensions of 50 mm × 20 mm × 20 mm was used to fabricate the interfacial adhesion specimens. Both ends of the fibres were mounted into the middle plane of the rubbers, which were placed at both ends of the mould. Pieces of rubber served to prevent the resin

from leaking out of the mould prior to solidification. A layer of wax was applied to the inner walls of the mould as a release agent. Epoxy mixed 2:1 with hardener was stirred gently and poured into the mould. The prepared samples were cured at 80 °C for 24 hours. The desired embedded length (20 mm) was obtained by drilling a hole through the specimen to cut the embedded fibre. The free end of fibre was placed into the clamp of the 100Q Standalone Universal Test System. The loading speed was set at 1 mm/min.

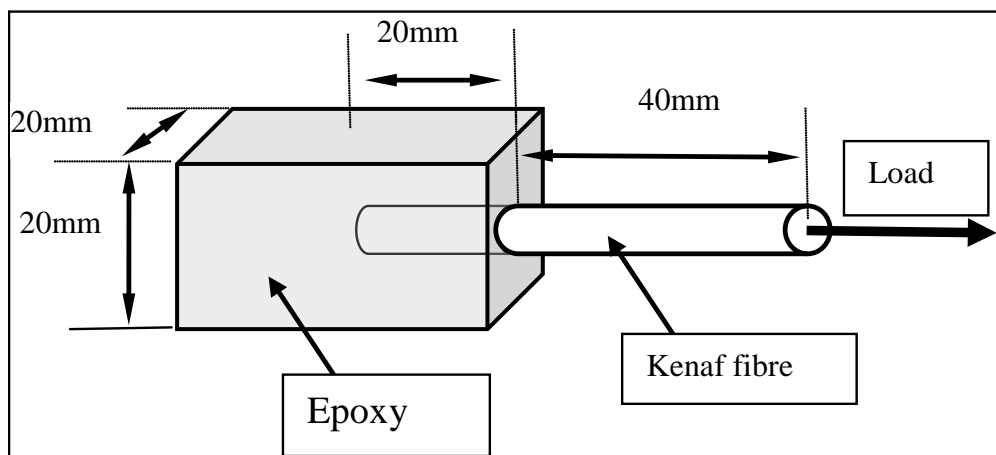


Figure 3.4 Schematic drawing describing the single fibre pull-out test

3.2.2.2 Sample Preparation for The Tensile, Flexural and Tribological Experiments

For the tensile and flexural experiments, three different materials were fabricated. These were NE, untreated KFRE and treated KFRE composites. The tensile samples were prepared according to ASTM standard D638; i.e., the samples were fabricated in the shape of a ‘dog bone’ with the dimensions given in **Figure 3.5a**. A Hounsfield Tensometer (250N–2500N) system was used to perform the tensile experiments, with

a crosshead speed of 1mm/min. Five samples were prepared and tested in each set of experiments. The average of the tensile strength, the modulus of the elasticity and the strain at fracture were determined.

For the flexural samples, a metal mould (10 mm × 10 mm × 100 mm) was coated with a layer of release agent (WD-40). The epoxy:hardener (2:1) mixture was stirred and poured into the mould. The untreated and treated kenaf fibres were prepared in unidirectional alignment, cut into lengths of 80 mm, and then placed into the mould. To ensure that bubbles were not trapped between the fibres a steel roller was used on the composite to remove any trapped air. Finally, the composite block was pressed, covered with mould cover and left to cure for 24 hours.

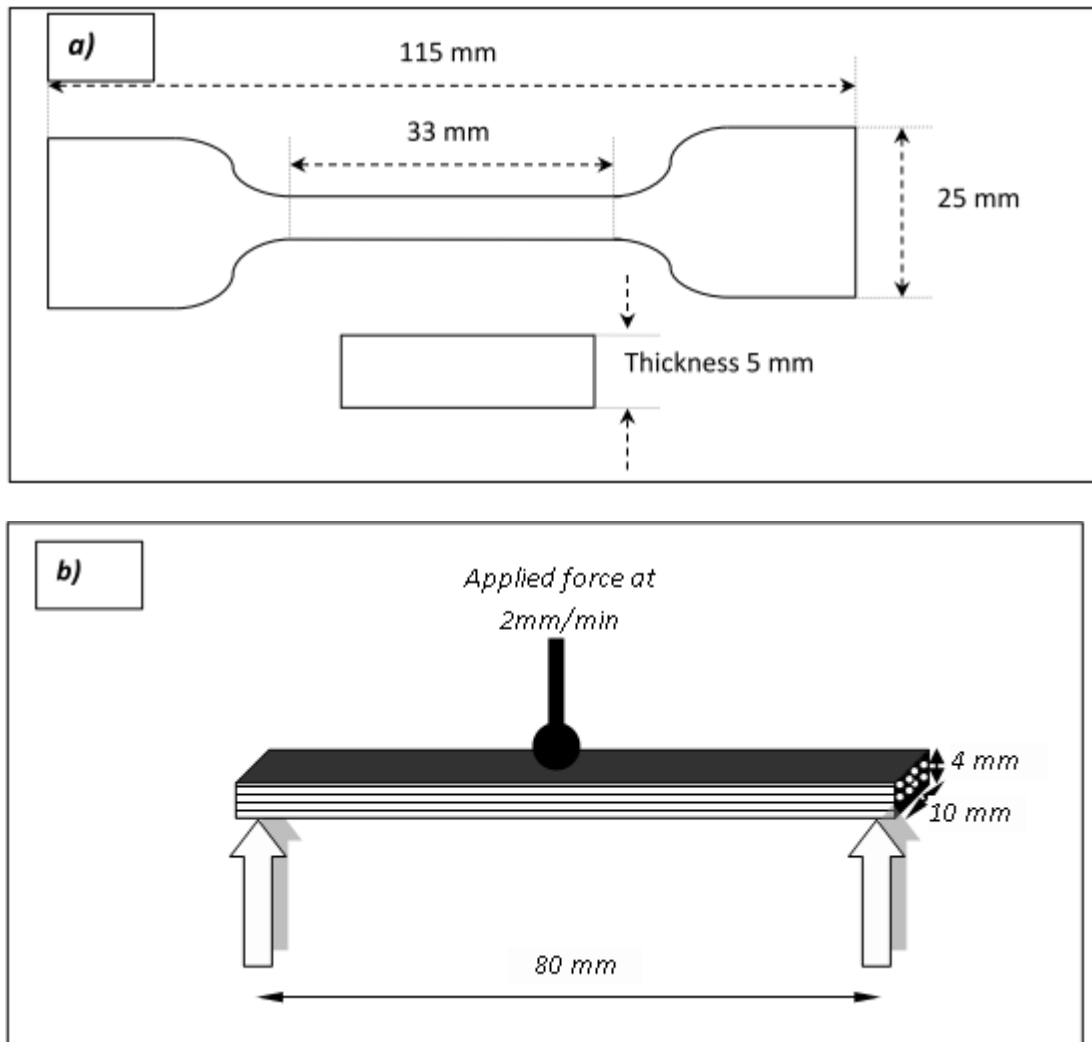


Figure 3.5 Specimen geometry and dimensions for the tensile and flexural tests

The same procedure was used for the treated kenaf fibres. The volume fraction of the fibre was determined (45–50 per cent). The amount of the fibres used was scaled and the resin used as well. Based on the density of both materials, the volume fraction was calculated. For the NE, the material was fabricated as described above without adding fibres. The prepared blocks were machined into specimens according to ASTM D790-07 standard test methods (80 mm × 10 mm × 4 mm), shown in **Figure 3.5b**. A three-point flexural technique was adopted in these experiments. A

Lloyd LR50K-Plus 50 kN Universal Testing Machine was used to perform the tests. The crosshead speed was set to 2 mm/min. For the tribological samples, a block of the treated kenaf fibre reinforced composite was prepared, then machined into small specimens in sizes of 10 mm × 10 mm × 20 mm. The tribological tests were conducted on 10 mm × 10 mm apparent contact areas.

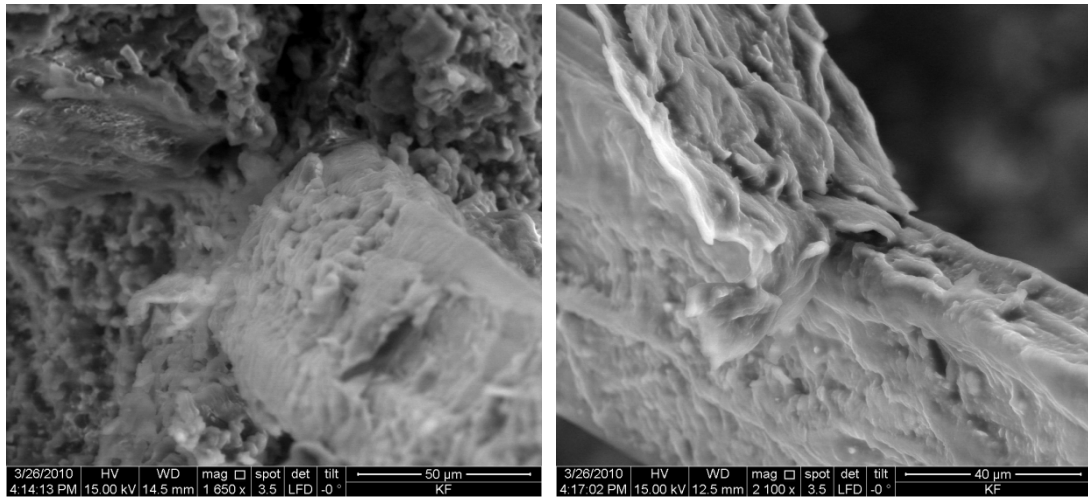
3.3 MECHANICAL PROPERTIES OF THE COMPOSITES

3.3.1 Interfacial Adhesion and Tensile Properties

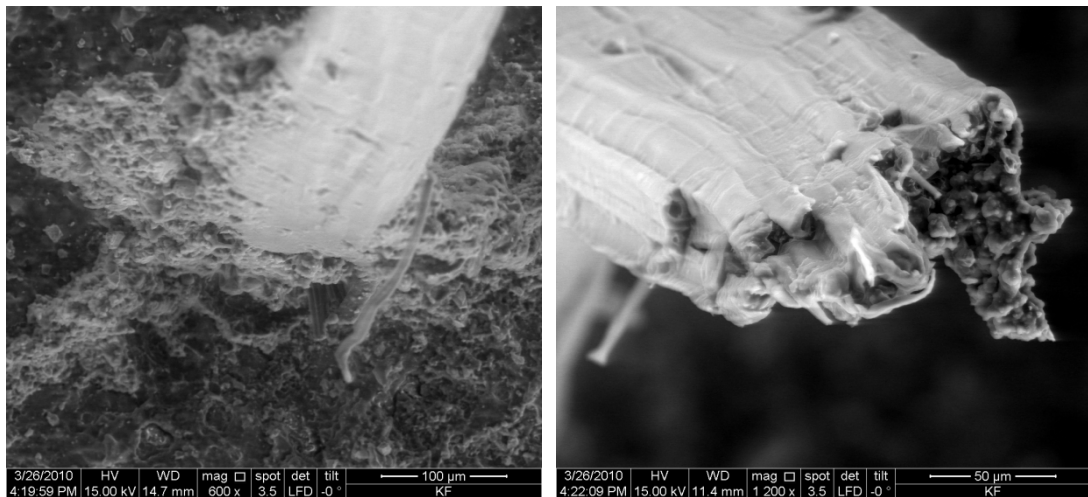
The pull-out results for both untreated and treated kenaf fibres embedded in the epoxy matrix revealed good interfacial adhesion of both the untreated and treated fibres and the matrix. In other words, during the pull-out process breakage occurred in the fibre, rather than it being pulled out. This is a promising result compared to other published work on oil palm (Jawaid, Abdul Khalil & Abu Bakar 2011; Yousif 2010), sugarcane (Vallejos et al. 2011; El-Tayeb, 2008) and jute (Mishra & Biswas 2013; Jawaid et al. 2011) fibres, which demonstrate poor interfacial properties with different synthetic matrices. **Figure 3.6** presents the micrographs of the pull-out samples for both untreated and treated kenaf fibres.

For both fibres, there were high adhesion signs on the fibres within the epoxy matrix, since there was no evidence of pull-out during the experiments. However, the untreated surface of the kenaf fibres was covered with a thin layer, which underwent either a peel-off process or tearing during the experiments. Such layers are found in

most of the natural fibres studied to date, including oil palm and sugarcane. NaOH treatment assisted in removing this layer and cleaned the fibre surface, which resulted in high bonding between the fibre and the matrix. On the other hand, after these experiments the maximum stress the fibres were subjected to were compared with the ultimate tensile strength of the fibres, and these were found to very close, at around 100 MPa and 150 MPa for the untreated and treated kenaf fibres, respectively. Some of the mechanical properties of these materials are summarised in **Table 3.1**. The addition of the kenaf fibres greatly enhanced the tensile strength of the epoxy composites, particularly when the kenaf fibres were chemically treated with NaOH. The ductility of the epoxy was also improved, and this indicates that the composites have ductile behaviour compared to the NE. On the other hand, there was a reduction of the modulus of elasticity.



a) Untreated kenaf fibre after the pull-out process



b) Treated kenaf fibre after the pull-out process

Figure 3.6 Micrographs of the pull-out samples for treated and untreated kenaf fibres embedded in epoxy matrix

Table 3.1 Mechanical properties of the prepared composites

Property	NE	Untreated KFRE	Treated KFRE
Fibre volume fraction (per cent)	0	≈48	≈48
Density (kg/m ³)	1,100±2	745±5	850±2
Modulus of elasticity (GPa)	20±2	12±2	14.5±2
Tensile strength (MPa)	78±5	97±7	135±2
Elongation (per cent)	3.5 ±0.2	9.2±3	6.5±2
Thermal conductivity (W/m*K)	0.17	0.09	0.11

3.3.2 Flexural Properties

The flexural results are summarised in **Figure 3.7 a-c**, showing the average strength, strain and flexural modulus associated with the maximum and minimum values of the readings. The figure clearly shows the significant improvement in the flexural strength and modulus of epoxy when it is reinforced with kenaf fibres. 20 and 36 per cent increases in the flexural strength of epoxy were achieved with the addition of untreated and treated KFRE, respectively. Moreover, the flexural modulus of the epoxy was improved by approximately 67 per cent after the addition of untreated KFRE and 74 per cent after the addition of treated KFRE. In addition, it appears that treated kenaf fibres have a greater effect on the flexural properties of the epoxy composite compared to untreated fibres. This is basically due to the enhancement of the surface characteristics of the kenaf fibres by NaOH treatment (**Figure 3.3c**). In the treated fibres, there was no debonding of fibres from the matrix; i.e., they show high interfacial adhesion.

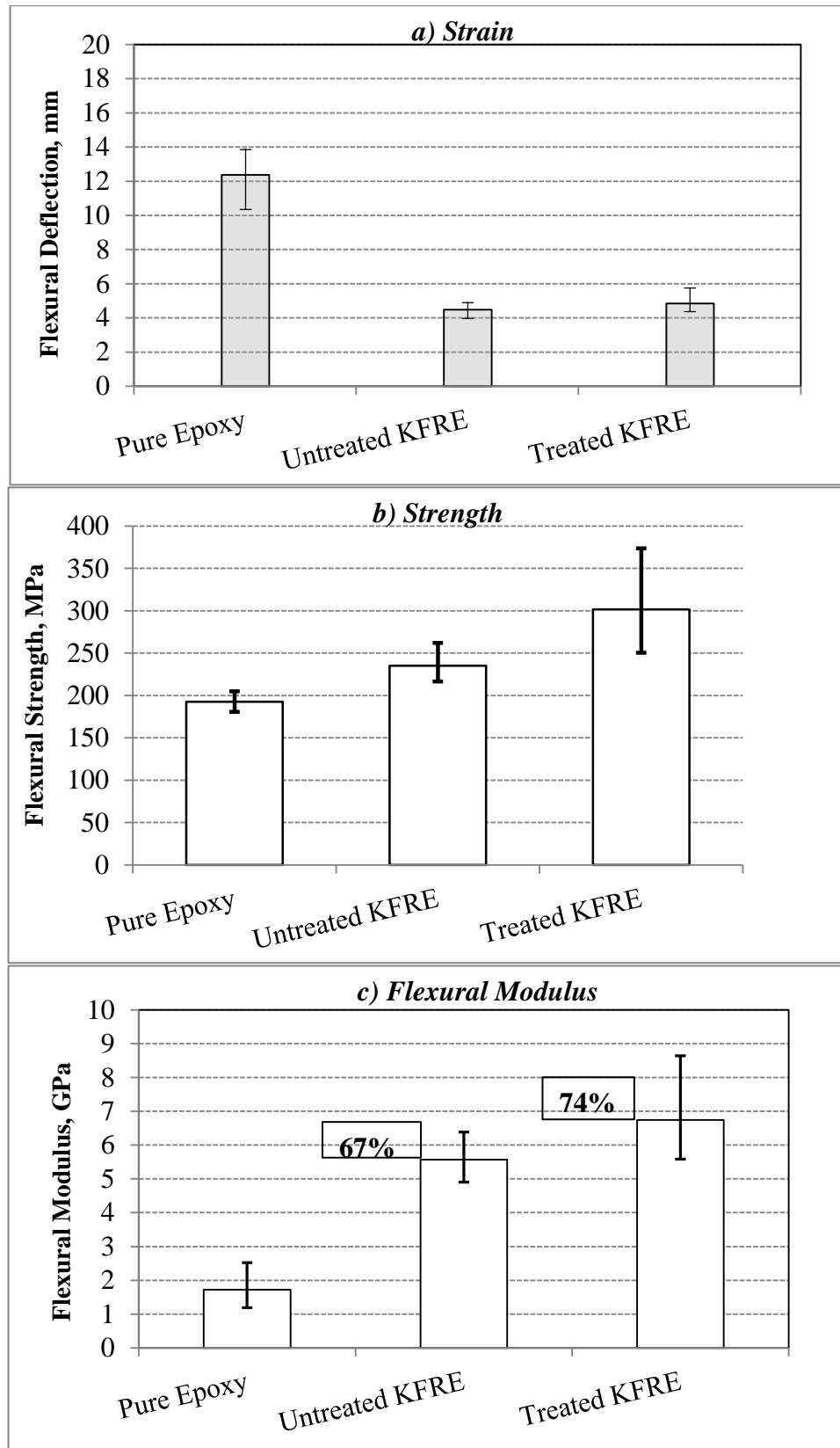


Figure 3.7 Bar charts of flexural properties of untreated KFRE and treated KFRE

This is due to two reasons. First, the rough surface achieved by removing the waxy layer on the fibre surface via NaOH treatment enhances bonding between the fibre and the matrix. Second, the low porosity of the treated composite is thought to also improve adhesion. This was confirmed in the micrographs of the fractured samples shown in **Figures 3.8** and **3.9**. In the case of the untreated fibres, the outer layer of the fibres prevents the epoxy entering the fibre bundles during the fabrication process. This weakens the interfacial adhesion of the fibre matrix. Removing of outer layer by treating the fibres allows the epoxy to enter the fibre bundle during the fabrication process, which locks the fibres in the composite and prevents debonding.

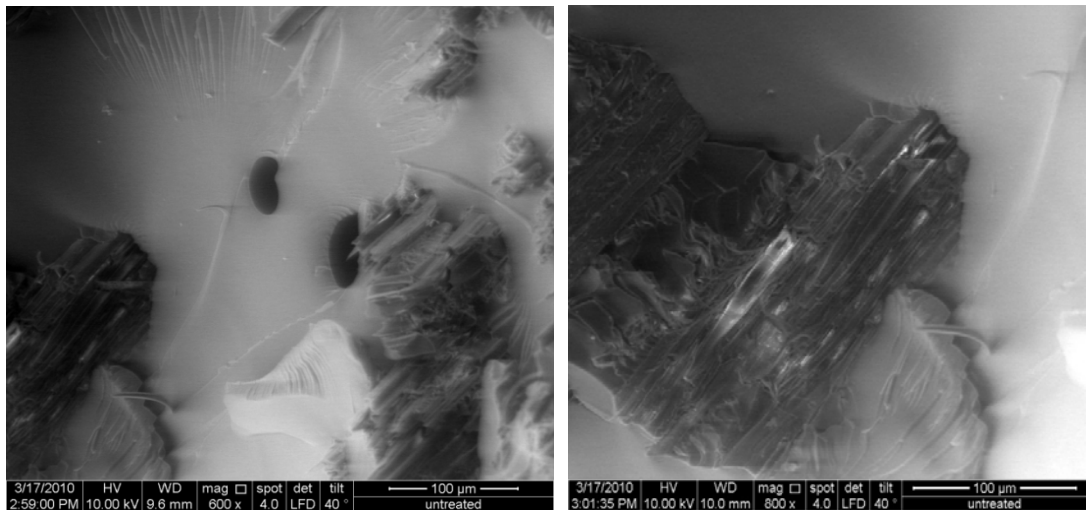


Figure 3.8 SEM micrographs of untreated KFRE after testing

On the other hand, debonding can be seen on the fracture surface of the untreated KFRE (**Figure 3.8**), which is the main reason for the poorer performance of the untreated KFRE. In contrast, the micrographs of the treated KFRE (**Figure 3.9**) show no debonding, detachment or pull-out on the composite surface. In addition, evidence

for epoxy entering the treated fibre bundles is obvious in **Figure 3.9c**, where the high magnification micrographs show epoxy debris between the fine fibres in the bundles, indicating that the epoxy has entered the fibres during fabrication process. This was absent in the case of untreated KFRE. Taken together, these results may explain the experimental results.

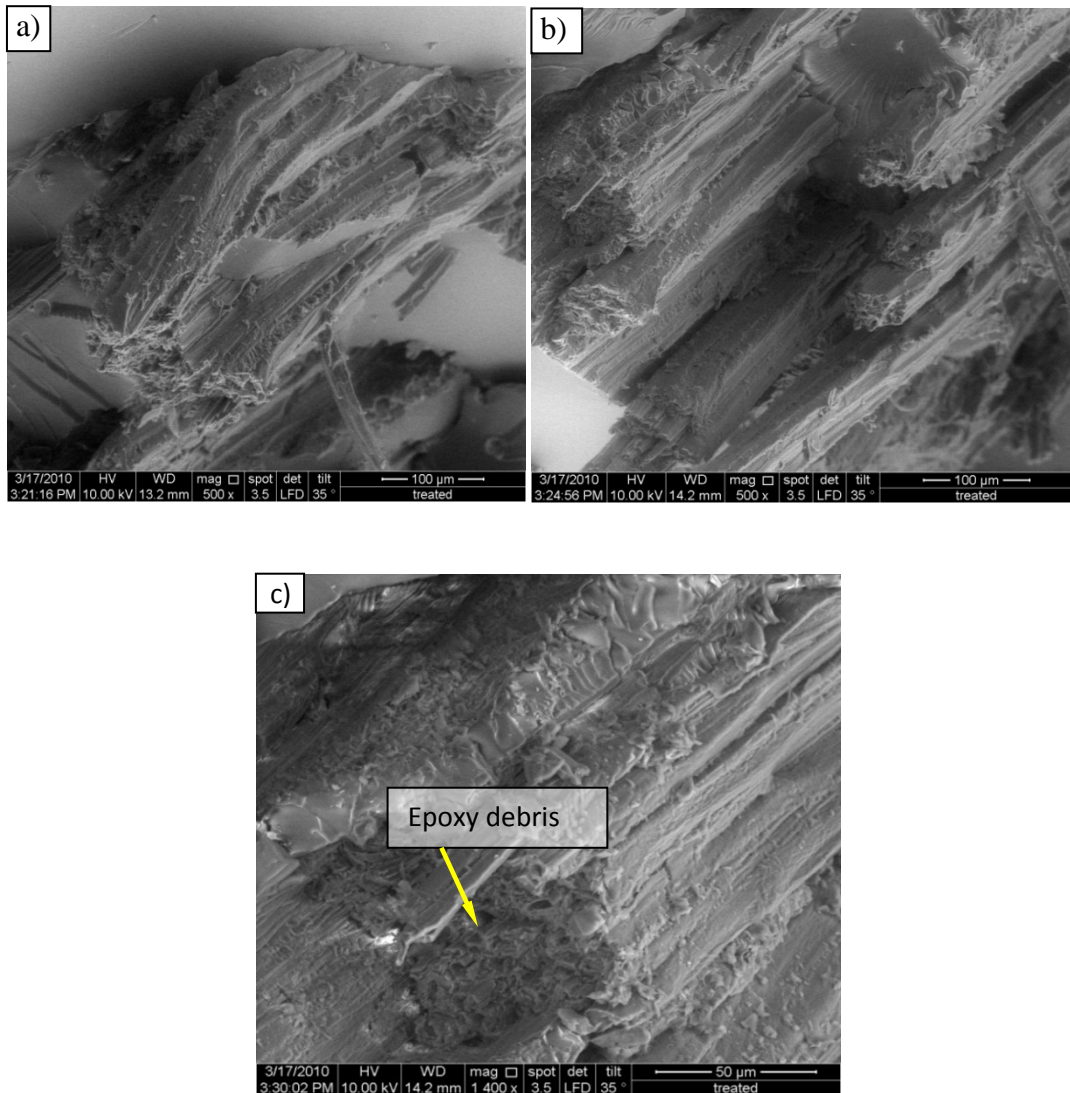


Figure 3.9 SEM micrographs of treated KFRE after testing

3.4 TRIBOLOGICAL EXPERIMENTS

Since the treated kenaf fibres exhibit better mechanical properties than the untreated ones, the treated KFRE composite was tested under tribological loading conditions and its performance compared with NE. Three different orientations of fibres with respect to the sliding direction of the counterface were considered: P-O, AP-O and N-O, respectively. A schematic drawing illustrating those orientations is presented in

Figure 3.10.

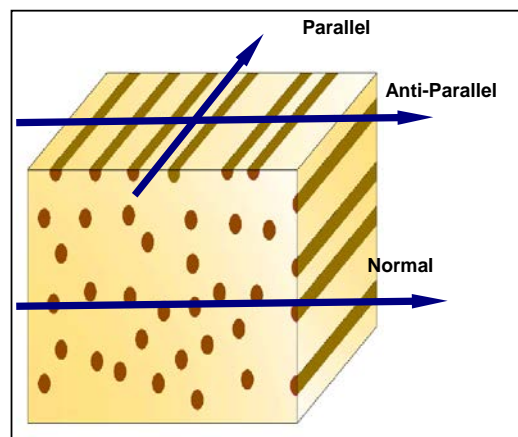


Figure 3.10 Fibre orientations with respect to the sliding direction

3.4.1 Dry/Wet Adhesive Wear Experiments

A BOD machine was used for these experiments, and is shown in **Figure 3.11**. The composite surface specimens (10 mm × 10 mm × 20 mm) were rubbed against a stainless steel (AISI 304, hardness=1,250 HB, Ra=0.1 μm) counterface under dry/wet contact conditions. For intimate contact between the specimen and the stainless steel counterface, the specimen's contact surface was polished by abrasive paper (Sic G2000) and then cleaned with a dry soft brush. The roughness of the

composite surface varied in each orientation. In the parallel and anti-parallel orientations, the average roughness of five measurements in different regions was around $0.30\ \mu\text{m}$ (**Figure 3.12a**). Meanwhile, in the N-O, the composite roughness values were an average of approximately $0.70\ \mu\text{m}$ (**Figure 3.12b**).

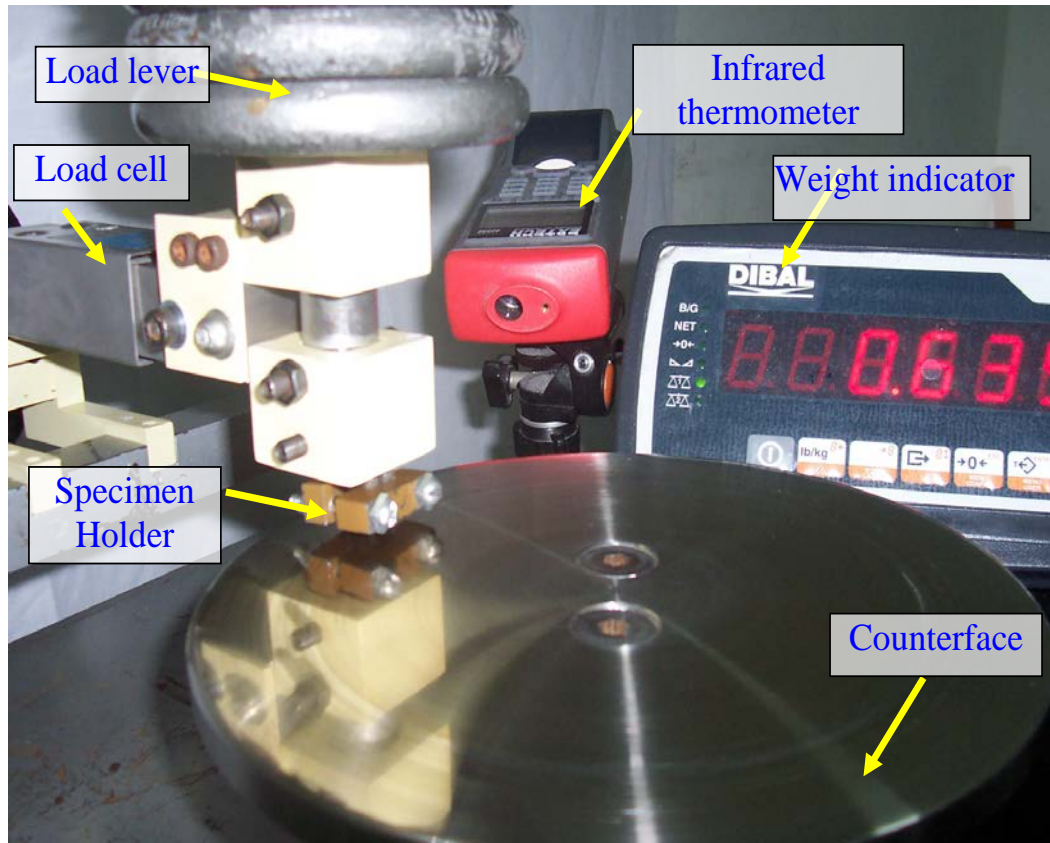


Figure 3.11 The BOD machine working under dry contact conditions

Before and after the test, the specimens were dried in an oven at $40\ ^\circ\text{C}$ for 12 hours.

A Setra balance ($\pm 0.1\ \text{mg}$) was used to determine the weights of the specimens. The specific wear rate (W_s) at each operating condition was determined using

Equation 3.1:

$$W_s = \frac{\Delta W / \rho}{L \times D} \quad (3.1)$$

Where:

W_s : Specific wear rate (mm^3/Nm)

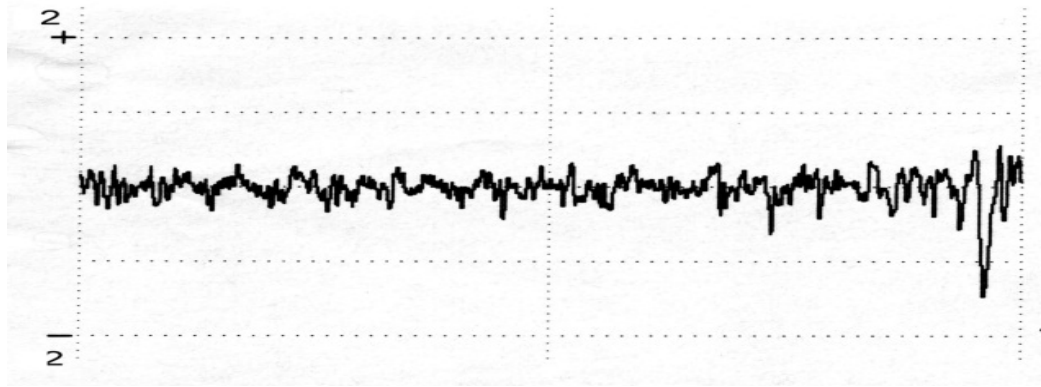
ΔW : Weight loss (mg)

ρ : Density (kg/m^3)

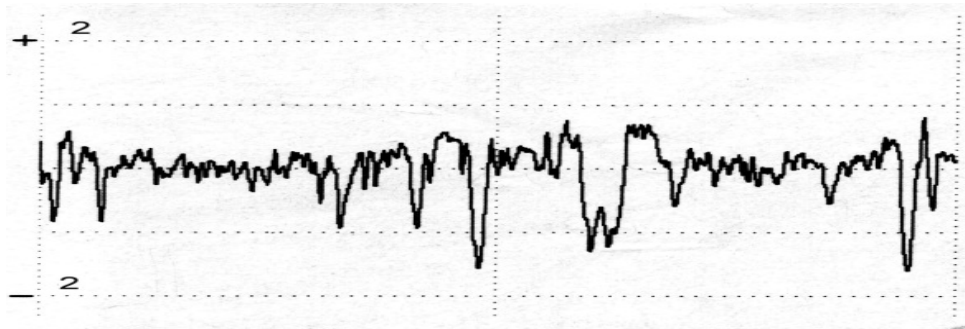
L : Applied load (N)

D : Sliding distance (m)

During the tests, frictional force was measured by a load cell, which was fixed at the middle of the lever that applied the loads.



a) P-O and AP-O, $R_a=0.336 \mu\text{m}$



b) N-O, $R_a=0.72 \mu\text{m}$

Fig. 3.12 Sample of the roughness profile of the composite surfaces in different orientations

For the wet adhesive wear test, tap water was supplied to the interface via a pump with flow rate of 0.2 l/min (**Figure 3.13**). After each test, the worn surface was coated with a thin layer of gold using an ion sputtering device (JEOL, JFC-1600) and a scanning electron microscope (JEOL, JSM 840) was used to observe the surface. Each tribological test was repeated three times and the average of the measurements were determined.

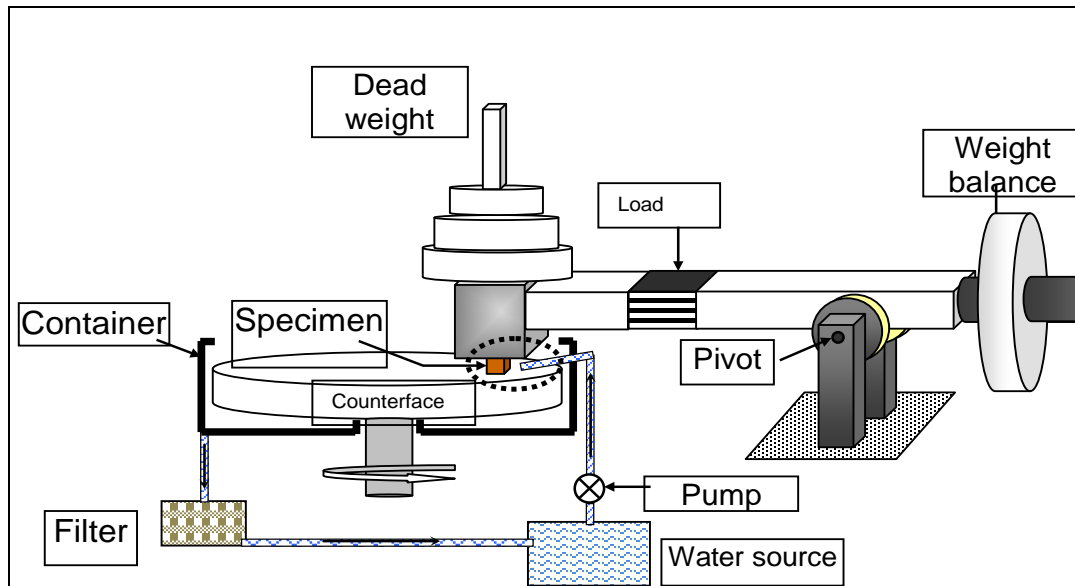


Figure 3.13 The BOD tribological machine operated under wet contact conditions

During the dry adhesive wear tests, an infrared thermometer (Extech 42580) was used to measure the initial interface temperature and calibration was performed to determine the interface temperature. In the calibration process, the infrared thermometer was pointed at the midpoint of interface between the specimen and the stainless steel counterface during the tests. The calibration of the temperature was carried out under stationary conditions. The counterface was heated using an external heat source. While the counterface was heated, a thermocouple was placed between the specimen and the counterface. The temperatures measured by both thermometers (infrared and thermocouple) were recorded simultaneously until the interface temperature reached approximately 80 °C. This process was repeated three times and the averages were determined. The measured temperatures (thermocouple) were plotted against each other and the fit line was determined using the calibration equation (**Figure 3.14**).

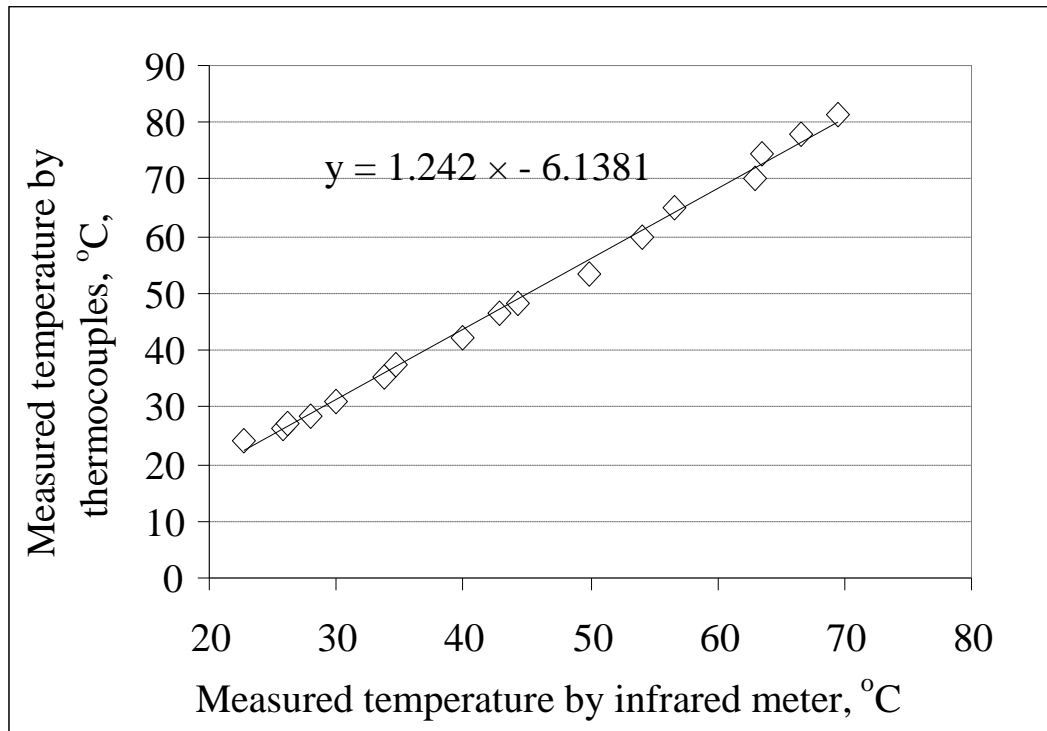


Figure 3.14 Calibration chart for measuring interface temperature

3.4.2 Three-body Abrasion Tests

As required for the standard test (the ASTM B 611), the prepared composite was machined into small specimens sized 20 mm × 25 mm × 58 mm and the tribological tests were conducted on 25 mm × 58 mm apparent contact areas. The high stress 3B-A wear experiments were conducted using an ASTM B 611 machine as shown in **Figure 3.15**.

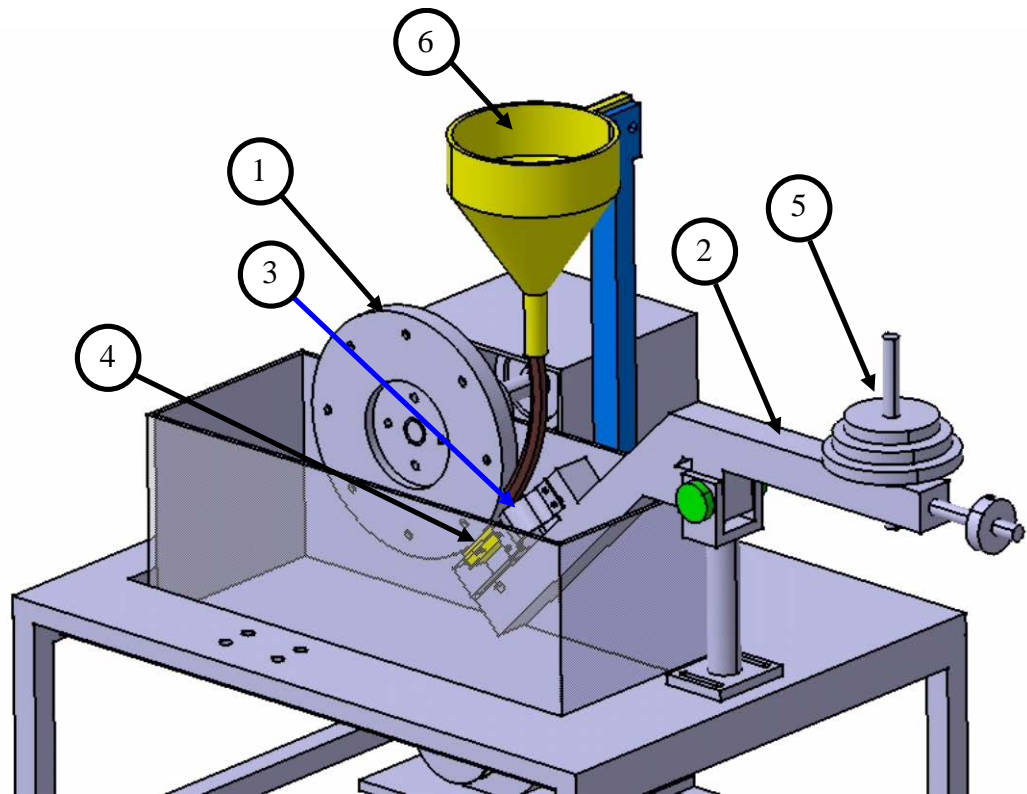
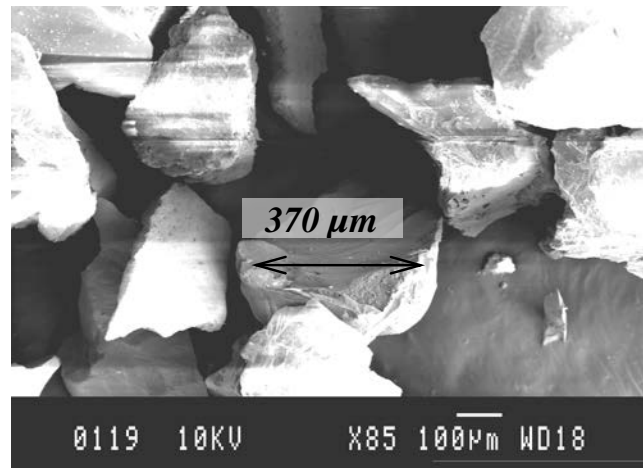


Figure 3.15 3B-A set-up (Yousif 2013)

*1-Counterface, 2-BOR load lever, 3-Load cells, 4-Specimens,
5-Dead weights, 6-Sand hopper*

The tests were performed against a stainless steel (AISI 304) counterface. The sand was collected from a beach in Melaka State, Malaysia. The sand particles were sieved (in the size ranges of 370–390 μm , 650–750 μm and 1,200–1,400 μm), cleaned, washed and then dried in an oven for 24 hours at 40 °C (**Figure 3.16**). The sand flow was fixed at a rate of 4.5 g/s. The 3B-A tests were conducted at a rotational speed of 100 rpm, corresponding to 1.152 m/s for 300 s at different applied loads (5–20 N).



a) *Small size*

b) *Intermediate*

c) *Large size*

Figure 3.16 Micrographs of three different sizes of sand particles before the tests

Before and after the tests, the prepared samples were cleaned with a dry soft brush. A Setra balance (± 0.1 mg) was used to determine the weights of the specimens before and after each test and then the weight loss was calculated. The wear rate under each operating condition was determined using **Equation 3.2:**

$$W_r = \frac{\Delta W}{N} \quad (3.2)$$

Where:

W_r : Wear rate (mm^3/Nm)

ΔW : Weight loss (mg)

N : Applied load (N)

During the tests, the frictional force was measured by a load cell, which was fixed in the middle of the lever. The composite surface morphology was studied using a scanning electron microscope (JEOL, JSM 840). Before using the microscope, the composite surfaces were coated with a thin layer of gold using an ion sputtering device (JEOL, JFC-1600). Each tribological test was repeated three times and the average of the measurements were determined.

3.5 DEVELOPMENT OF THE ARTIFICIAL NEURAL NETWORK MODEL

The ANN modelling technique was employed in the current study to predict the influence of applied load, sliding distance and sliding velocity on the frictional behaviour of the KFRE composite in N-O. The experimental data was used for developing, training and verifying the ANN models. The data was divided into two groups: training data and verification data, with 70 per cent of the 1,095 frictional values being used for training, while the remaining 30 per cent of data were reserved for verification purposes. Matlab (R2010b) was used in developing, training and simulating the models. Simulations were performed using a multi-layer perception network for non-linear mapping between the input and output variables. Several architectures were evaluated and trained to obtain the optimum performance for the model. A back propagation algorithm was employed for training all ANN models, as recommended by authors such as Nasir et al. (2010), Zhang and Friedrich (2003), Zhang, Friedrich and Velten (2002) and Ray and Roy Chowdhury (2009). This algorithm changes each weight of the network based on its localised portion of the input value and the error. These changes must be relative (a scaled version) to the product of the input and error quantities.

3.5.1 The Optimum Learning Rule and Transfer Function

In the current study, there are three operating parameter inputs (applied load, sliding distance and sliding velocity) and one output (friction coefficient), as shown in **Figure 3.17**. The output layer consists of one neuron, while the input layer has three

neurons for each individual model. The number of neurons in the hidden layer(s) can be adjusted to suit the complexity of the problem and the dataset. In the initial stage of developing the ANN model, one hidden layer with a fixed number of neurons was set up. The activation function for the hidden layers was varied for each test to find the optimum function for these experimental sets, as shown in **Figure 3.18**. A scaled conjugate gradient (SCG) method and the Levenberg-Marquardt (LM) algorithm were used as learning rules. There are several types of transfer function available; for example, satlins, or symmetric saturation linear transfer functions; purelin, or linear transfer functions; Soft Max (SM) and Logsig, or log-sigmoid transfer functions.

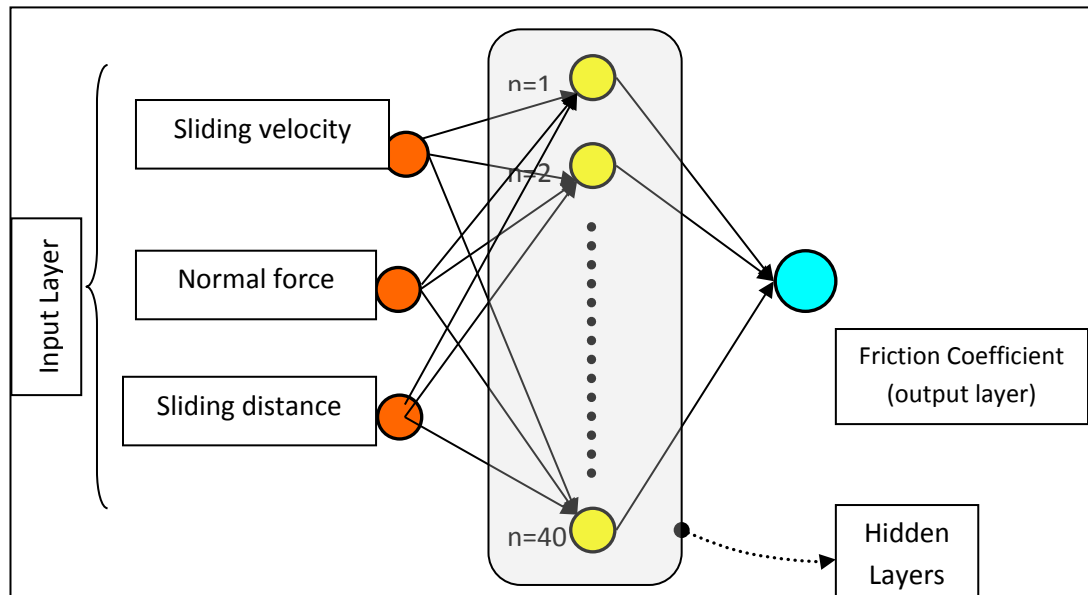


Figure 3.17 ANN configuration for prediction of the friction coefficient

The average of the error percentage of the different models developed with different learning and transfer functions are presented in **Figure 3.18** for two hidden layer models with different functions. **Figure 3.18** shows that the optimum functions are the SCG for the learning rule and the log-sigmoid transfer function. A total of 1,000

epochs and a mean square error of $1e^{-4}$ were used to measure the model quality by simulating the network size and training performance. According to Akaike's theory (Akaike 1974), the best performance of an ANN is determined by the smallest error. Based on this, the SCG learning rule and the log-sigmoid transfer function provided the best ANN model for this study.

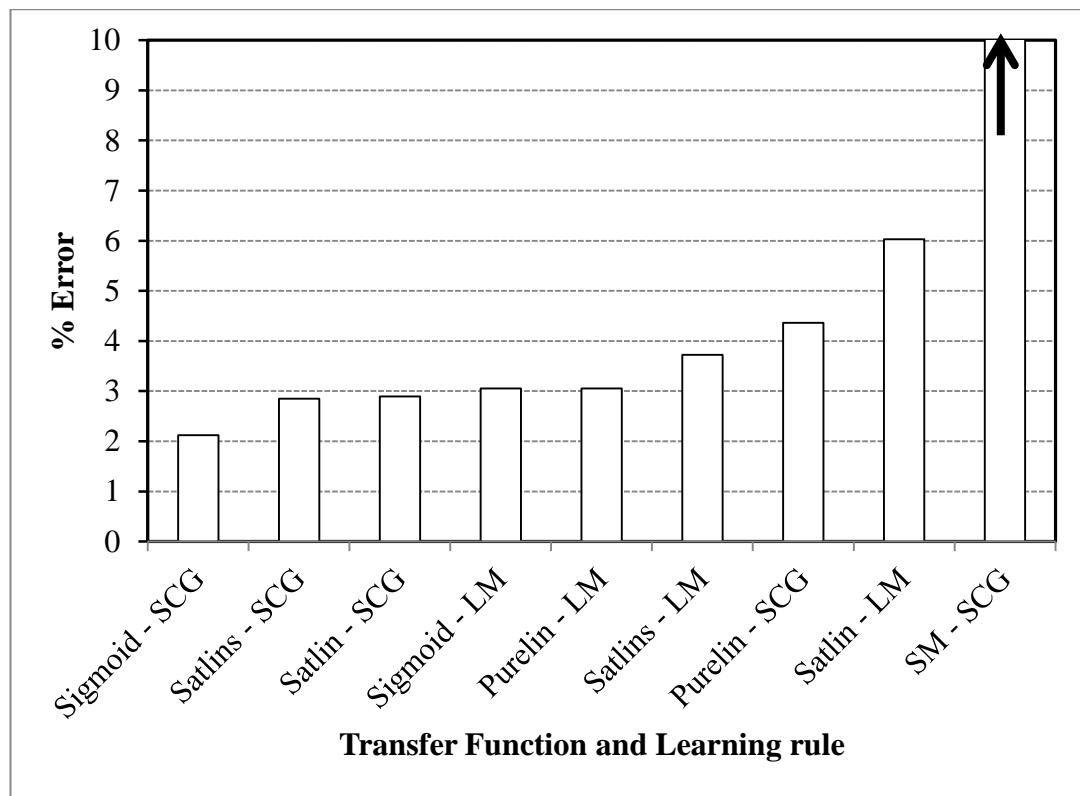


Figure 3.18 Transfer function and learning rules versus error percentage of ANN models

3.5.2 Optimum Number of Neurons

Based on **Figure 3.18**, the SCG learning rule and log-sigmoid transfer function were used for developing the ANN model for the prediction of the friction coefficient. To study the influence of the number of neurons in the first hidden layer, the error percentage versus the number of the neurons was obtained and these are represented in **Figure 3.19**. For this study, it seems that there is an optimum number of neuron that produces fewer errors compared to others. In this study, 50 neurons in the hidden layer provided the least error, which indicates better prediction performance since the error was about 0.6 per cent. The final optimum model consisted of 50 neurons in the first hidden layer. This model will be verified and used to predict the friction coefficient at different operating parameters than those used in the input data. The details of the steps involved in developing the ANN models are given in **Appendix A**.

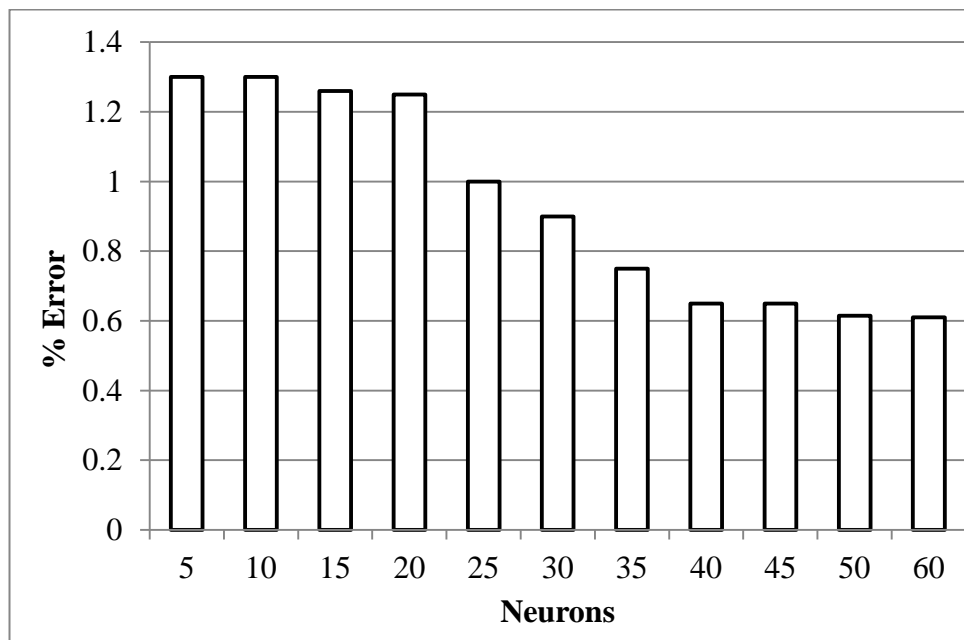


Figure 3.19 Number of neurons versus error percentage of ANN models

These steps are summarised in the flow chart in **Figure 3.20**, which shows the general procedure for developing a successful ANN model. Such a flow chart has not been proposed in the literature (Gyurova & Friedrich 2011; Aleksendric 2010; Zhang, Friedrich & Velten 2002), where trial and error has generally been used (Aleksendric 2010). To gain a comprehensive overview of all the possibilities in developing an ANN model, it is recommended to follow the steps presented in **Figure 3.20**. This will assist in reducing error, selecting a suitable training function and generating good predictions.

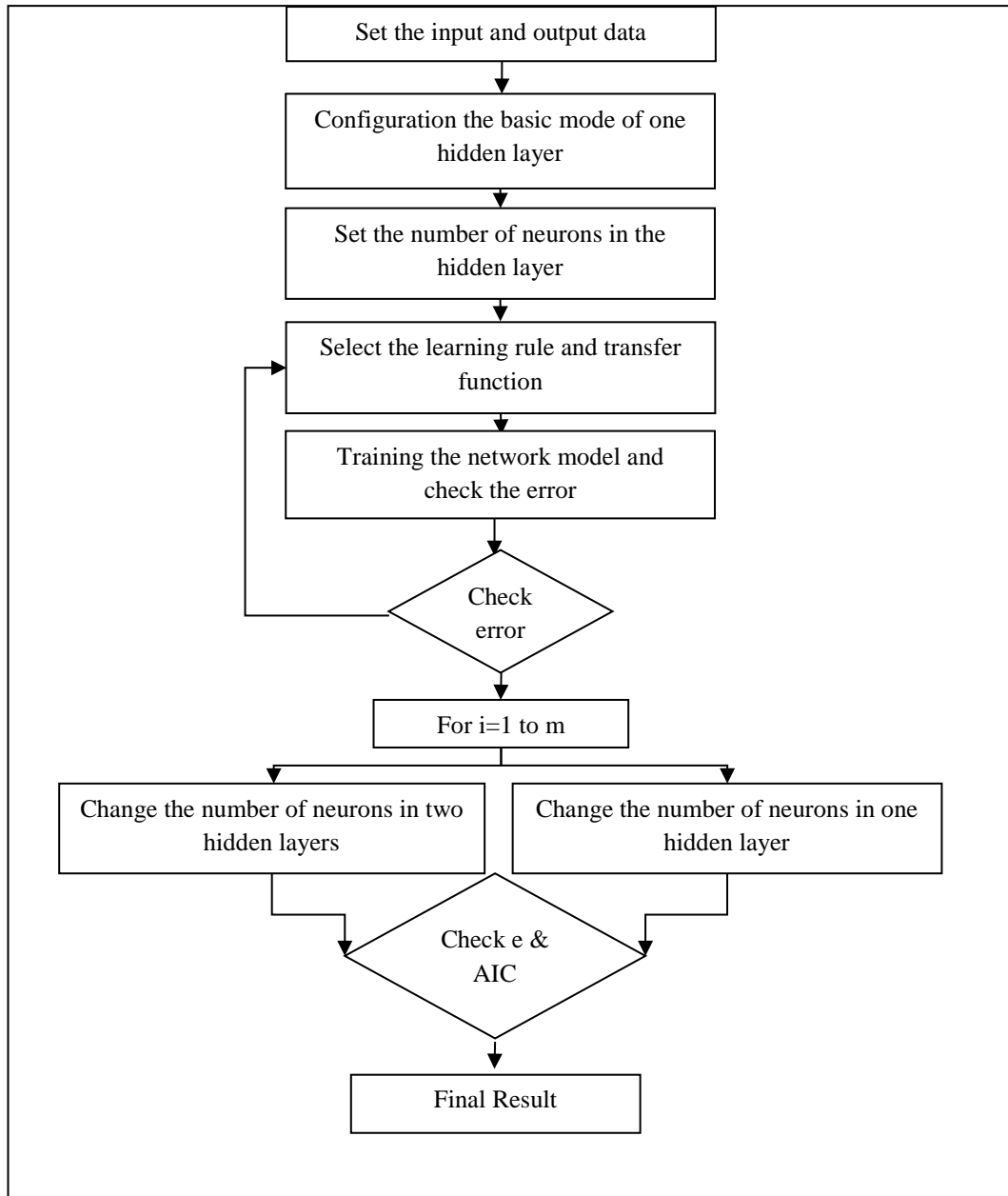


Figure 3.20 Flow chart representing the procedure for the development and selection of a suitable ANN model configuration

CHAPTER 4: ADHESIVE WEAR AND FRICTIONAL BEHAVIOUR OF THE COMPOSITES

4.1 INTRODUCTION

This chapter presents the adhesive wear results of the KFRE composites. The sliding wear and frictional behaviour of the composites were studied against a polished stainless steel counterface using a BOD machine set at different applied loads, sliding distances and sliding velocities. The effect of the fibre orientations (P-O, AP-O, N-O) with respect to the sliding direction was considered, and the morphology of the worn surfaces of the composite was studied using a scanning electron microscope and the surface roughness determined. The averages of these measurements were determined and are presented in this Chapter. The standard deviation of the results for all materials, at all sliding distances, sliding velocities and loads is listed in **Table 4.1**.

Table 4.1 Typical experimental values of the standard deviation of W_s and the friction coefficient

	W_s	Friction coefficient
NE	± 0.30	± 0.11
KFRE (P-O)	± 0.33	± 0.21
KFRE (AP-O)	± 0.46	± 0.28
KFRE (N-O)	± 0.15	± 0.10

4.2 DRY ADHESIVE WEAR AND FRICTIONAL BEHAVIOUR

The W_s values of the NE (NP) and KFRE composites (in three different orientations: P-O, AP-O and N-O) at different operating parameters are presented in **Figures 4.1–4.10**, along with micrographs of the worn surfaces.

4.2.1 Dry Adhesive Wear Behaviour

4.2.1.1 Wear Behaviour Under Different Sliding Distances

The adhesive wear behaviour of the composite materials at various sliding distances under a 50 N applied load is presented in **Figure 4.1**. In general, there was a fluctuation in the W_s values of all the materials in the first stage of sliding, which represented the running-in period. At this stage of rubbing, the asperities of both surfaces are at the initial contact stage where there is relatively high removal of materials for intimate contact between the asperities. This is a well-known phenomenon in the dry adhesive wear behaviour of most composites (Jeantrakull et al. 2012; Basavarajappa & Ellangovan 2012). Other than the sudden dip and boost at sliding distances of 1.5 and 2 km respectively, the W_s values displayed a relatively steady state for all the materials. From **Figure 4.1**, it appears that after a sliding distance of around 3–4 km, a complete adaption between the asperities in contact was achieved. At the steady state, there may be a film transfer from the soft part (resin) to the hard counterface (stainless steel), which assists in steadying the wear behaviour and reduces the W_s . NE showed the highest W_s at all sliding distances. The addition of the kenaf fibres to the epoxy reduced the W_s at all fibre orientations, as shown in **Figure 4.1**. Moreover, orienting the fibres normally to the counterface

(N-O) resulted in the lowest W_s value; i.e., the composite in N-O possessed the highest wear resistance. In summary, an approximately 83 per cent reduction in W_s was achieved when kenaf fibres were used as a reinforcement. This reduction in W_s may be attributed to a number of reasons, including mechanical and/or thermo-mechanical reduction in the loading at the interface. This will be explained in the following sections. In term of specific wear trends, similar trends have been reported with different materials such as glass fibre-polyester (Yousif 2013a), betelnut-polyester (Nirmal et al. 2010b) and jute-epoxy (Mishra & Biswas 2013).

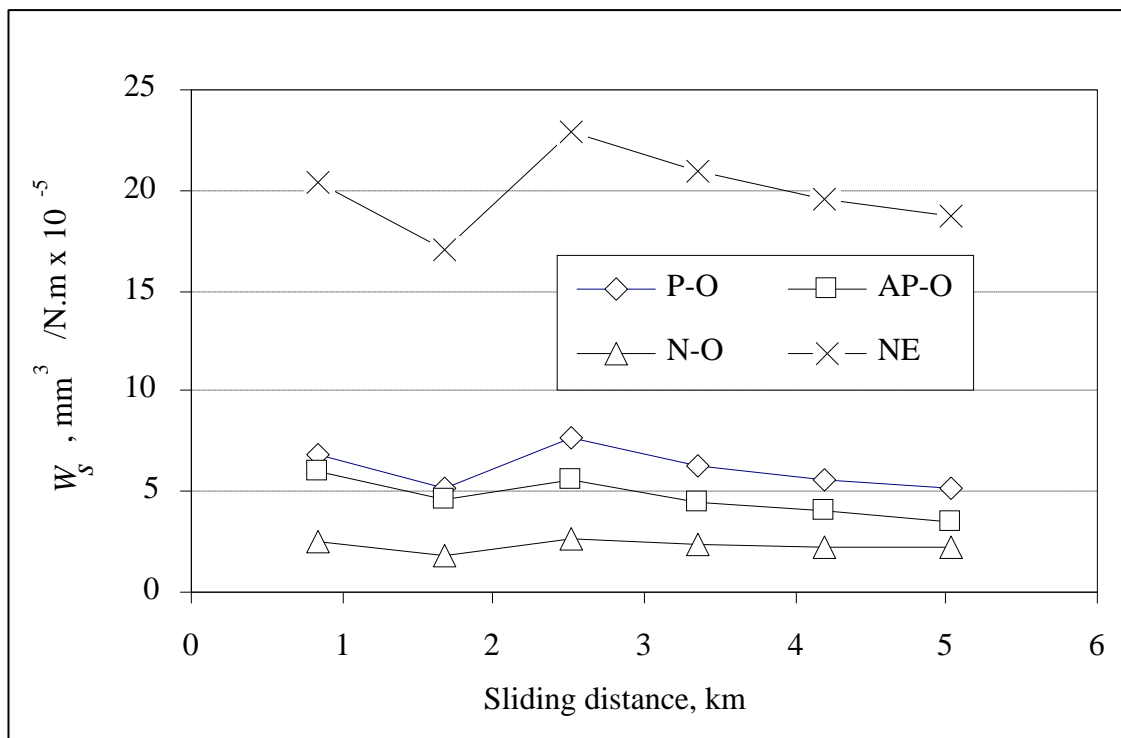


Figure 4.1 W_s versus sliding distance at a 50 N applied load

4.2.1.2 Dry Adhesive Wear At Different Applied Loads

To understand the influence of the applied load on the wear behaviour of the composites, W_s was determined under different applied loads. **Figure 4.2** illustrates the trend and variation of the W_s value of NE and its composites against applied loads of 30–100 N at a sliding velocity of 2.8 m/s. There was an increase in the W_s values of NE and the KFRE composites (in AP-O and N-O) at the lower range of applied load (30–50 N). An increase in the applied load of more than 50 N had no significant effect on the W_s values, especially for the KFRE composite in N-O. Moreover, the composites in all three orientations had better wear performances than NE. Thus, kenaf fibres assist in reducing the W_s of the epoxy, especially when the fibres are oriented in N-O. In this orientation the wear performance of the NE was enhanced by about 85 per cent. A similar finding was reported in the previous section, in which the KFRE (N-O) showed better performance compared to other materials at different sliding distances.

The applied load has been reported to have no influence on the adhesive wear behaviour of betelnut fibre reinforced polyester composites (Nirmal et al. 2010b). Moreover, the W_s of synthetic fibre reinforced thermoset polymers such as carbon fibre-polyetherimide (Bijwe & Rattan 2007), glass fibre-polyester (Yousif 2013a) and glass-epoxy (Arhaim, Shalwan & Yousif 2013) has been demonstrated to exhibit similar trends at different applied loads, especially at higher ranges of applied loads. The reason for these findings may be that less modification occurs on the contact surfaces when the applied load is increased; in other words, the applied load has little

influence on the material removal rate. The stability of the film transfer onto the counterface and the smaller change in the roughness value of this film may be the main reason for this finding. Further explanation of this hypothesis will be given later in this chapter, with the assistance of roughness profile and SEM data.

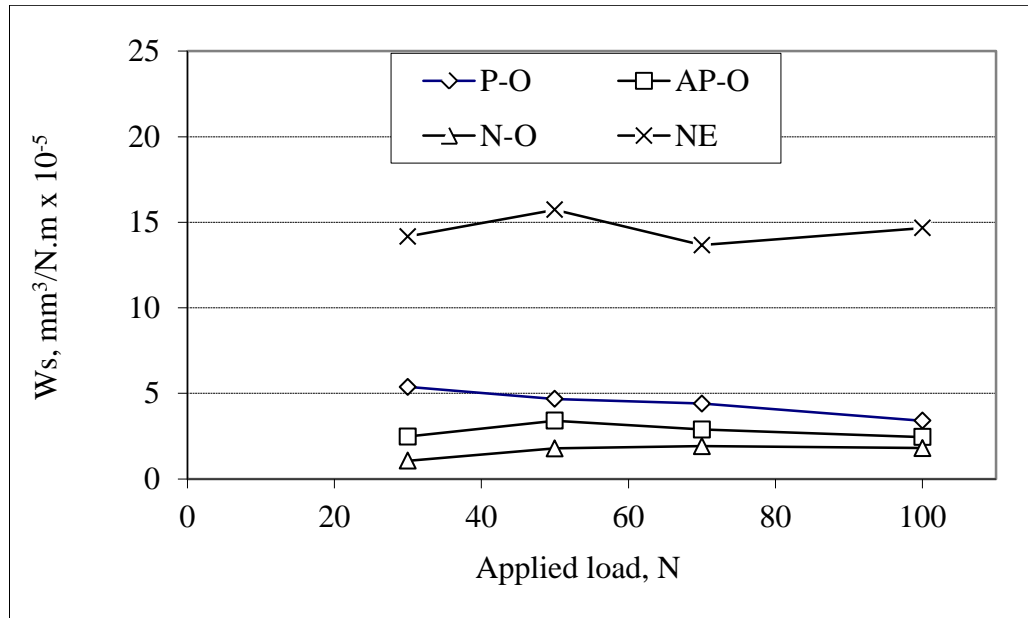


Figure 4.2 W_s versus applied load after sliding distance of 3.36 km at a sliding velocity of 2.8 m/s

4.2.1.3 Dry Adhesive Wear At Different Sliding Velocities

The W_s values of the KFRE composites and NE were determined at different sliding velocities with a 50 N applied load over a 5 km sliding distance. The influence of sliding velocity on the wear performance of the composite is presented in **Figure 4.3**. The figure shows that sliding velocity did not greatly affect the W_s of the KFRE composites in all orientations; i.e., the wear behaviour of the composites was not dependent on the sliding velocity. However, NE showed an increase in W_s when the sliding velocity increased. Similar to the previous results, the KFRE composite in N-

O showed better wear performance at all sliding velocities, followed by the composites in AP-O and P-O. In most reported studies of synthetic fibre-polymer composites, such as glass-epoxy (Arhaim, Shalwan & Yousif 2013), glass-polyester (El-Tayeb & Yousif, 2005; El-Tayeb, Yousif & Yap 2006) and carbon-polyetherimide (Tiwari, Bijwe & Panier 2011), an increase in either the applied load and/or the sliding velocity leads to a high W_s . The current findings show that sliding velocity has no influence on the wear behaviour of kenaf-epoxy composites in any of the selected orientations. This could be due to the fact that kenaf fibres are less abrasive than the synthetic fibres, especially glass fibres, which in turn reduces their effect on the stability of the contacted surfaces. In the case of the glass fibre-polyester composites, there is a significant increase in the roughness of the counterface at higher sliding velocities, which leads to the low wear resistance of the composites at the higher range of sliding velocities (El-Tayeb, Yousif and Yap 2006). This argument will be supported with evidence from the roughness profile data presented later in this chapter.

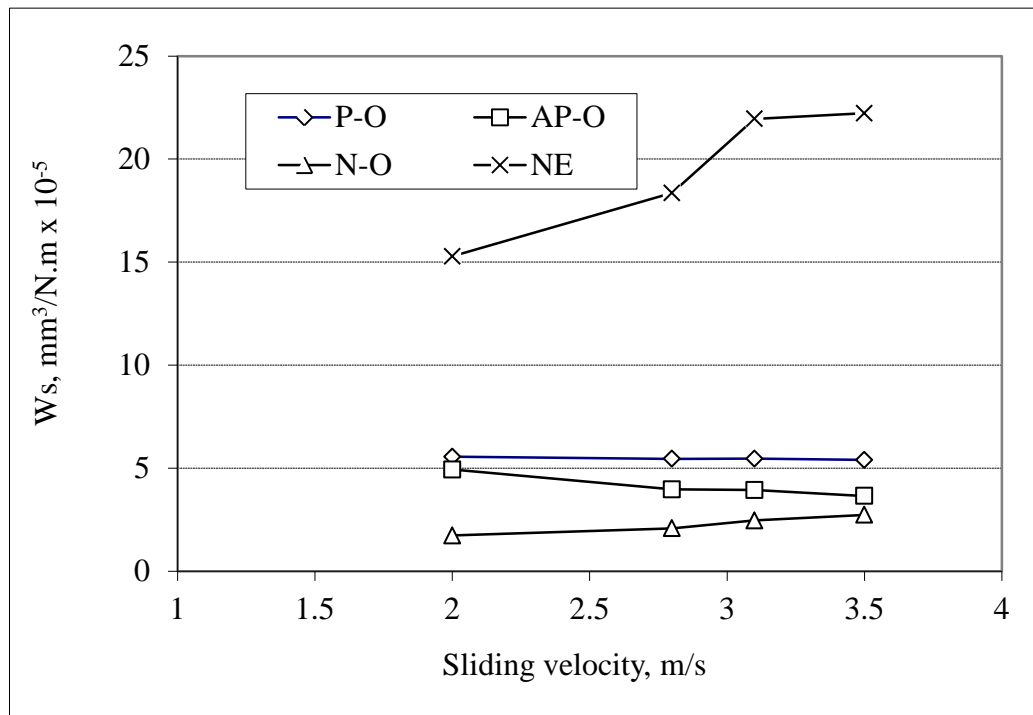


Figure 4.3 Ws versus sliding velocity at 50 N applied load

4.2.2 Dry Adhesive Frictional Behaviour of the Composites

The frictional force was captured during each experiment for all operating parameters. Due to the large volume of data collected, it was summarised and is presented in this section. The friction coefficients versus the sliding distances at different applied loads and velocities for the NE and the KFRE composites were developed and a sample of the frictional data is given in **Figure 4.4**. The figure displays the friction coefficient against the sliding distance for the KFRE composite at N-O under different applied loads at a sliding velocity of 2.8 m/s. All materials showed similar frictional behaviour at all the operating parameters tested; i.e., the frictional coefficient was high at the start of the sliding (running-in) and then reached a steady state after a sliding distance of approximately 4 km. This behaviour is

common in both natural fibre-polymer and synthetic fibre-polymer composites, since there is a high shear force in the contact zone in the first stage of the adoption process between the asperities in contact. After this stage, a steady state friction coefficient is achieved if there is no change in the contacted surfaces. For synthetic fibre-polymer composites, stability of the friction coefficient has been reported in studies of carbon-epoxy (Zhou, Sun & Wang 2009), glass or a carbon-aramid hybrid weave-epoxy and three-dimensional braided carbon fibre-epoxy (Wan et al. 2006). The instability of the friction coefficient of the synthetic fibre-polymer composites is mainly due to the modifications that occur on the track surface of the counterface (Yousif 2013a).

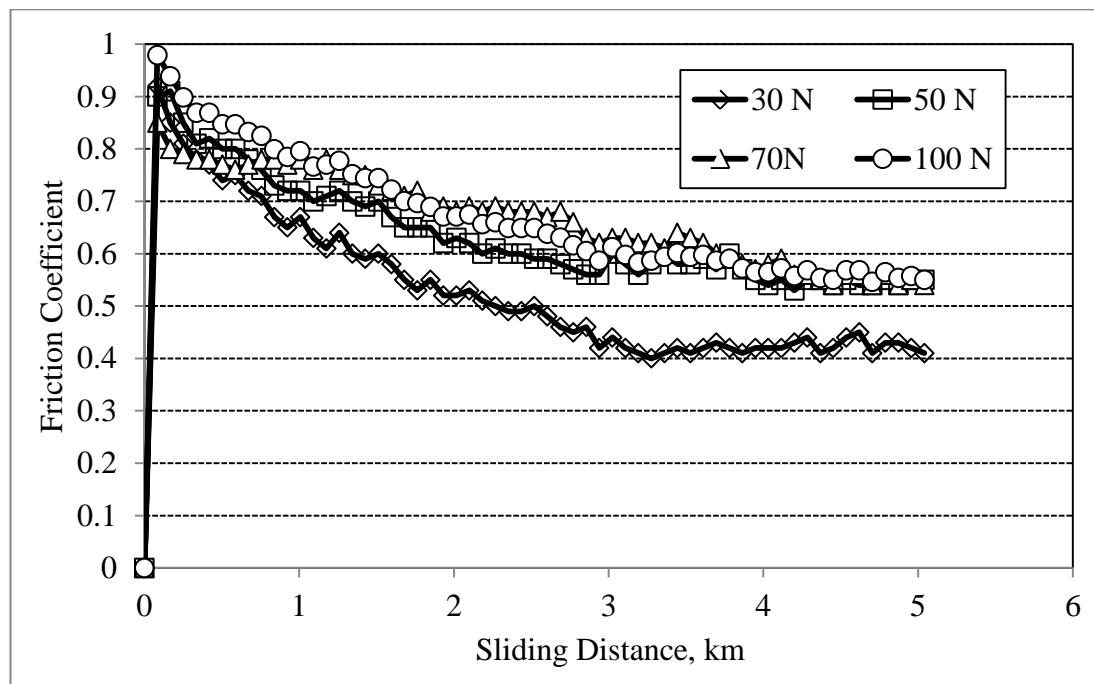


Figure 4.4 Sample of the frictional data showing the coefficient versus sliding distance of KFRE in N-O at a sliding velocity of 2.8 m/s

To examine the influence of the applied load on the friction coefficient and frictional behaviour of the composites, the average of the friction coefficient after a 5 km sliding distance was determined for all materials under different applied loads and is presented in **Figure 4.5**. NE and KFRE in N-O exhibited higher friction coefficients (0.5–0.75) than the other composites. KFRE in AP-O exhibited a relatively low friction coefficient (0.32–0.42). From the wear behaviour (see Section 4.2.1), the wear resistance in the KFRE composite in N-O is higher than that of other composites, which indicates high resistance at the interface and reflects the high friction coefficient at this fibre orientation. In the case of the NE, the wear property was much lower than its composites and hence the frictional behaviour of NE is relatively poor compared to its composites. It appears that the film transfer on the counterface has high adhesion characteristics, which causes stickiness between the asperities and leads to a high friction coefficient. This is followed by detachment of the film, resulting in high levels of material removal. This is illustrated in **Figure 4.6** and will be discussed further in a later section.

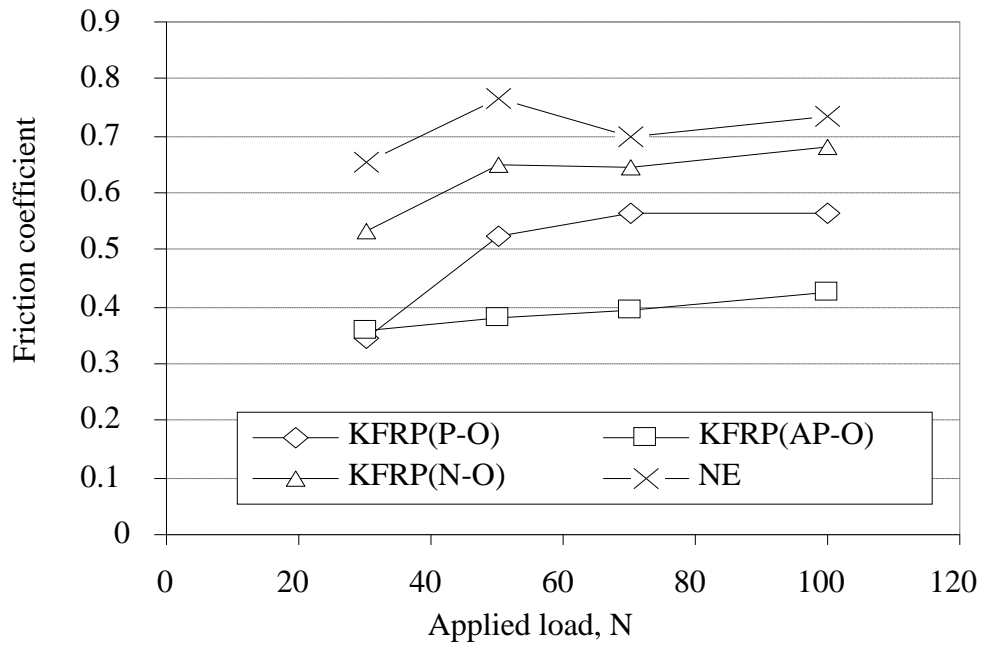


Figure 4.5 Friction coefficient versus applied load for NE and KFRE at different orientations

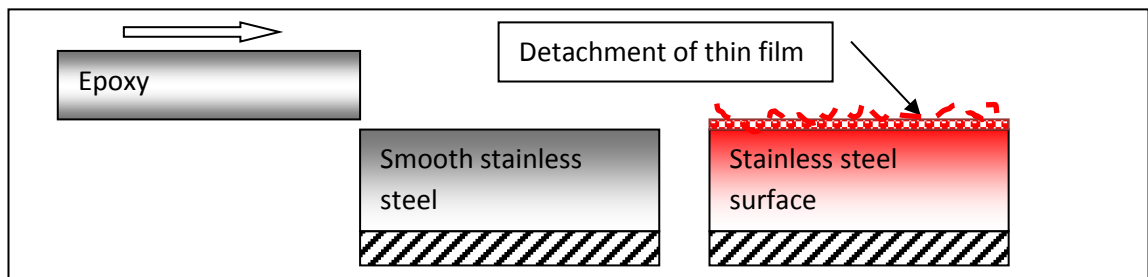


Figure 4.6 Film transfer behaviour of epoxy against stainless steel

As a result of dry sliding, heat is generated at the interface, which can play an important factor in determining the wear mechanism of the materials. **Figure 4.7** delineates the maximum interface temperature that was measured during the rubbing at the longest sliding distance of 5 km at different applied loads. Due to the high friction coefficient of the NE and the KFRE composite in N-O, higher interface

temperatures were produced compared to KFRE composites in P-O and AP-O. Despite the high interface temperatures, the maximum temperature did not reach the T_g of the epoxy (approximately 125 °C). However, the presence of the heat associated with the shear loading at the interface may combine with the load at the interface to become thermo-mechanical and then cause deterioration of the soft surface. A plastic deformation and/or softening process may be expected to take place in the resinous regions of the composites during sliding.

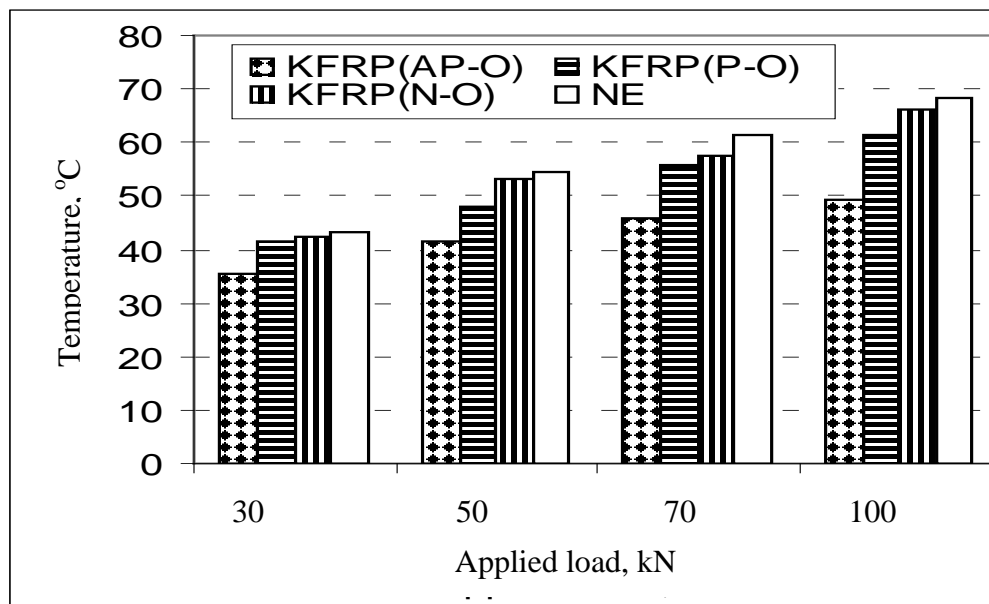


Figure 4.7 Interface temperature versus applied load

4.3 DISCUSSION AND SURFACE OBSERVATION

The adhesive wear and frictional results under dry contact conditions showed that the presence of kenaf fibres in the epoxy matrix can enhance the wear and frictional performance of the NE. This enhancement was pronounced in N-O orientation. This

demonstrates that fibre orientation has a significant influence on the wear characteristics of KFRE composites. This can be further explained by the proposed wear mechanism for the KFRE composite in the three tested orientations depicted in **Figure 4.8**. In this study, it was found that the damage features in the fibrous regions are different in each orientation; they are dependent on the sliding force with respect to the fibre direction. In P-O (**Figure 4.8a**) two damage features can be seen; breakage or bending of fibres along the sliding direction. This is controlled by the interfacial adhesion characteristics of the fibres with the matrix. If the interfacial adhesion is strong enough to prevent bending and/or debonding of the fibres, tear and breakage may occur. However, if the side force is higher than the interfacial adhesion, debonding, bending and then detachment of the fibres may take place. This can be seen when the KFRE composite is oriented in AP-O (**Figure 4.8b**). On the other hand, in the case of N-O, when the ends of the fibres are exposed to the counterface (**Figure 4.8c**), there is no possibility of detachment due to the deep embedding of the fibres (20 mm) in the bulk of the composite. However, there is a possibility of generating cracks close to the fibres and perpendicular to the sliding direction, due to the side shear force (**Figure 4.8c**). This can be further clarified by observing the worn surface of the composite.

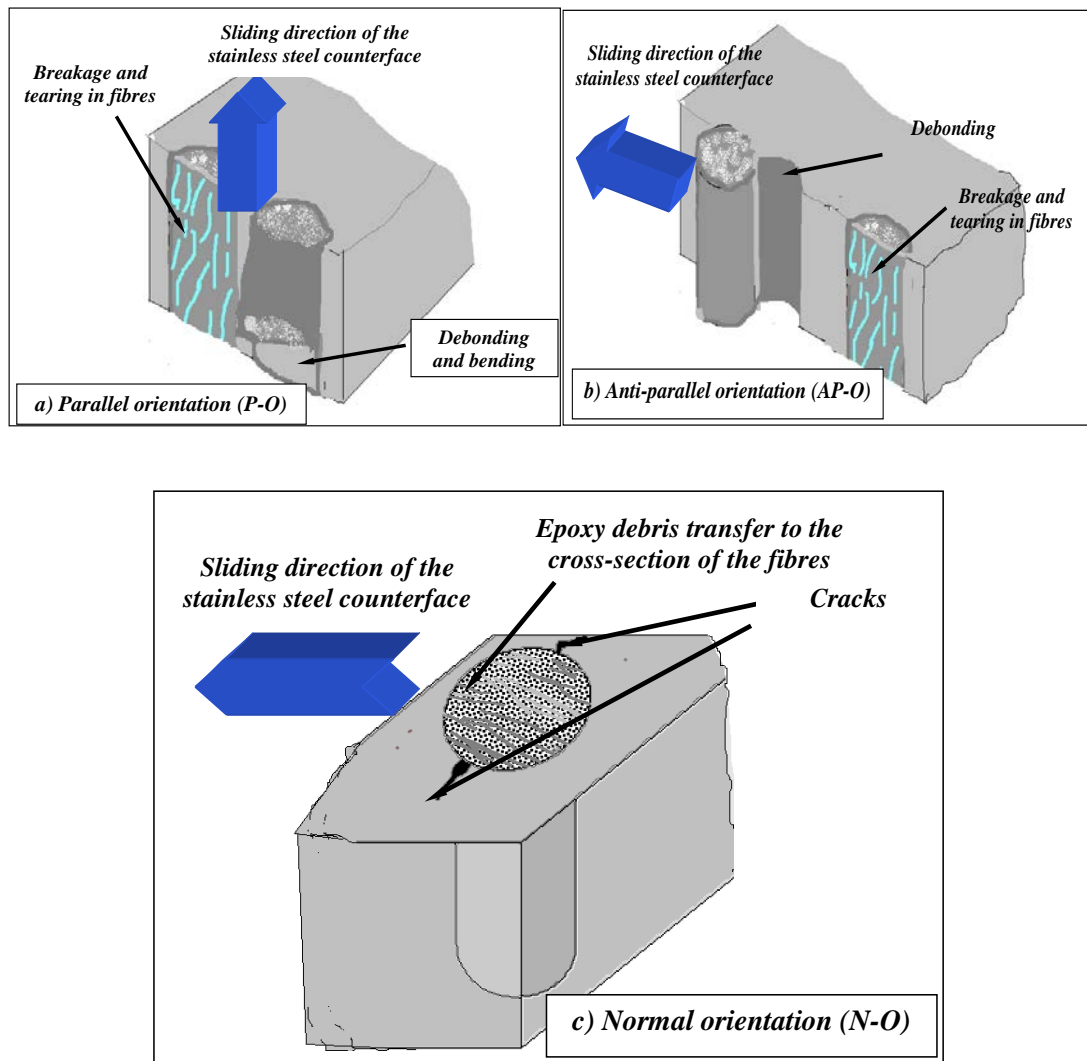


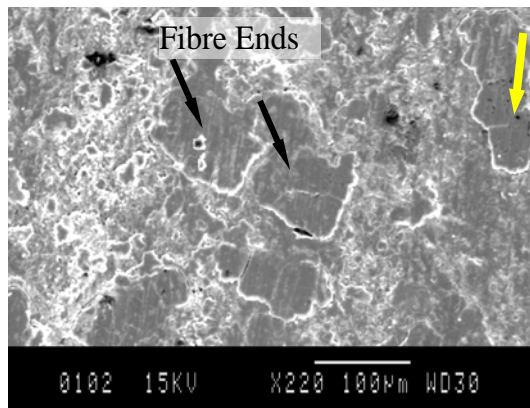
Figure 4.8 Proposed wear mechanisms of the KFRE composite in three different orientations

The worn surfaces of the KFRE composites and NE at different operating parameters are shown in **Figures 4.9–4.11**. The worn surface of the KFRE composite in N-O under a 50 N applied load and a sliding velocity of 2.8m/s (**Figure 4.9a**) showed that the resinous regions were deformed and softened. Meanwhile, the fibre ends were still well adhered in the matrix and there was no sign of debonding or pull-out. The cross-section of the fibres was covered with an epoxy layer generated by either back-transfer film or debris transformation from the resinous regions, which in turn

reduces material removal from the composite surface, leading to lower W_s (**Figure 4.1**). At a higher applied load (70 N) **Figure 4.9b** showed debonding of fibres. This is due to the high thermo-mechanical loading, which increases the rate of material removal from the resinous regions and weakens the interfacial area between the fibres and the matrix. Despite this, the fibre ends appear to carry some of the load during the sliding. In addition, there was no sign of pull-out of fibres. At a higher applied load (100 N), micro-cracks appeared on the surface, due to the high side force. This indicates the high wear resistance of the composite at the rubbing zone. This can also be seen at the higher sliding velocity of 3.9 m/s (**Figure 4.9d**). Under severe conditions (high load and/or velocity) the wear mechanism of the KFRE composite in N-O is dominated by micro-cracks, which confirms the proposed wear mechanism (**Figure 4.9c**) in this orientation.

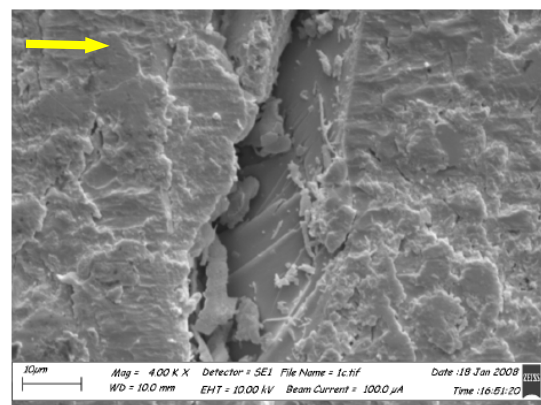
When the KFRE composite in P-O was tested at a lower applied load of 50 N and a sliding velocity of 2.8 m/s (**Figure 4.10a**), the damages seen were similar to those observed when the composite was tested at the same applied load in N-O (**Figure 4.9a**); i.e., the epoxy regions were softened and deformed, while the fibres were still in good condition. At the higher sliding velocity of 3.9 m/s under an applied load of 50 N, debonding of fibres was evident (**Figure 4.10b**). However, there was no sign of fibre detachment, which indicates the higher interfacial adhesion property of kenaf fibres with the matrix. The worn surfaces of NE showed deformation and softening of the epoxy due to the high interface temperature, associated with high side force

(Figure 4.11). This deteriorated the surface and micro-cracks could be seen under severe condition (Figure 4.11b).



a) At 50 N applied load and 2.8 m/s sliding velocity for a 3.36 km sliding distance

b) At 70 N applied load and 2.8 m/s sliding velocity for a 3.36 km sliding distance



c) At 100 N applied load and 3.9 m/s sliding velocity for a 3.36 km sliding distance

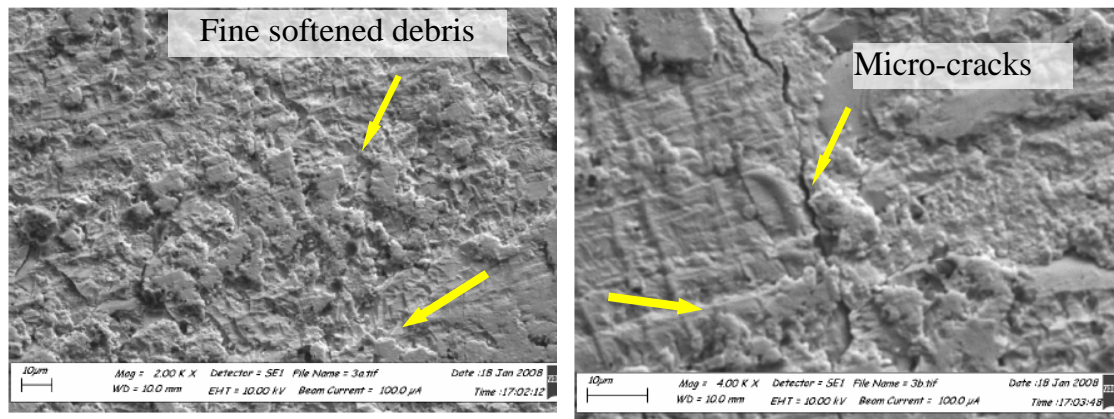
d) At 70 N applied load and 3.9 m/s sliding velocity for a 3.36 km sliding distance

Figure 4.9 Worn surface of the KFRE composite tested in N-O at different operating parameters

a) At 50 N applied load and 2.8 m/s sliding velocity for a 3.36 km sliding distance

b) At 50N applied load and 3.9 m/s sliding velocity for a 3.36 km sliding distance

Figure 4.10 Worn surface of the KFRE composite tested in P-O at different operating parameters



a) At 50 N applied load and 2.8 m/s sliding velocity for a 3.36 km sliding distance

b) At 50 N applied load and 3.9 m/s sliding velocity for a 3.36 km sliding distance

Figure 4.11 Worn surface of the NE at different operating parameters

The effect of the composites sliding on the roughness of the stainless steel counterface is shown in **Figure 4.12** under two conditions: before and after cleaning the wear track with acetone. It should be mentioned that the initial roughness of the counterface (before the tests) was about $R_a=0.11 \mu\text{m}$. The wear track roughness increased after the tests of all the materials. This indicates that either some debris or

film transfer was generated on the wear track. After cleaning, the roughness was reduced, which confirmed the generation of a film transfer on the counterface during the sliding. Further, the film transfer appeared to be rough when NE was tested ($R_a=0.21\ \mu\text{m}$), and this was clear in the case of the KFRE in P-O as well. This could be one of the reasons for the high W_s of NE and the low W_s of KFRE in N-O compared to the other orientations. On the other hand, KFRE in N-O and AP-O showed less effect on the roughness of the counterface.

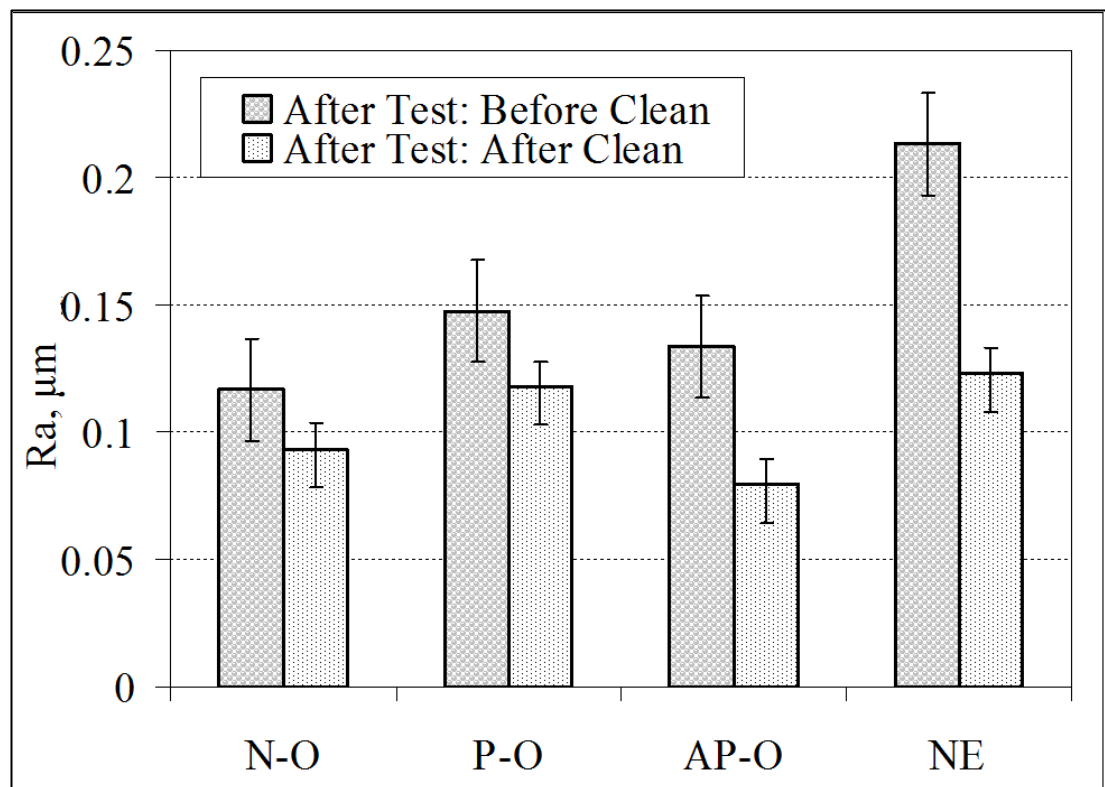


Figure 4.12 Counterface roughness after tests: before cleaning and after cleaning

Due to the changes in the roughness of the wear track, the roughness of the composite surface was also modified. Averages of five readings (before and after the tests) are displayed in **Figure 4.13**. Samples of the roughness profiles of the composite surfaces after the tests are shown in **Figure 4.14**. The surface roughness of the composites (in the three orientations) and NE was significantly increased. **Figure 4.14** shows that the roughness of the composite surfaces and NE increased, except for that of KFRE tested in N-O.

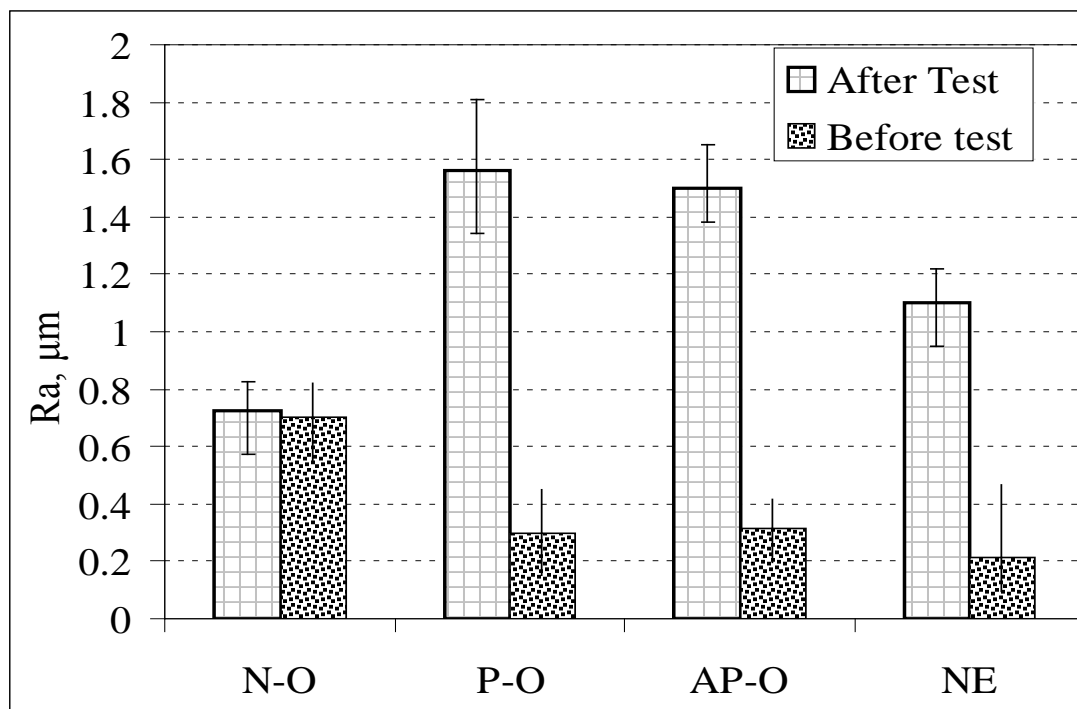
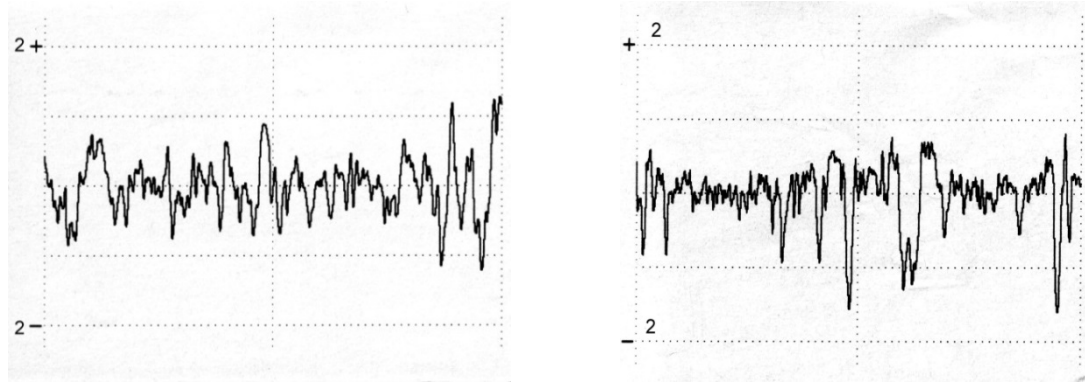
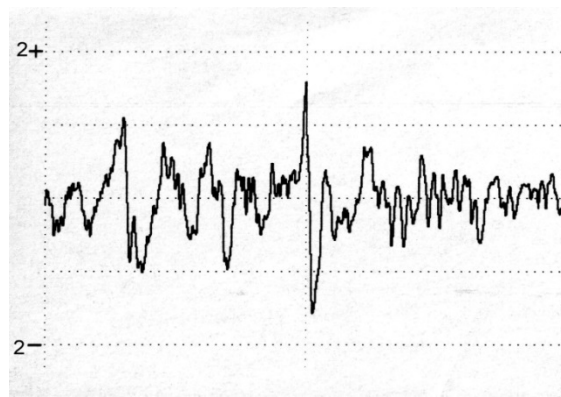


Figure 4.13 Composite roughness after tests



a) NE, $R=1.033 \mu\text{m}$

b) KFRE N-O, $R_a=0.7 \mu\text{m}$



c) KFRE AP-O, $R_a=1.558 \mu\text{m}$

Figure 4.14 Roughness of the worn surface of the composite and NE after tests at a sliding velocity of 2.8 m/s under a 50 N applied load and 3.36 km sliding distance

4.3.1 Dry Adhesive Wear Behaviour in the Published Literature

Table 4.2 summarises the ranges of W_s values and friction coefficients of polymeric composites based on natural (jute, sugarcane and oil palm) and synthetic (glass) fibres from the literature and from this study. In general, one can say that polymeric composites based on kenaf fibres have a better wear and frictional performance than the other composites. Polymeric composites based on cotton, oil palm and jute fibres

exhibited very high friction coefficients, which led to higher interface temperatures, causing greater deformation and softening in their resinous regions. In addition, pull-out, breakage and detachment of these fibres have been reported. In contrast, in the current study, epoxy composites based on kenaf fibres show high interfacial adhesion, leading to the high wear resistance. Moreover, kenaf fibres have given promising results in replacing glass fibres for tribological applications when compared to sugarcane, oil palm and jute fibres.

Table 4.2 Ws values and friction coefficients of some previous studies

Fibre-polymer composites	Range of Ws, $\text{mm}^3/\text{N.m } 10^{-5}$	Friction coefficient	Remarks
Kenaf in N-O	0.15–2	0.52–0.68	Low wear, no pull-out or delamination of fibres
Cotton-polyester, (Hashmi, Dwivedi & Chand 2007)	0.1–6.0	0.6–1.0	Low wear, very high friction
Oil palm-polyester, (Yousif & El-Tayeb 2007a)	35–60	0.6–0.92	Moderate wear, high friction
Jute-polyester, (El-Sayed et al. 1995)	Not available	0.75–1.0	High friction
Sugarcane-polyester, (El-Tayeb 2008)	5,000–10,000	0.02–0.25	Very high wear, low friction, pull-out and delamination of fibres
Glass fibres-polyester, (Yousif & El-Tayeb 2007e)	0.2–0.6	0.4–0.6	Low wear, moderate friction

4.4 WET ADHESIVE WEAR AND FRICTIONAL BEHAVIOUR

The adhesive wear and frictional characteristics of the KFRE composites with different fibre orientations were investigated under wet contact conditions with different applied loads (50–200 N) and sliding distances (0–30 km). It should be noted that the applied loads and sliding distances selected for wet contact conditions are much higher than the operating parameters for the dry contact conditions. This is primarily due to the fact that no weight loss can be measured at low values of loads and/or sliding distance. A summary of the W_s values of NE (NP) and the KFRE composites in the three different orientations is presented in **Figures 4.15–4.18**.

4.4.1 Wear Behaviour Under Wet Contact Conditions

Figure 4.15 shows the relationship between W_s and the sliding distance. A decrease in the W_s values of all materials was observed with increasing sliding distances, since the running-in process occurs from the start of rubbing until a sliding distance of approximately 20 km. Under dry contact conditions, the steady state was reached at around 4–5 km, while this is achieved at approximately 20 km under wet conditions. This is normal behaviour, since under wet contact conditions the adhesion between the asperities required to reach the steady state is interrupted by the presence of the water at the interface. Further, the presence of the water helps in cleaning away the debris at the interface and cooling the contact areas, which in turn prevents the film transfer found under dry contact conditions. This is illustrated in **Figure 4.16**.

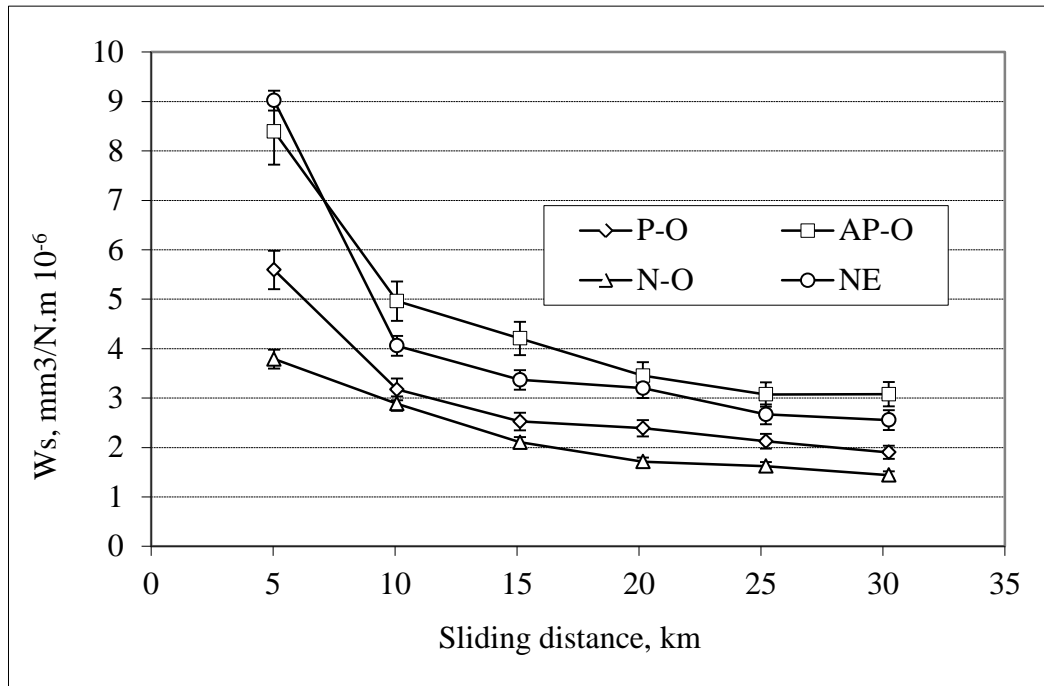


Figure 4.15 W_s results of the epoxy composites at different sliding distances at 2.8 m/s sliding velocity and 100 N applied load

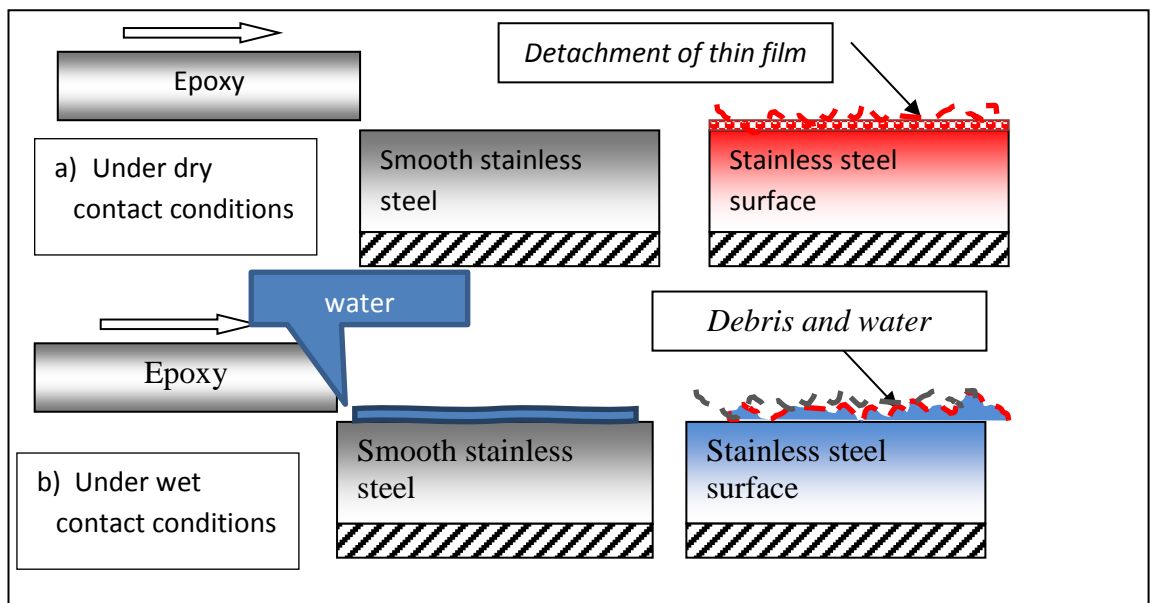


Figure 4.16 Adhesive wear behaviour under wet and dry contact conditions

Figure 4.15 shows that while the addition of kenaf fibres assisted in reducing the W_s of the epoxy, this was not the case for all fibre orientations, and the orientation of the fibres greatly influenced the wear behaviour of the composite. The KFRE composite performed more poorly than NE when the kenaf fibres were oriented in AP-O. The cooling and cleaning mechanisms associated with the water were found to make the NE very competitive with the composites in terms of wear resistance. On the other hand, the KFRE composite exhibited better wear performance in N-O compared to the other orientations, with an improvement of 35–57 percent. In N-O, the ends of the fibres are exposed to the rotating counterface while the fibres are embedded in the bulk of the matrix. In this orientation, pulling out or detachment of fibres is not possible. In contrast, when the fibres are parallel or perpendicular to the shear force, they are subject to detachment, bending, tearing and breakage, as shown in the scanning electron micrographs.

Figure 4.17 shows the W_s values of the materials at different applied loads. At the low applied load of 30 N, the W_s values appeared to be low due to the fact that there is less pressure at the interface in the presence of the water. An increase in the W_s values was noticed at an applied load of 50 N, which subsequently reduced at higher applied loads for all materials. Hence, it seems there is relatively low material removal from the surface at higher applied loads. This could be due to the high stress at the interface, which stabilises the surfaces and prevents the occurrence of 3B-A. Previous studies have suggested that under wet contact conditions the removed material could act as a third body at the interface (Wu & Cheng 2006; Shekar et al.

2010), which in turn transforms the adhesive wear into 3B-A wear and results in high levels of material removal. This may explain the high W_s values seen at 50 N applied load. Similar behaviour has been reported when glass fibre reinforced polyester composites and date palm fibre reinforced polyester composites were tested under the same conditions (Yousif & El-Tayeb 2010a, 2010b).

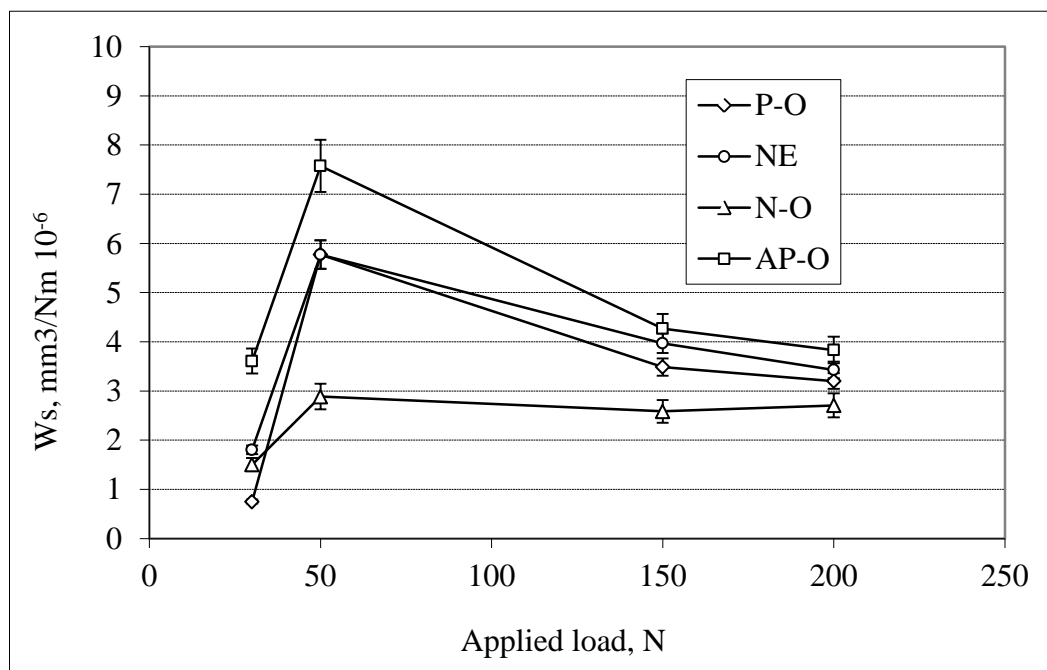


Figure 4.17 W_s results of the epoxy composites at different applied loads at 2.8 m/s sliding velocity for 30 km sliding distances

4.4.2 Frictional Behaviour Under Wet Contact Conditions

Under dry contact conditions, the friction coefficient of all the materials was above 0.3. To determine these values under wet contact conditions, friction coefficients were collected under different applied loads and at different sliding velocities and sliding distances. At all operating parameters, the friction coefficient did not exceed

0.05, which was very low compared to the dry contact conditions. The averages of the friction coefficients associated with the maximum and minimum values are presented in **Figure 4.18** for different sliding distances under an applied load of 150 N and at a sliding velocity of 2.8 m/s. From this figure it is evident that the trends in the friction coefficient of all the materials are almost the same, and that increasing the sliding distance gradually reduced the friction coefficient. Higher friction coefficients were exhibited by the KFRE composites in the N-O and AP-O orientations. However, the values of these friction coefficients (0.035–0.045) are very low due to the presence of the water at the interface, which assists in removing any trapped debris from the rubbing zone. This leads to low interactions between the asperities in contact and results in a low friction coefficient.

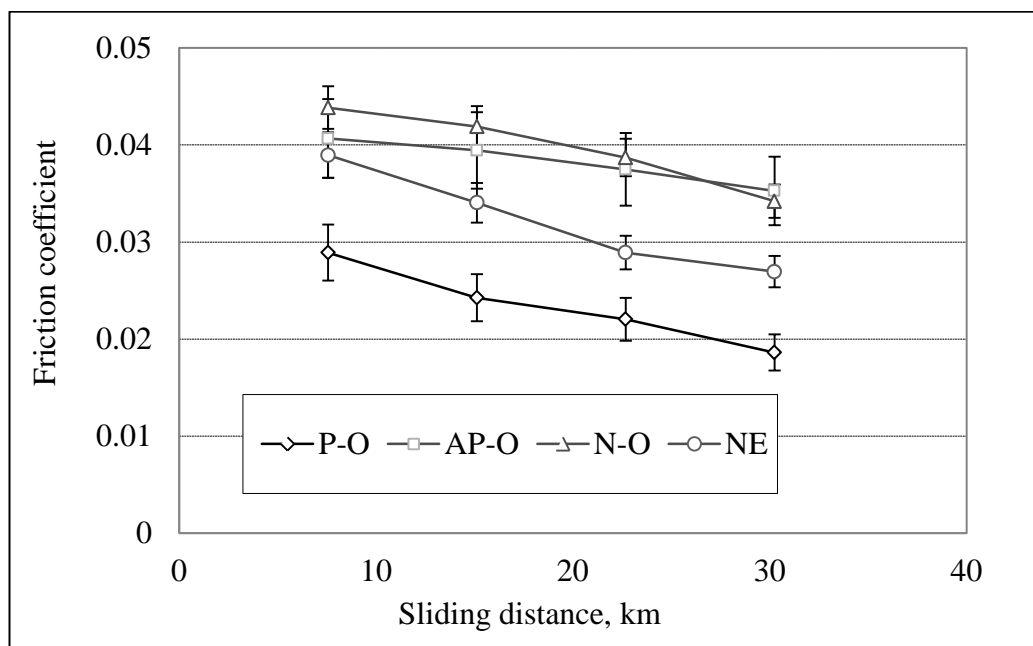


Figure 4.18 Averages of the friction coefficient of the composites at different sliding distances under 150 N applied load at a sliding velocity of 2.8 m/s

This hypothesis was confirmed by the SEM micrographs presented in the next section. These results are in high agreement with previous studies on glass-PEEK (Shekar et al. 2010) and glass-polyester composites (Yousif & El-Tayeb 2010a).

4.4.3 Surface Observation of Worn Surfaces Subjected to Wet Adhesive Wear

Figure 4.19 displays the scanning electron micrographs of the worn surfaces of the KFRE composites in different orientations and applied loads. In AP-O, **Figures 4.19 a** and **b** clearly show that the predominant wear mechanisms were the debonding of fibres (marked as ‘*De*’) and abrasive in nature (marked as ‘*Ab*’). Debonding occurred due to the shear force in the rubbing area that was exposed to the debonding region, leading to weakening of the interfacial adhesion of the fibres with the matrix. The abrasion observed in the resinous regions of the surface was due to debris rolling at the interface, which is in agreement with the arguments given to explain the low friction coefficient (**Figure 4.18**). Both debonding and abrasion increased the material removal from the composite surface. This explains the poor wear results of the composite in AP-O, as shown in **Figure 4.15** and **Figure 4.17**.

In P-O (**Figure 4.20**), the wear mechanism was peeling of fibres (marked as ‘*Pe*’), which can be observed in the fibrous regions for both applied loads of 150 N and 200 N. Peeling took place due to the parallel direction of the shear force, which attempted to tear and peel the fine fibres from the bulk of the kenaf fibre. However, the less abrasive nature of the P-O surfaces compared to the AP-O surface resulted in lower levels of wear removal from the surface and a better wear performance for the

composite in P-O compared to AP-O, as reported in the experimental data given in the previous section. Further, the smooth surface appearance of the composite in P-O (at a load of 200 N) in the resinous area (marked as 'Ss') could explain the lower friction coefficient of the composite in this orientation.

Figure 4.21 showed that there was less damage on the KFRE surface oriented in N-O compared to that seen on the P-O and the AP-O surfaces. In N-O, the ends of fibres were still well adhered in the matrix and no debonding, pull-out and/or peeling was evident, especially at the load of 150 N. Interestingly, the end of the fibres resisted the rubbing process and protected the resinous regions. This showed that kenaf fibres oriented in N-O support the epoxy composite well. However, at an applied load of 200 N, debonding appeared at a portion of the edge of the fibre (**Figure 4.21b**). Nevertheless, high resistance to the shear force was evident at the fibre ends. In spite of the slight debonding of the fibres, no significant surface damage was observed. On the other hand, some of the removed materials acted at the interface and attempted to damage the end of the fibre. The high resistance of the composite in this orientation could explain its high friction coefficient compared to that of the composite in P-O (**Figure 4.18**). This resistance aided in maintaining the surface characteristics of the composite and prevented high removal of the materials, resulting in the low W_s values of the composite in N-O, as shown in **Figure 4.15** and **Figure 4.17**.

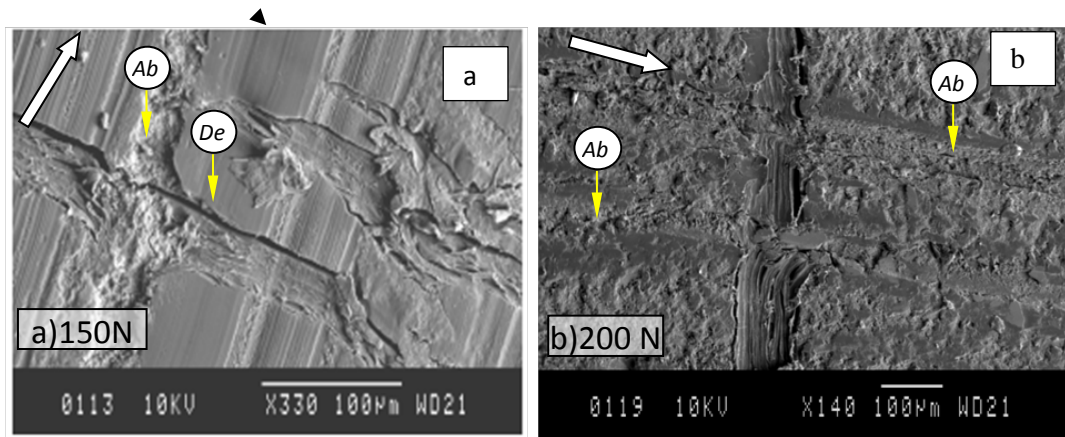


Figure 4.19 Micrographs of KFRE worn surface at AP-O after a 30 km sliding distance

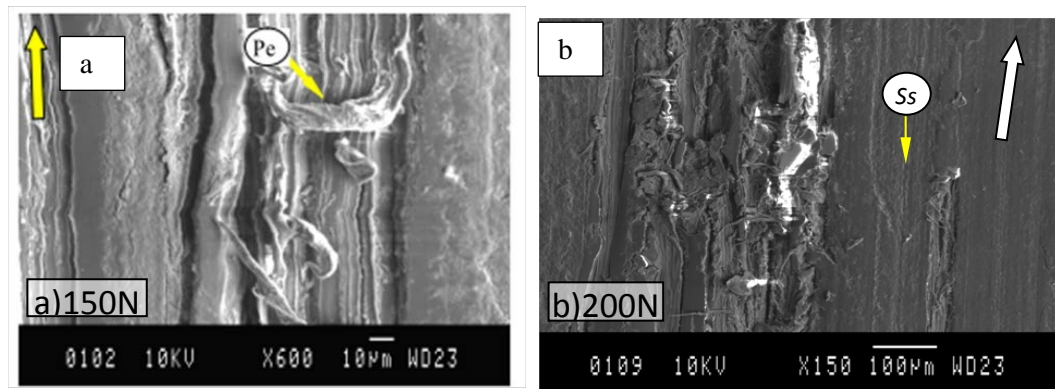


Figure 4.20 Micrographs of KFRE worn surface at P-O after a 30 km sliding distance

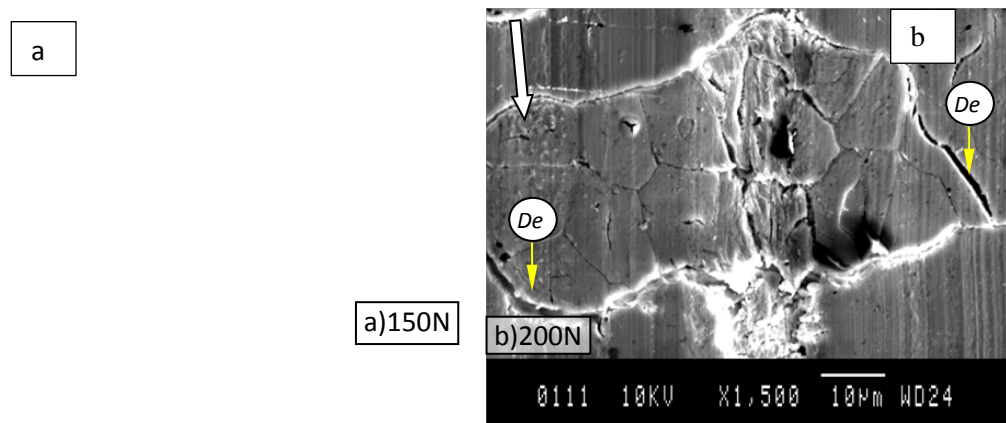


Figure 4.21 Micrographs of KFRE worn surface at N-O after a 30 km sliding distance

To explore the possibility of replacing synthetic fibres with kenaf fibres for tribological applications, the results of this study can be compared with previously reported studies of glass-polyester composites that have been tested under the same conditions (Wu & Cheng, 2006; Yousif & El-Tayeb 2010c). The W_s value of the glass-polyester composite was in the range of $0.7\text{--}3.0 \times 10^{-6}$ mm under wet contact conditions with the same operating parameters used in the current study. This range is almost similar to the W_s of KFRE ($1.2\text{--}3.5 \times 10^{-6}$ mm) tested in N-O. This suggests that kenaf fibres have strong potential as a replacement for glass fibres for tribological applications under wet contact conditions.

4.5 ARTIFICIAL NEURAL NETWORK RESULTS

4.5.1 Comparison of the Experimental and ANN Results

The derivation of an optimum ANN model based on the log-sigmoid transfer function and SCG learning rule with 50 neurons in the first hidden layer was outlined in Section 3.5. The model was then trained and run to predict the results at the same operating parameters. Figure 4.22 displays samples of the experimental and ANN results of the determination of the friction coefficient under different applied loads and sliding distances at a sliding velocity of 2.8 m/s. In general, the predicted frictional value is very close to the experimental ones which indicate good agreement between the experimental results and those of the ANN model especially for the 10 N and 100 N applied load.

At applied loads of 30 N, 50 N, 70 N and 90 N, the correlation coefficient (R) between the experimental and ANN results were 0.953, 0.934, 0.975 and 0.981

respectively. In a recent study using an ANN model for tribological applications, the sliding friction of polyphenylene sulphide composites was evaluated by Gyurova and Friedrich (2011). They found that the ANN prediction profiles for the characteristic tribological properties of these composites exhibited good agreement with the experimentally measured results since there is less than 1% error. However, their study did not give clear information on how their model was developed. Similar findings have been recently reported for different materials (Yang et al. 2013; Nasir et al. 2010).

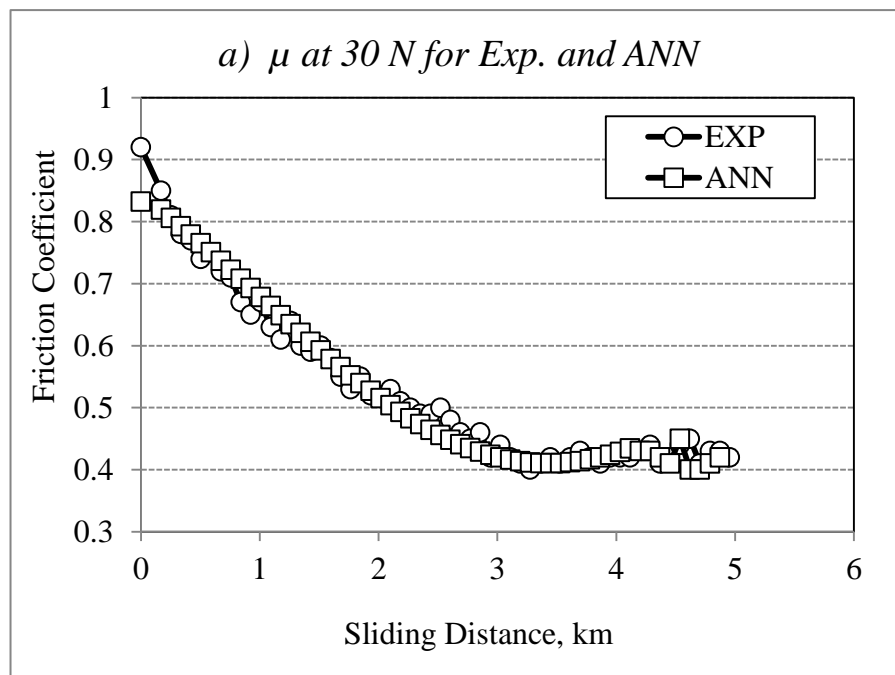


Fig. 4. 22 continued

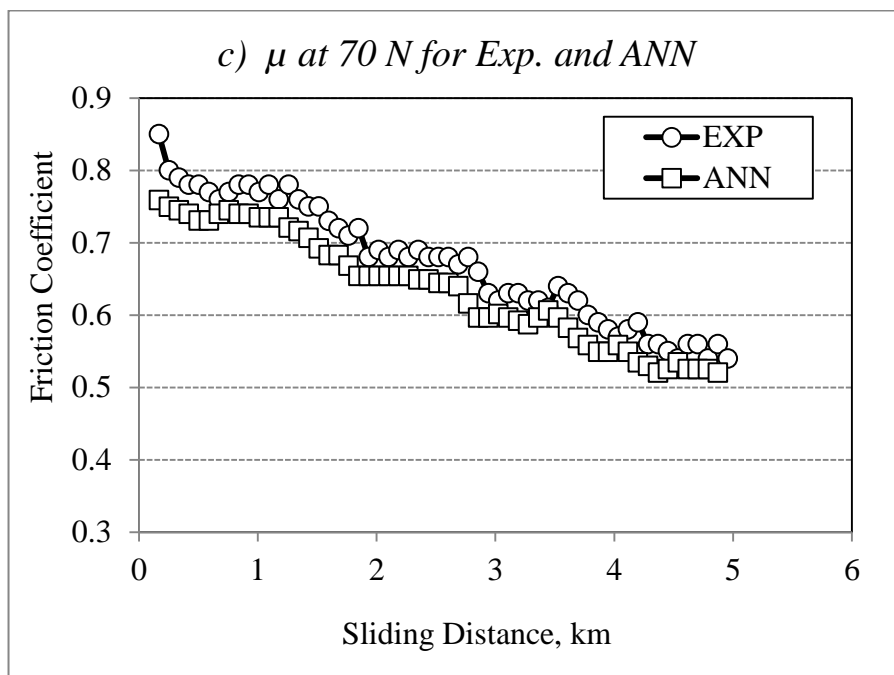
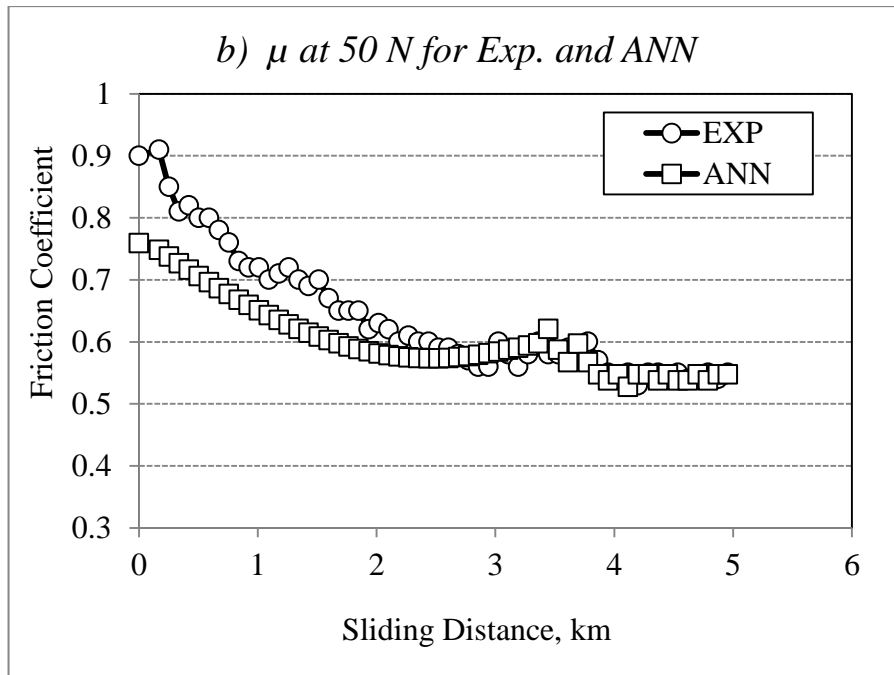


Fig. 4. 22 continued

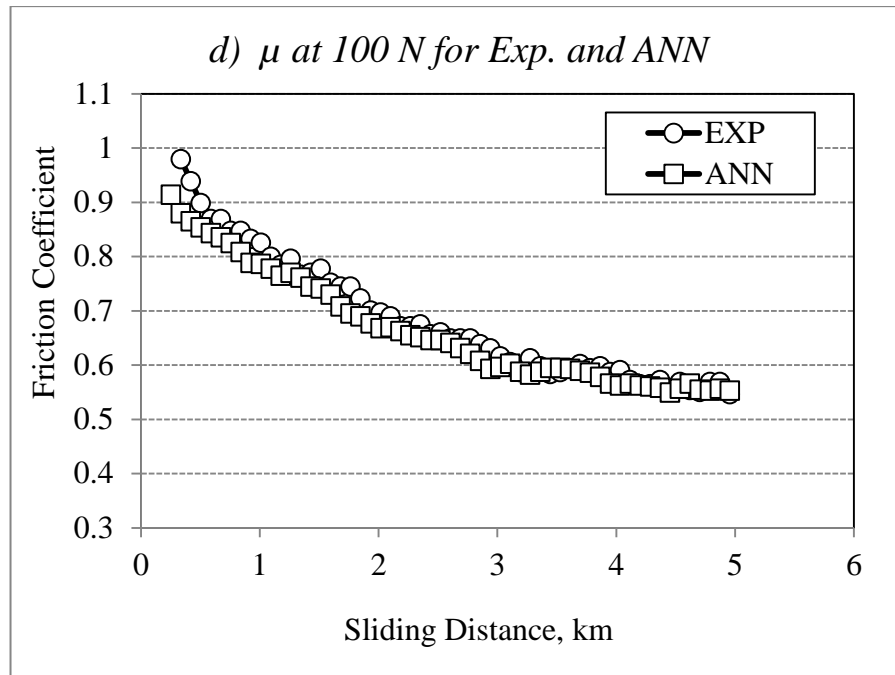


Figure 4.22 Experimental measurement and modelling of the friction coefficient of KFRE composite at different applied load at a sliding velocity of 2.8 m/s

In spite of the difference in the training function between the current study and the published reports, the current findings are in strong agreement with those of Gyurova and Friedrich (2011), Aleksendric (2010) and Zhang, Friedrich and Velten (2002). In the most recent study by Gyurova and Friedrich (2011), the minimum square error obtained was <0.10 , which was very low compared to previous studies. However, the number of data points used in the training process was 60. In the current study, 1095 data points were used, many more than those in the study by Gyurova and Friedrich (2011) and resulted in a lower error (<0.10). In addition, the training and learning functions used in this study were selected based on the low error obtained.

4.5.2 Verification of the ANN Model

To evaluate the ANN model, the experimental data was used for verification purposes. For this investigation, different numbers of neurons were used in the evaluation and the correlation between the experimental and the predicted values of friction coefficients are displayed in **Figure 4.23**, which also shows the square errors and the trendline equations. This figure clearly shows that 50 neurons exhibit better correlations than the other models, since the R^2 value is approximately 0.97, which represents a very high correlation between the experimental and the ANN results.

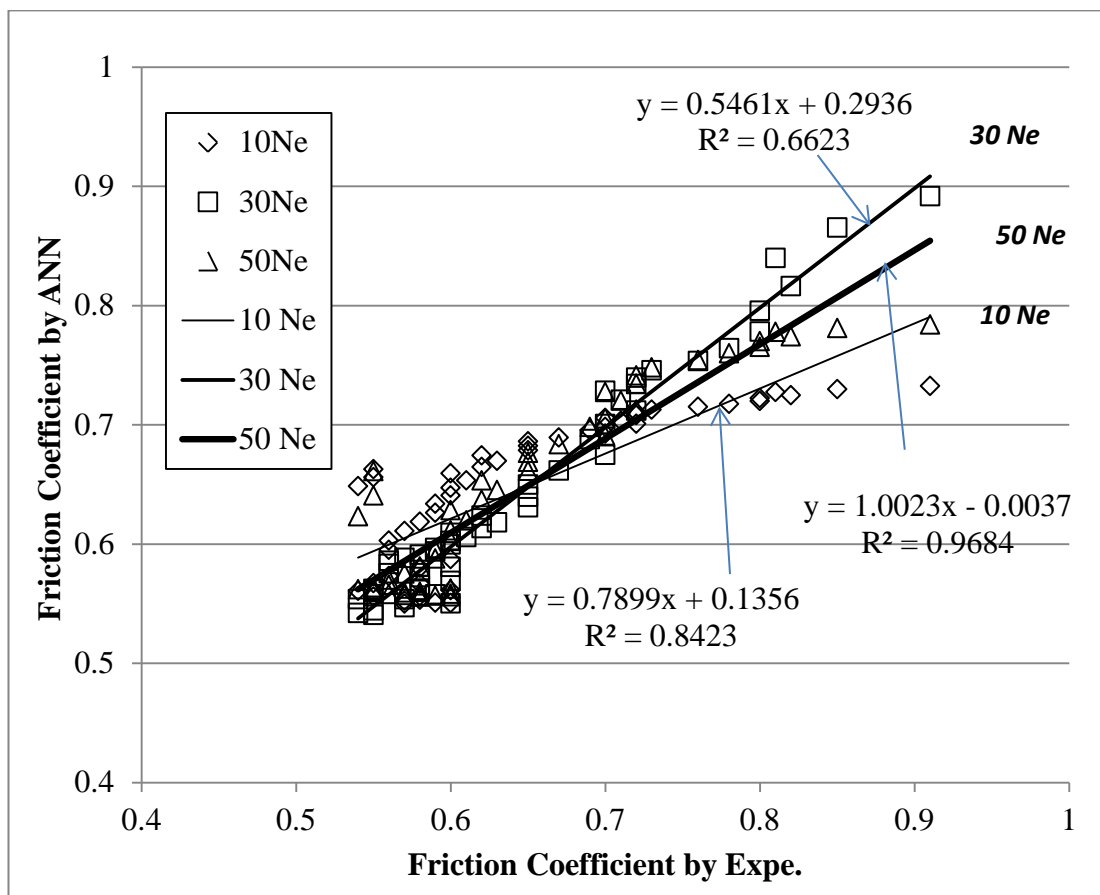


Figure 4.23 Correlation between the experimental and ANN friction coefficients

4.5.3 Prediction of the Friction Coefficient Using Artificial Neural Networks

Figure 4.24 shows the predicted friction coefficient values of the composites plotted against the sliding distance for operating parameters other than those selected for the experiments. The figure shows that the friction coefficient is relatively high at higher sliding velocities, which is in agreement with the frictional data obtained, where higher sliding velocities resulted in high interface temperatures and sticking phenomena at the interface.

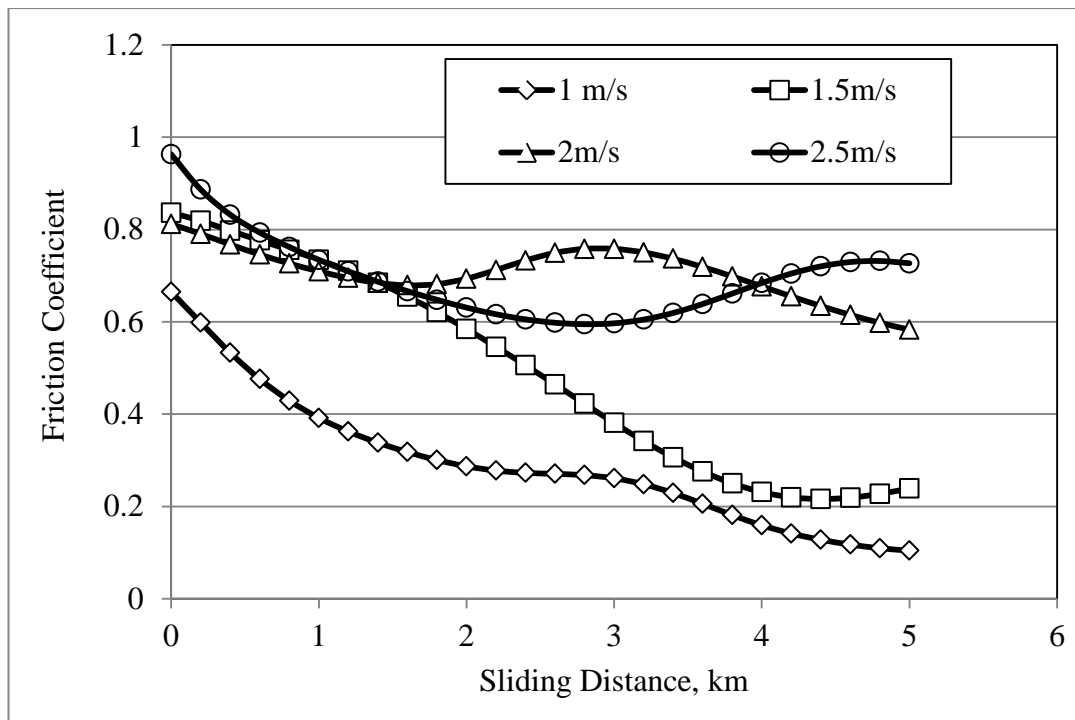


Figure 4.24 Prediction results of the KFRE friction coefficient at different orientations

4.6 SUMMARY

From the results obtained and the observations of the surface morphology of the composites after testing, several conclusions can be drawn:

1. The operating parameters have less influence on the wear and friction behaviour of the composites than the orientation of the fibres does. The KFRE composite exhibited high wear performance in N-O; in this orientation the wear performance of the epoxy could be improved by approximately 85 per cent under dry contact conditions. The high resistance at the interface in the composite in N-O resulted in the generation of micro-cracks; however, debonding of the fibres and deformations in the resinous regions were observed when the composites were tested in P-O.
2. The presence of water at the interface reduced the friction coefficient to a range of 0.03–0.045, which is very low compared to the dry frictional values. This was mainly due to the removal of debris in the interface and cooling of interface by the water, which led to the low interaction between the aspirates.
3. The ANN results revealed that this model was able to predict the friction coefficient of the composites since low error (<0.1) exhibited when the ANN results compared with the experimental data.

CHAPTER 5 THREE-BODY ABRASION BEHAVIOUR OF THE EPOXY COMPOSITE

5.1 INTRODUCTION

The chapter aims to address the effects of sand particle size, applied load, sliding distance and kenaf fibre orientation on the 3B-A wear behaviour of epoxy composites subjected to high stress. Experiments were conducted using a dry sand/steel wheel apparatus at different applied loads (5–20 N) and sliding distances (0–0.18 km). The tests were performed at a rotational speed of 100 rpm (corresponding to 1.152 m/s). The sizes of the sand particles were in the ranges of 370–390 μm , 650–750 μm and 1,200–1,400 μm , with a fixed flow rate of 4.5 g/s. The composite was tested in three different orientations: P-O, AP-O and N-O. SEM was used to observe the damage features on the worn surfaces of the composite.

5.2 WEAR BEHAVIOUR OF THE COMPOSITE UNDER THREE BODY ABRASION

Most of the studies on the abrasive wear performance of similar composites reported in the literature have presented wear data in the form of wear data and wear rate. For the comparative purposes, the abrasive wear data in this study is presented as the wear rate and weight loss at the sliding distance or applied load tested.

5.2.1 Three-Body Abrasive Behaviour at Different Sliding Distances

The wear rate of NE and its KFRE composites in different orientations plotted against sliding distance is presented in **Figure 5.1** for the three particle sizes 370–390 μm , 650–750 μm and 1,200–1,400 μm . In general, all these materials showed a similar trend, since in each case a reduction in the wear rate was observed with an increase in the sliding distance. This is due to the increase in the contact area of the materials with the counterface. In the first stage of the sliding process, the contact between the materials and the stainless steel counterface is in line. As material is removed from the interface the contact between the bodies increases, allowing more particles into the interface. Since the applied load is fixed with the increase of the sliding distance and the contact area, there is a load distribution on the numbers of particles. In other words, there is a reduction in wear rate with the increase of the sliding distance, since there are more particles and they share the stress. **Figure 5.2** illustrates this argument, which is supported by the literature (Harsha 2011; Koottathape et al. 2012; Molazemhosseini et al. 2013).

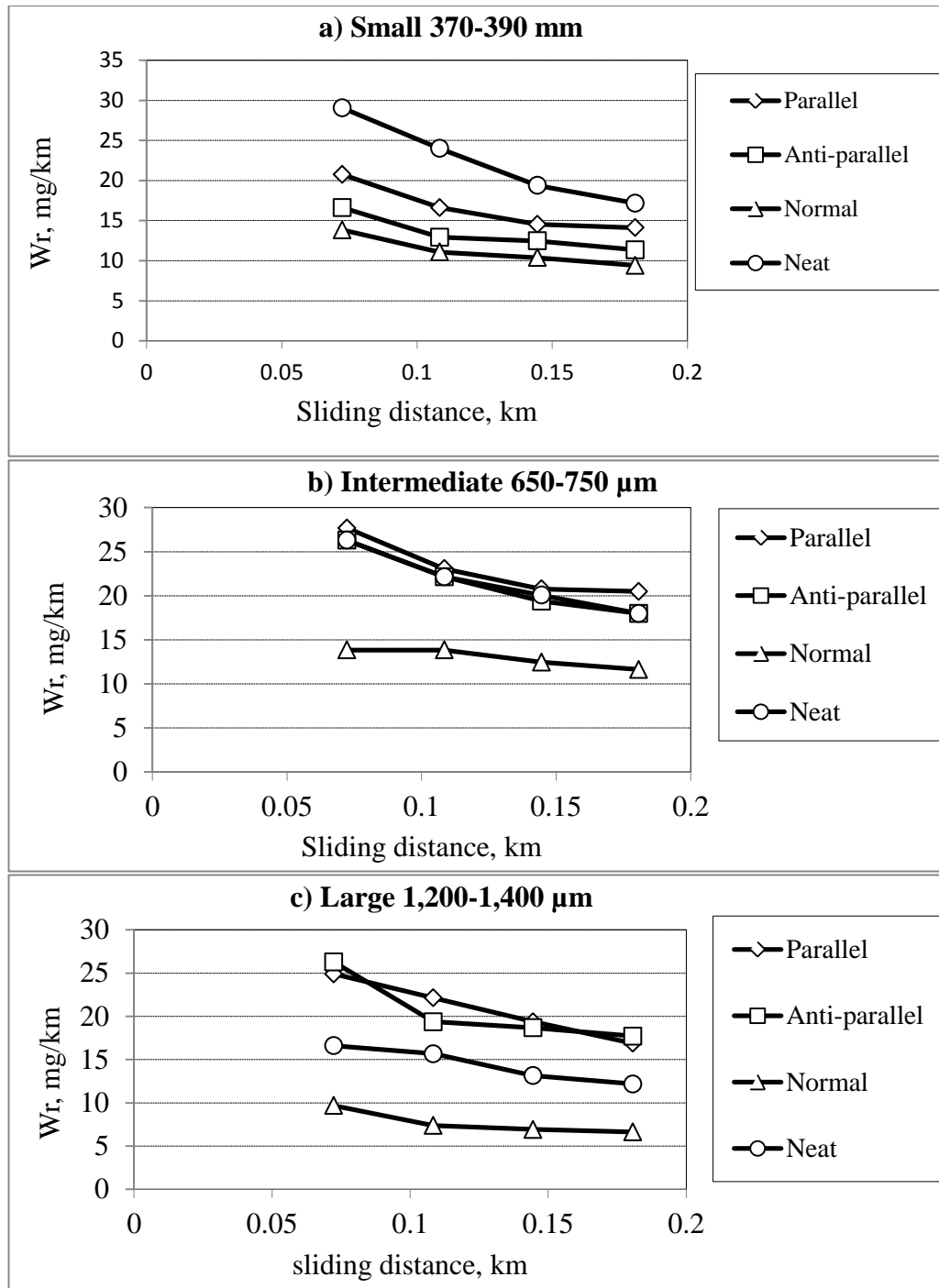


Figure 5.1 Wear rate versus sliding distance with different particle sizes and an applied load of 20 N

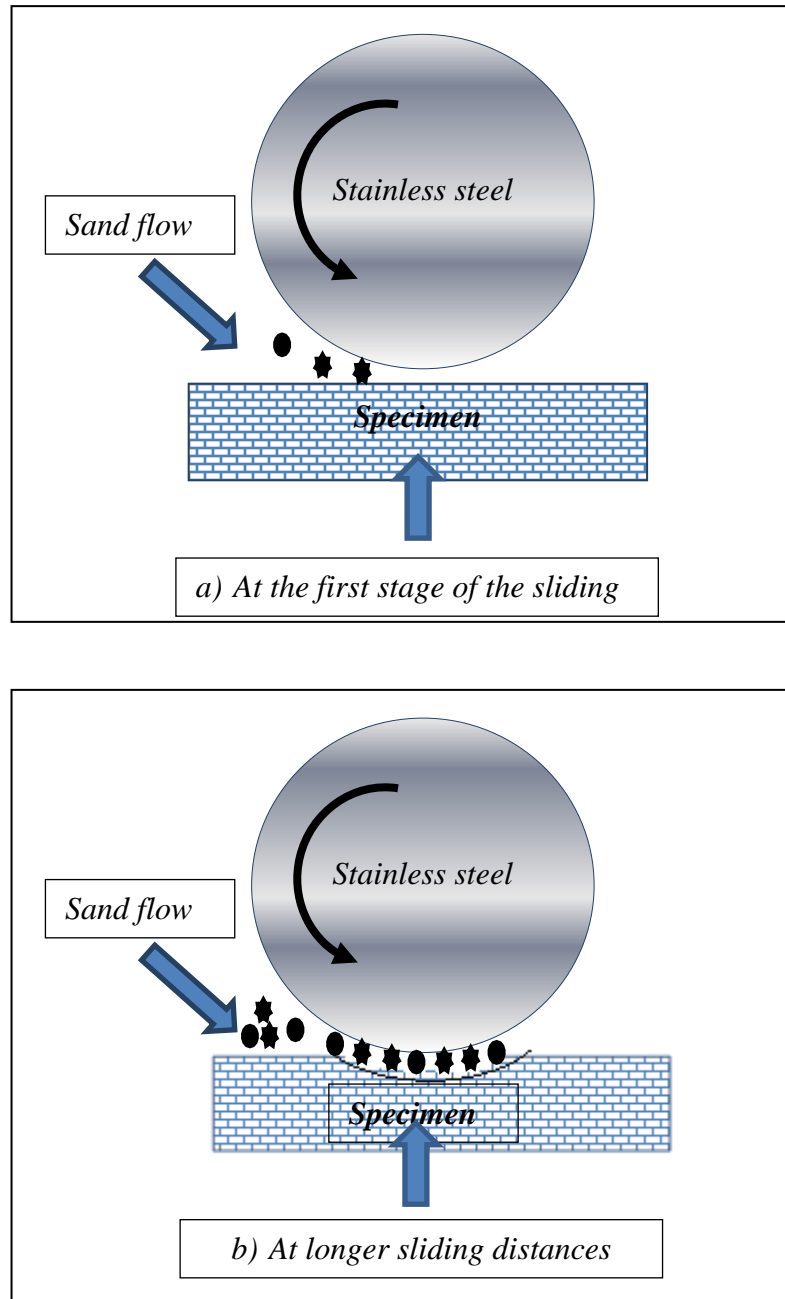


Figure 5.2 Schematic drawing showing the contact and the number of particles in the interface at short and longer sliding distances

5.2.2 Three-Body Abrasion Behaviour at Different Applied Loads

The wear rate of the KFRE composites and NE versus applied load is presented in **Figure 5.3** for the three different size ranges of particles sizes after a 0.18 km sliding distance. The figure indicates that increasing the applied load reduces the wear rate for all materials at all particle sizes. This behaviour has been reported in other studies (Yousif & El-Tayeb 2008a; Trezona & Hutchings 1999; Allsopp, Trezona & Hutchings 1998). Other published studies have shown that the applied load does not have a significant influence on the wear rate in low stress 3B-A (Shipway & Hodge 2000). With regard to the effect of the orientation of the kenaf fibres on the performance of the epoxy composites, when kenaf fibres in N-O were included there was reduction of approximately 50–75 per cent in the wear rate compared to that of the NE. On the other hand, with intermediate and large particles sizes, the performance of the composites in P-O and AP-O was poorer than that of the NE. This is clearly shown in **Figure 5.4**, which gives a summary of the wear results, showing that particle size affects the wear behaviour of the materials differently. At low applied loads, KFRE composites showed a high wear rate when the composites was tested in AP-O and P-O with intermediate and large sized particles. Meanwhile, the NE and the KFRE in N-O showed lower wear rate values when intermediate and large particles were used compared to those seen with small particles. Hence, both fibre orientation and particle size have a significant effect on the wear behaviour of the materials.

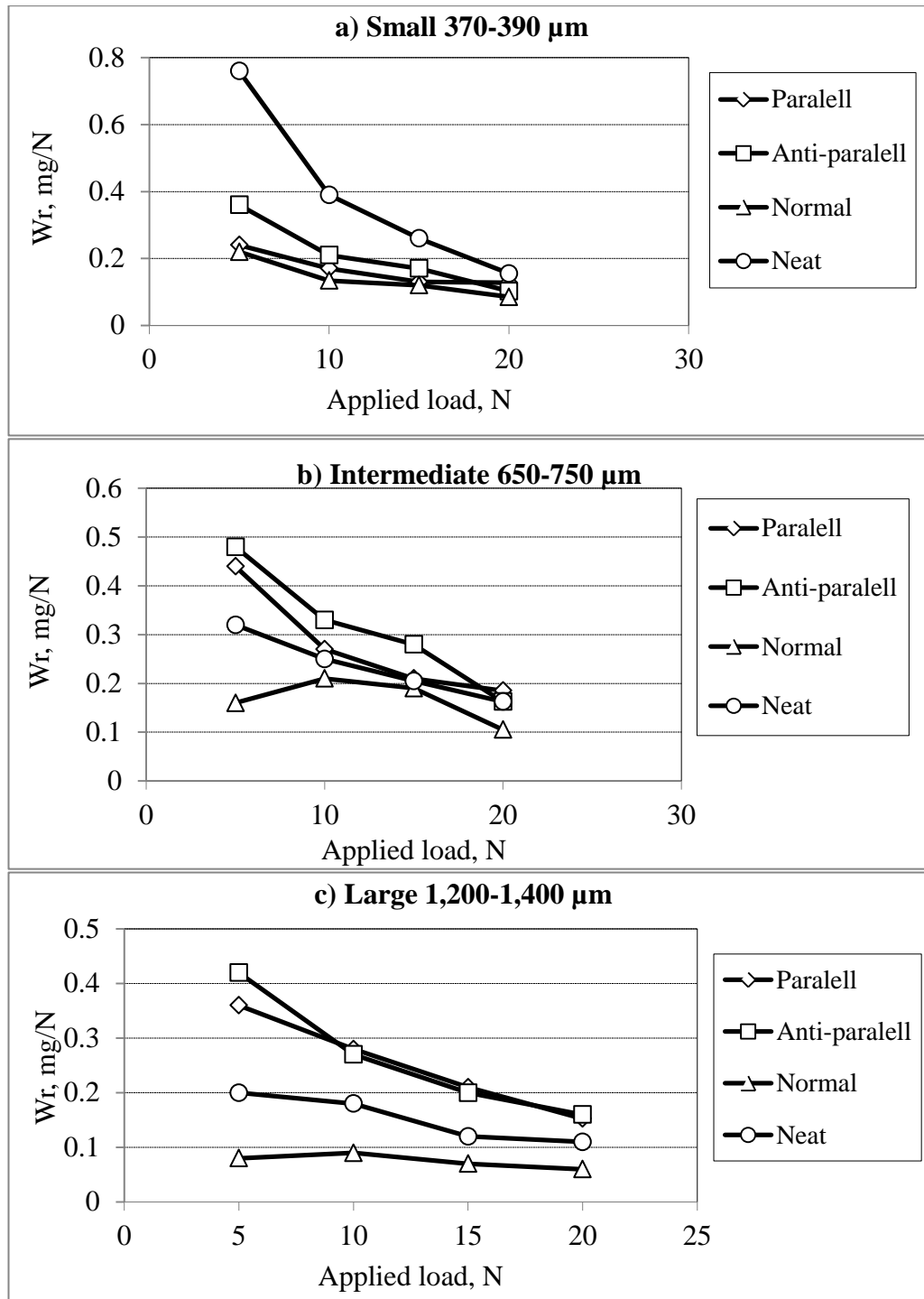


Figure 5.3 Wear rate versus applied load with different particle sizes after a 0.18 km sliding distance

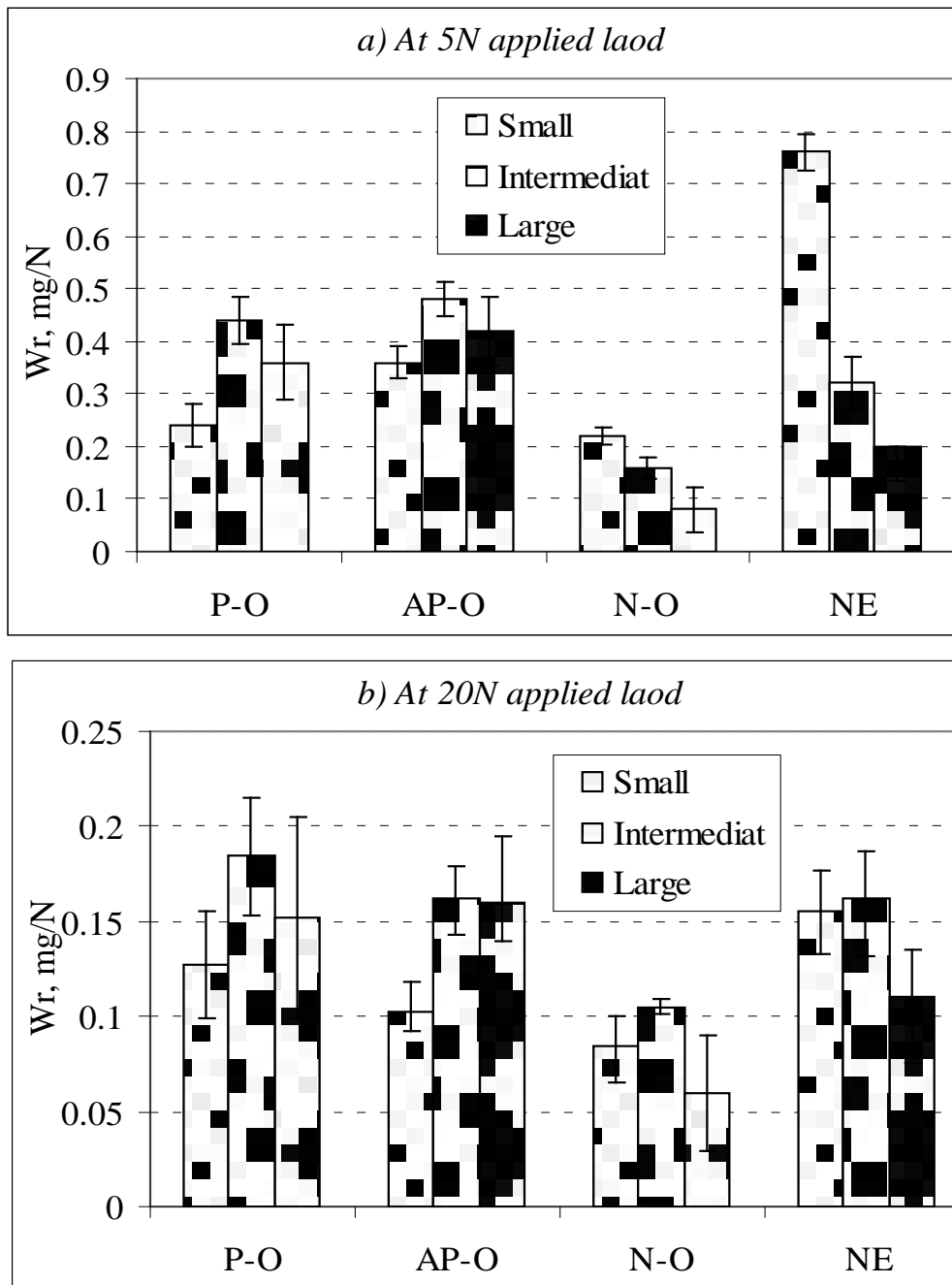


Figure 5.4 Wear rate of the materials with different particle sizes under 5 N and 20 N applied loads after a sliding distance of 0.18 km

5.3 FRICTIONAL RESULTS OF THE COMPOSITES UNDER THREE-BODY ABRASION

In the previous chapter, the friction coefficients of the composites under dry adhesive were always above 0.3, most likely due to the direct interaction between the two rubbed surfaces. Under wet contact conditions, the water assisted in reducing the interaction between the asperities in contact, leading to a reduction of the friction coefficient, which became less than 0.1. In this chapter, there is a third body in the interface; the sand particles, and thus there are two possibilities for the way the materials will behave. The first is that the particles will roll in the interface, which will lead to a very low friction coefficient. The second is that the particles will slide after penetrating the soft surface, which may lead to a high friction coefficient. This issue will be addressed and clarified in the following sections.

5.3.1 Three-Body Abrasion Frictional Behaviour at Different Sliding Distances

The friction coefficient was captured at each test for different applied loads, sliding distances and particle sizes. Plots of the friction coefficient versus the sliding distance at all applied loads showed a similar trend. Samples for the friction coefficient versus the sliding distance are presented in **Figure 5.5** for different sand particle sizes and composite orientations. From these, it is immediately evident that all materials showed an increase in the friction coefficient with an increase in the sliding distance, with all the sizes of sand particles used.

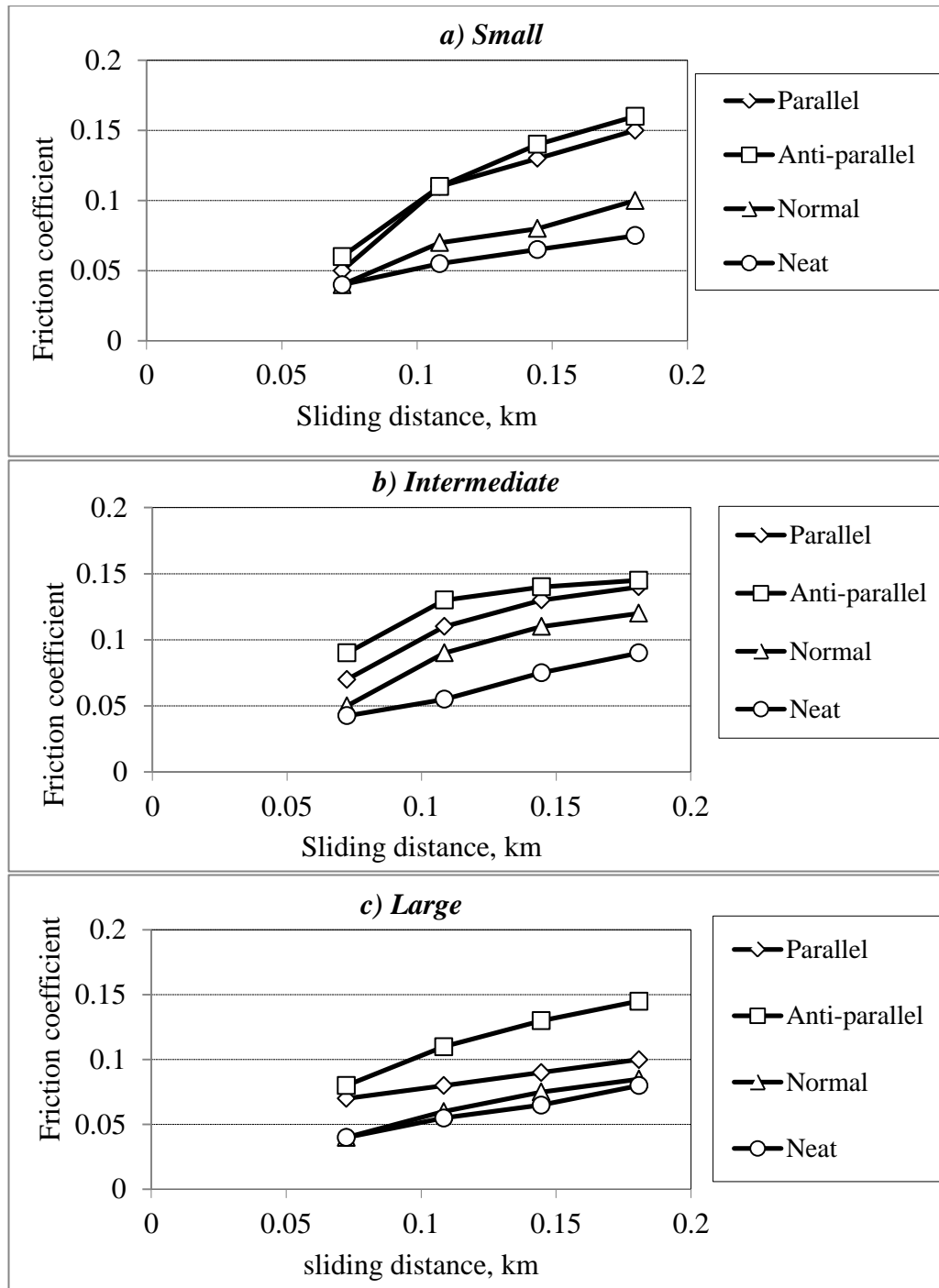


Figure 5.5 Friction coefficient versus sliding distance with different particle sizes at an applied load of 20 N

Figure 5.1 showed that the wear rate reduces with increased sliding distance; i.e., there was high resistance at the interface at longer sliding distances. This can be explained by the fact that large numbers of particles are present in the interface at later stages of sliding compared to the initial stage. This also explains the friction coefficient results, since the increase in the value of the friction coefficient at longer sliding distances indicated high resistance and a lower wear rate. This finding is in agreement with other recently published works (Boissonnet, Duffau & Montmitonnet 2012; Harsha 2011).

5.3.2 Influence of Particle Size and Applied Load on Three-Body Abrasion Frictional Behaviour

The friction coefficient of the materials was determined at different applied loads and sliding distances. The friction coefficient reached its steady state after a sliding distance of approximately 72 m. The averages of the friction coefficients of the materials under the different applied loads and particle sizes are presented in **Figure 5.6**. In general, the friction coefficient values were low at all applied loads and particle sizes. This indicates that the particles at the interface are rolling rather than sliding. Particle size did not appear to have a significant effect, particularly in the case of the composite in AP-O. The lowest friction coefficients were seen for the NE, which may be due to its homogeneous surface compared to the composites. This would result in fewer obstacles preventing the particles from rolling rather than sliding. The presence of fibres on the composite surface may disturb particle movement, leading to a higher friction coefficient, especially in P-O and AP-O.

Further explanation of this hypothesis is given in the next section, where the SEM micrographs of the worn surfaces are presented.

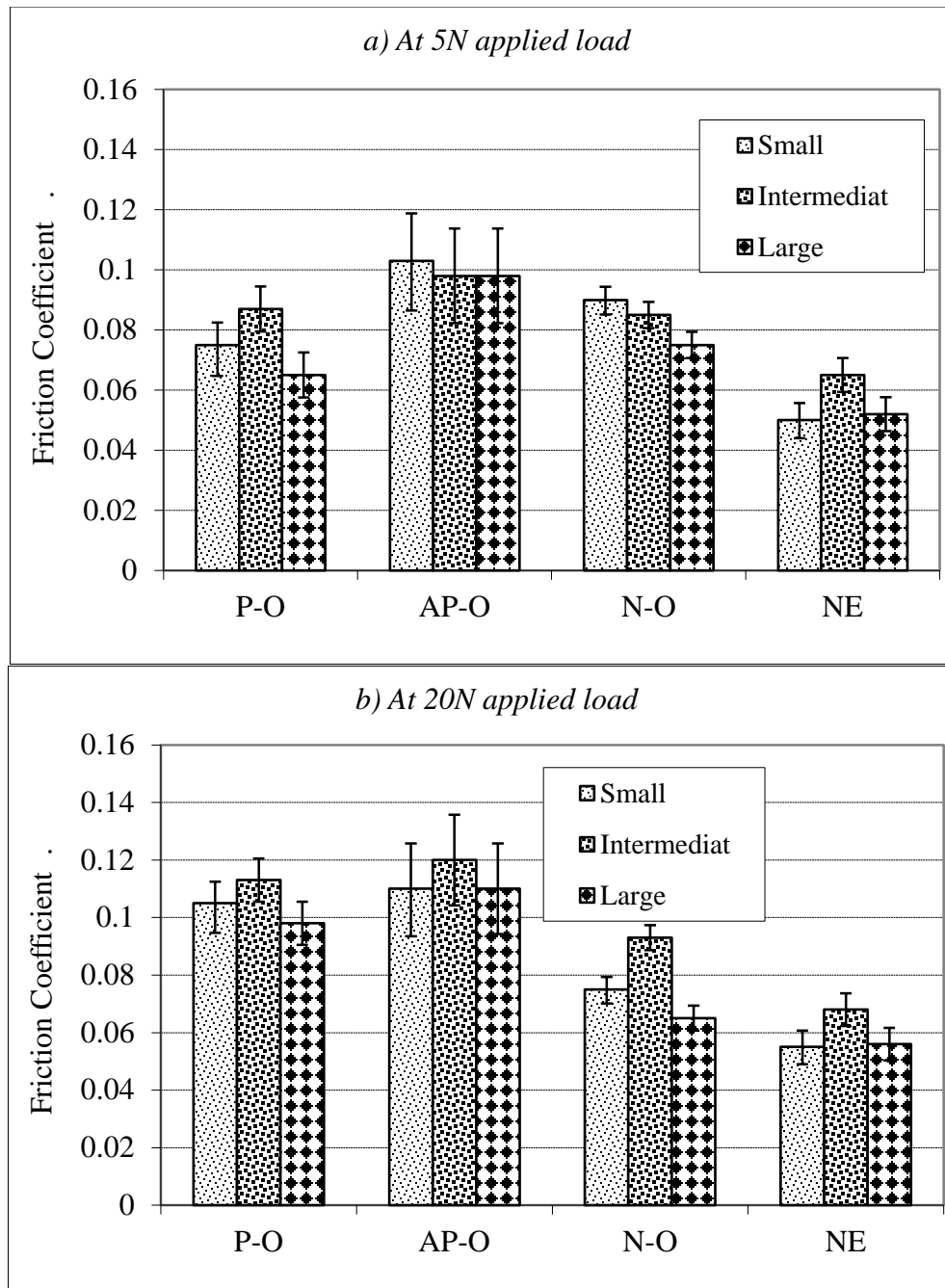


Figure 5.6 Averages of the friction coefficients associated with maximum and minimum values at different applied loads and particle sizes

5.4 DISCUSSION OF THE THREE-BODY ABRASION RESULTS

5.4.1 Rolling and/or Sliding of Particles

The 3B-A wear results revealed that the KFRE composite performed better in N-O compared to the other orientations, as well as the NE. It is important to understand the way that particles behave at the interface in the different composite orientations. There is an ongoing discussion in the literature that attempts to explain this (Yousif et al. 2010; Yousif & El-Tayeb 2010b; Wang & Essner 2001; Trezona & Hutchings 1999; Qiu & Chen 2010; Osara & Tiainen 2001). In these studies, the tests were performed on neat polymer, randomly oriented fibres and/or composites in one orientation (P-O). To clarify this issue, it is proposed that the way particles move at the interface is a key factor determining a material's wear performance, along with the material's characteristics.

Figure 5.7 illustrates the possible movement of the particles at the interface when different orientations of KFRE are exposed to the rubbing area. It proposes that when the particles move on the composite surface, their movement direction can be disturbed by transfer from the resinous (epoxy) phase to the fibrous (kenaf) phase. In the case of N-O, the particles may either move on the end of the fibres or on the hard part of the composite in the epoxy regions. Since the surface is uniform along the sliding pathway; i.e., both at the ends of the fibres and in the resinous regions, there are fewer obstacles to the movement of the particles and the possibility of rolling is higher than that of sliding. This results in less removal of materials (**Figure 5.1**) and

a low friction coefficient (**Figure 5.5**). These factors could explain the results obtained for KFRE in N-O.

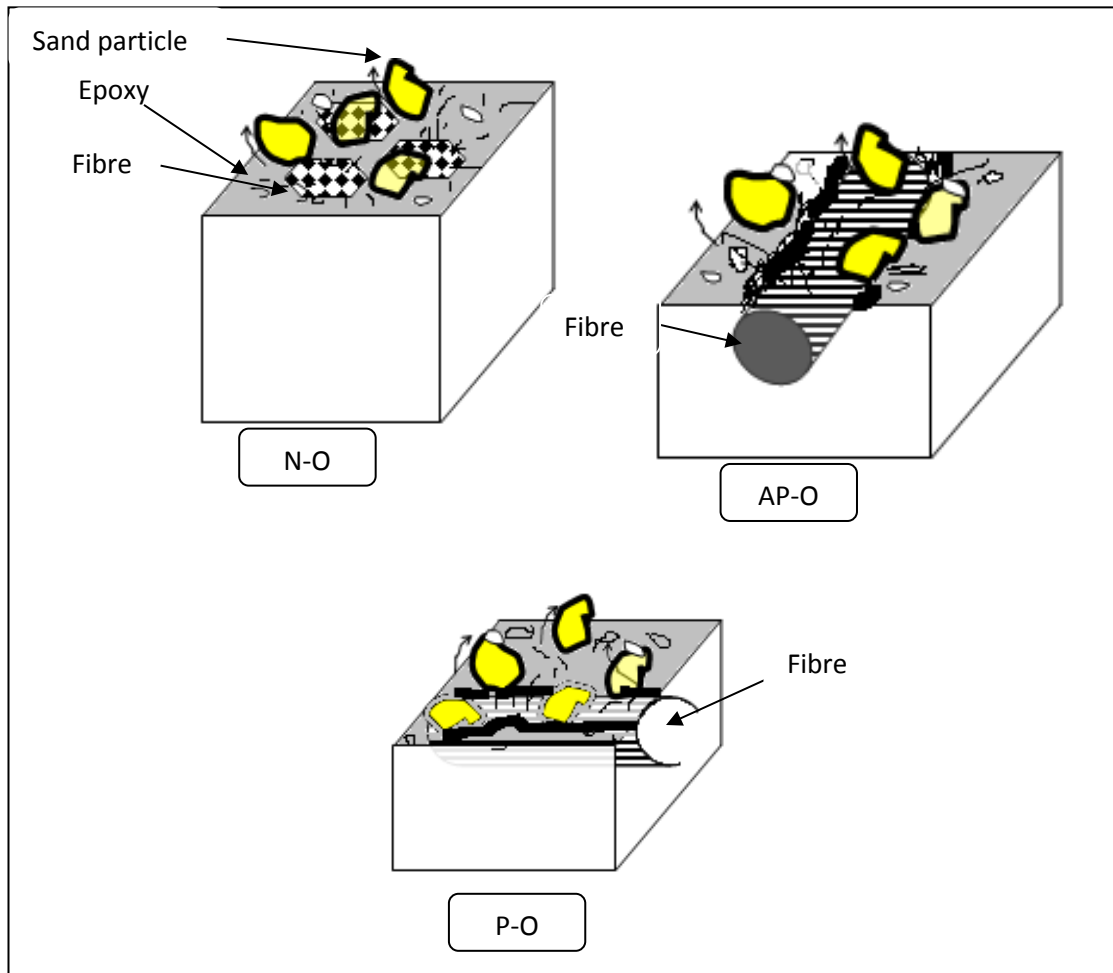


Figure 5.7 Proposed particle movements on the composite surface for fibres in three different orientations

Meanwhile, for KFRE in P-O, it is proposed that the particles show both rolling and sliding movements, where there is strong possibility that particles may penetrate within the large exposed areas of the fibres. Penetration of particles (pitting) into the surface of the composites will disturb other particle movements and may cause

accumulation of particles at the interface. This will lead to high levels of material removal from the surface, which may explain the poor performance of the KFRE composites in P-O. This wear behaviour and mechanism can also be applied to the composite in AP-O. Moreover, the fibres are oriented perpendicular to the particle sliding direction, which increases the disturbance of particle movement and can result in more material removal in this orientation; KFRE has the poorest behaviour in AP-O (**Figure 5.3**). Further, particle size may control the movement behaviour of the particles at the interface as well. In the next section, scanning electron micrographs of the collected sand particles and worn composite surfaces after the tests will help to explain these arguments.

5.4.1.1 Morphology of The Sand Particles After The Tests

The sand particles were collected after each test and some were observed using the SEM. Samples of the collected particles are presented in **Figure 5.8**, which shows the micrographs of the different sized sand particles after a test conducted at an applied load of 20 N with a sliding distance of 0.18 km. After all tests, particularly those at high applied loads, the particles showed fracturing during the sliding process. This can be seen in the intermediate and large (**Figure 5.8 b&c**) particles, which confirms that high stress 3B-A occurred when the intermediate and large particles were used. With particles in this size range (650–1,400 μm), fewer are present at the interface than when smaller particles (370–390 μm) are used, which means that fewer particles carry higher stress loads. The presence of this high stress at the interface leads to fracture of the particles; i.e., a 3B-A process is taking place.

In contrast, the small particles (370–390 μm) (**Figure 5.8a**) exhibited no obvious reduction in their size and there was no evidence of fracturing. This is due to the large number of particles at the interface, with the stress being evenly distributed between them, allowing them to maintain a relatively well preserved shape compared to the larger particles under the same conditions. Despite the fact that the rubbing process occurs between polymer and stainless steel in the presence of sand particles, it appears that with the smaller particles, a low stress 3B-A process takes place. This is in agreement with the study by Gates (1998), who reported that high stress 3B-A occurs when particles fracture during the rubbing process. Meanwhile, under low stress there is no damage to the particles. Similar findings have been reported elsewhere (Yousif et al. 2010). Therefore, 3B-A tests using a metal counterface do not necessarily produce high stress conditions. Investigation of particle morphology is strongly recommended after testing to determine the type of 3B-A mechanism.

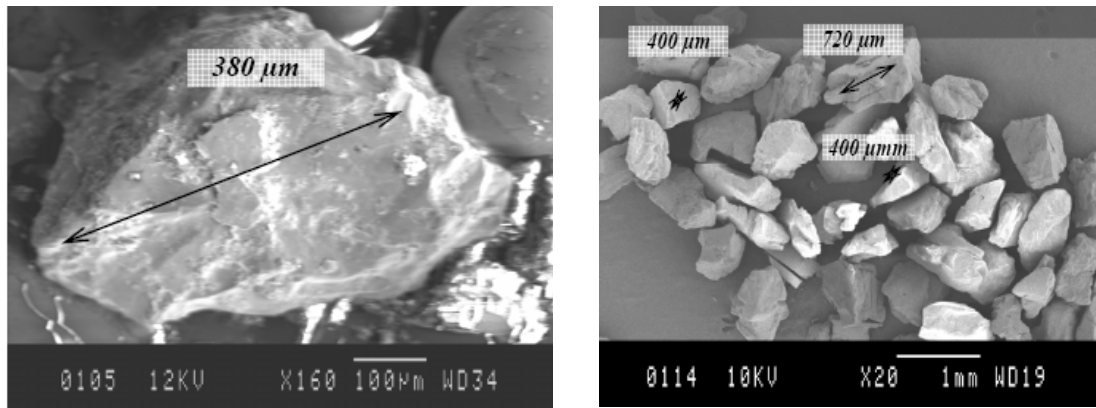
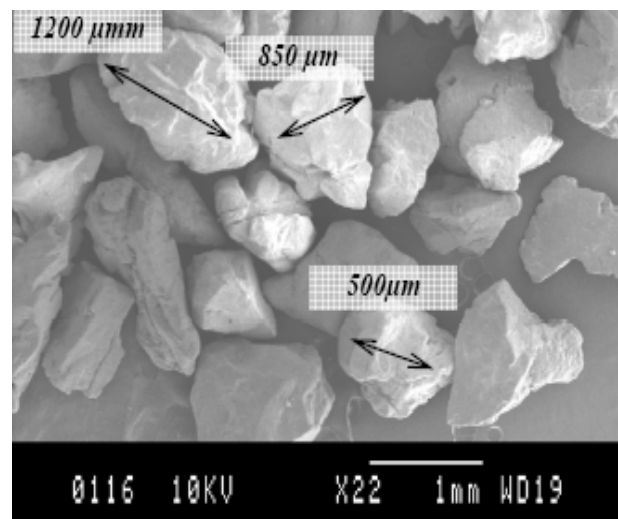
a) *Small size*b) *Intermediate size*c) *Large size*

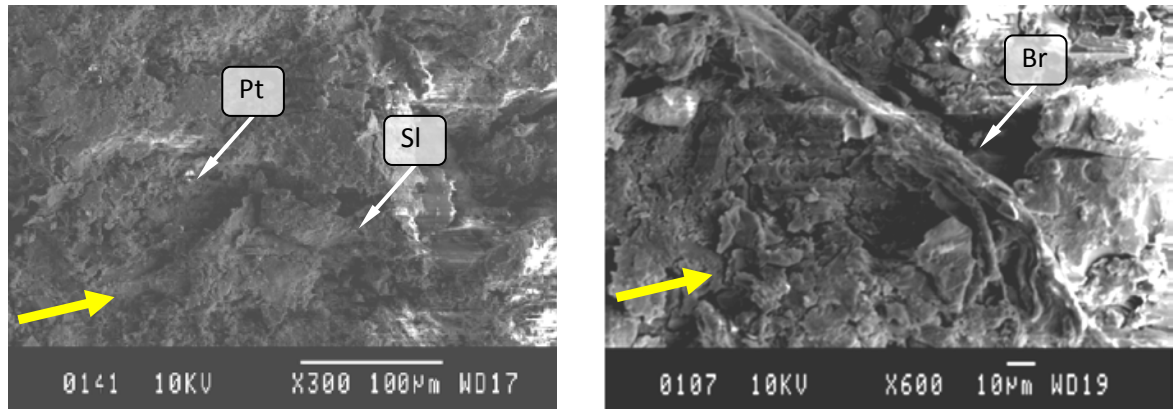
Figure 5.8 Micrographs of three different sizes of sand particles after the test at an applied force of 20 N

5.4.2 Worn Surface of the Composites after the Three-Body Abrasion Tests

5.4.2.1 Observations on KFRE at AP-O

The micrographs of the composite surface after the tests at AP-O under different operating parameters are shown in **Figures 5.9–5.11** for all three sizes of sand particles. In general, severe damage was seen in both the resinous and the fibrous regions when the composite was tested in AP-O (**Figure 5.9a**). While the particles were moving perpendicular to the fibres, breakage, delamination and pulling out of fibres occurred, as shown in **Figure 5.9b**. Moreover, the resinous regions were exposed to pitting (*'Pt'*), sliding (*'Sl'*) and sand penetration processes. This can be observed in both micrographs (applied loads of 5 N and 20 N). It is proposed that when small sand particles are used, there are a large number of particles at the interface and the stress is distributed evenly between them. Despite this, there were high levels of damage on both the resinous and the fibrous regions in the presence of small sand particles. This was mainly due to the orientation of the fibres, where obstacles to the particles' movements result in penetration of the particles and damage to the bonding of the fibres with the matrix. Despite this, the small particles did not demonstrate any fracturing. As reported in Section 5.4.1.1, the particles released their energy and impact on the composite surface. Further, it is well known that sand particles are much harder than the epoxy matrix, kenaf fibres and steel, which allows the particles to preserve their shape and size while damaging the composite surface. Suresha et al. (2013) reported similar findings when carbon fabric reinforced epoxy composites were tested against small sand particles. In their study, the orientation of the carbon fibres was similar to the AP-O used in the current work.

Despite the fact that carbon fibre is much stronger than kenaf fibre, the damage to the epoxy composites based on carbon fibres was similar to that seen in the current study. Hence, it appears that small particles damage the composite surface because the particles are harder than the composites.



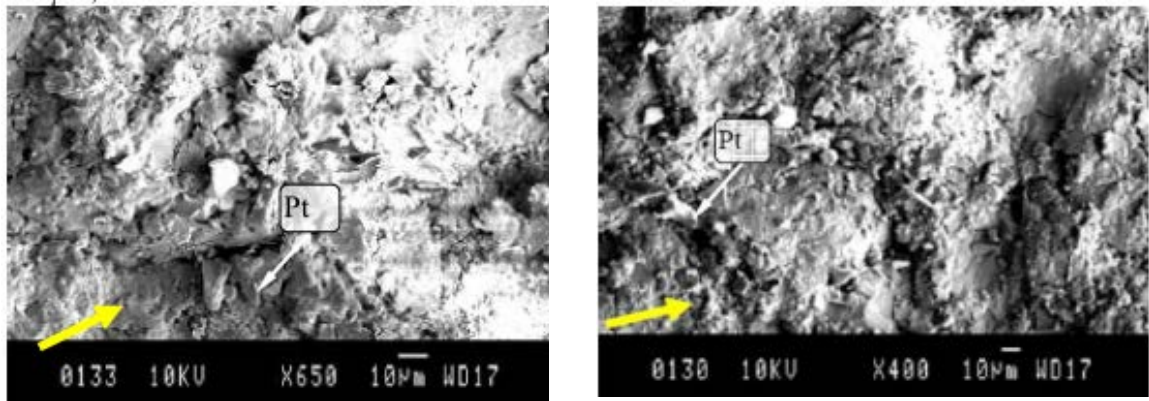
a) At a load of 5 N, particle size of 370–390 μm

b) At a load of 20 N, particle size of 370–390 μm

Figure 5.9 SEM micrographs of KFRE composites in AP-O tested under different conditions against a particle size of 370–390 μm (Br: Breakage; Pt: Pitting; SI: Sliding)

Figure 5.10 a&b presents the micrographs of the KFRE composite worn by intermediate sized particles (650–750 μm) at applied loads of 5 N and 20 N respectively. Pitting, fractures and defragmentation occurred during the 3B-A test, particularly in the epoxy regions. This indicates the presence of fatigue loading at the interface, which represents a rolling movement of the particles at the interface, associated with deep penetration. This may explain the poor wear and frictional performance of the composites in this orientation (**Figures 5.3 and 5.5**). Further, the large sand particles (1,200–1,400 μm) cause greater damage on the surface of the composites in AP-O, as can be seen in **Figure 5.11**. At the low applied load of 5 N,

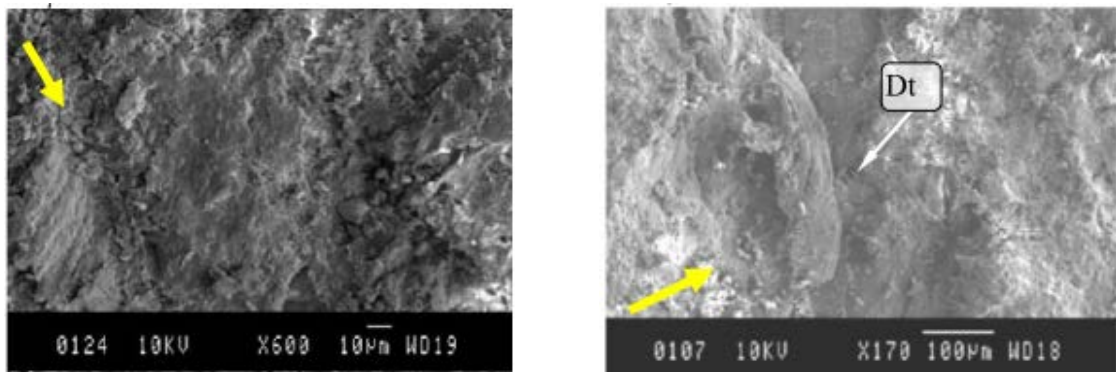
Figure 5.11a shows the ploughing caused by the sand particles on the surface of the composite. At the higher applied load of 20 N, ploughing processes were taking place since deep penetration of the particles in the surface was evident, followed by sliding and then rolling. This resulted in detachment and peeling of the fibres, leading to high levels of material removal and poor wear performance (**Figure 5.3c**). Since there are fewer intermediate and large particles at the interface, they carry a high stress and energy load, leading to the deep penetration associated with the ploughing process. This behaviour has been reported in the literature under both high and low stress 3B-A. Under high stress 3B-A, glass fibre reinforced polyester composites exhibited similar damage, despite the presence of hard reinforced fibres such as glass at the interface (Yousif & El-Tayeb 2010b). Further, severe detachment and delamination of the glass fibres was seen, which is in agreement with the current study. It appears that the brittleness of the glass fibres significantly worsened the polyester composite surface. The wear rate of the glass-polyester composites was above 5 mg/N at similar operating parameters to those of the current study, which showed that KFRE has a wear rate of less than 1 mg/N. In other words, natural fibres such as kenaf help to absorb the 3B-A load more efficiently than glass fibres, and confer high levels of protection to the resinous regions of the matrix.



a) At a load of 5 N, particle size of 650–750 μm

b) At a load of 20 N, particle size of 650–750 μm

Figure 5.10 SEM micrographs of KFRE composites in AP-O tested under different conditions against a particle size of 650–750 μm
(Pt: Pitting)



a) At a load of 5 N, particle size of 1,200–1,400 μm

b) At a load of 20 N, particle size of 1,200–1,400 μm

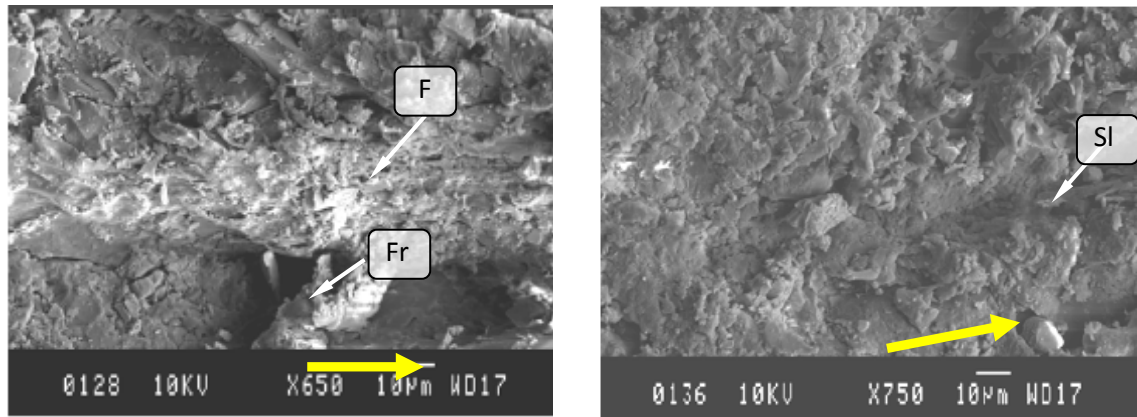
Figure 5.11 SEM micrographs of KFRE composites in AP-O under different conditions against a particle size of 1,200–1,400 μm
(Dt: Detachment)

5.4.2.2 Observations on KFRE at P-O

In the case of composite in P-O, the fibre is parallel to the sliding direction and directs the sand particles in a way that is different from that seen in the AP-O. The composite in AP-O may distribute the movement of the particles, while the P-O cannot. **Figure 5.12** shows the micrographs of the KFRE composite in P-O subjected to 3B-A with fine sand particles (370–390 μm). At applied loads of 5 and 20 N, there were clear signs of a ploughing process during the sliding, which were very apparent on the resinous regions. The surface was exposed to fracture loading in the initial stage of the sliding process, generating grooves on the surface. This was followed by particles sliding and rolling, leading to the ploughing process. Moreover, since the particles were relatively small, they were able to penetrate between the fibres, where the damage was more pronounced than in the epoxy regions. Despite this, the fibres were still well adhered to the matrix, and there was no evidence of delamination or pull-out of fibres. Thus, it appears that the high level of material removal from the resinous regions is the main reason for the low performance of the composites in this orientation.

When particle sized between 1,200 and 1,400 μm were used the damage was more severe than that caused by the small particles (**Figure 5.13**). This is due to the high pressure caused by the particles, which caused debonding of the fibres and deep penetration of the particle into the composite surface. **Figure 5.13a** shows the composite surface after testing with the low applied load of 5 N and the large sand

particles. Defragmentation and fracture in the resinous areas, particularly those covering the fibres, was evident, since the fibres are exposed.

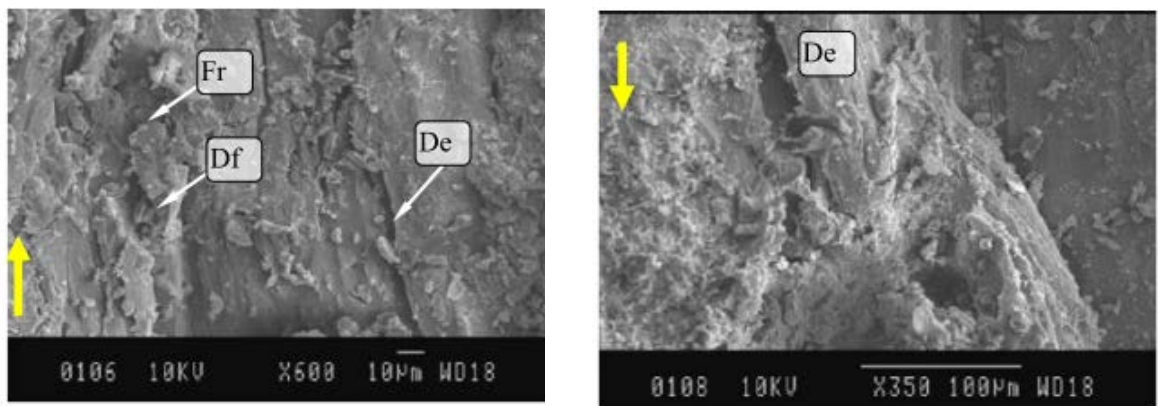


a) At a load of 5 N, particle size of 370–390 μm

b) At a load of 20 N, particle size of 370–390 μm

Figure 5.12 SEM micrographs of KFRE composites in P-O tested at different conditions against particles of 370–390 μm

(F: Fibre; Sl: Sliding; Fr: Fracture)



a) At a load of 5 N, particle size of 1,200–1,400 μm

b) At a load of 20 N, particle size of 1,200–1,400 μm

Figure 5.13 SEM micrographs of KFRE composites in P-O tested under different conditions against particles sizes of 1,200–1,400 μm

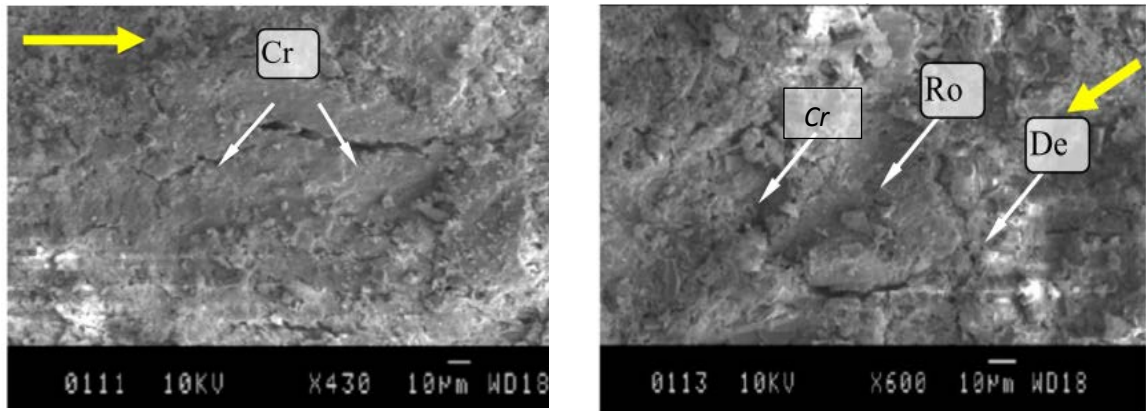
(De: Debonding; Fr: Fracture; Df: Defragmentation)

5.4.2.3 Observations on KFRE at N-O

In the previous sections, the micrographs of the worn surfaces of the composites in P-O and AP-O showed severe damage, including delamination, debonding and pull-out of fibres, in the resinous regions of the composites. In these orientations, the whole fibres are exposed to the high stress 3B-A and this exposure results in the detachment and the damage to the fibres. Further, in the case of the P-O, the sand particles create a pathway by ploughing the resinous regions, which results in damage to the composite surface.

When the composite is oriented in N-O, the ends of the fibres are exposed to the rubbing area while the whole fibres are in the bulk of the composite, which makes pull-out and detachment of the fibres difficult compared the other orientations. **Figure 5.14** displays the micrographs of the composite in N-O tested with fine particles. Micro-cracking on the fibre ends, combined with slight debonding of a small area and pitting, especially with the high applied load of 20 N, was evident, although there was no detachment or pull-out of fibres. With the intermediate sized of particles, similar wear mechanisms occurred (**Figure 5.15**). At the higher applied load and with larger particles, pitting and penetration of the particles was found, as depicted in **Figure 5.16**. However, the damage appeared to be much less significant than that exhibited when the composites were tested in P-O and AP-O. This strengthens the argument outlined in **Figure 5.7**. Moreover, there was no sign of particle sliding, implying that the particles were in a rolling movement. This supports

the lower friction coefficient and wear rate of the composite in this orientation (Figures 5. 3 and 5. 5).

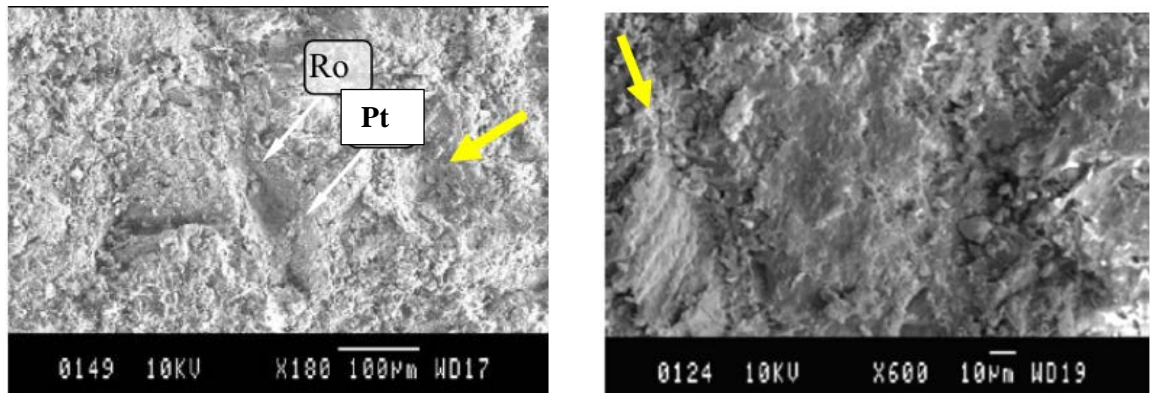


a) At a load of 5 N, particle size of 370–390 μm

b) At a load of 20 N, particle size of 370–390 μm

Figure 5.14 SEM micrographs of KFRE composites in N-O under different conditions against a particle size of 370–390 μm

(Ro: Rolling; De: Debonding; Cr:Crack)

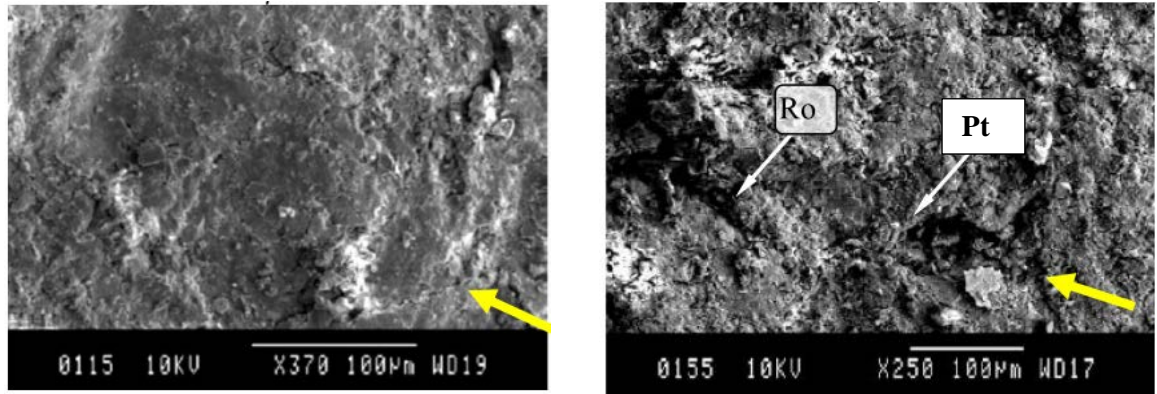


a) At a load of 5 N, particle size of 650–750 μm

b) At a load of 20 N, particle size of 650–750 μm

Figure 5.15 SEM micrographs of KFRE composites in N-O tested under different conditions against a particle size of 650–750 μm

(Pt: Pitting; Ro: Rolling)



a) At a load of 5 N, particle size of 1,200–1,400 μm

b) At load of 20 N, particle size of 1,200–1,400 μm

Figure 5.16 SEM micrographs of KFRE composites in N-O tested at different conditions against a particle size of 1,200–1,400 μm

(Pt: Pitting; Ro: Rolling)

5.5 SIMULATION OF THE DAMAGE MECHANISM TO THE COMPOSITE SURFACE

In this section, an attempt to study the high stress 3B-A wear behaviour of polymeric composites based on kenaf fibres was made by simulation. A simulation model was developed using ABAQUS software to study the damage features on the composite surface at different pressures and particle angles in three different fibre orientations. The pressure was determined by the flow rate and the applied load observed during the experiments, with the load assumed to be static. The contact between the fibre and the matrix is bonded. Finite element analysis was performed by constructing a simple model consisting of a sand particle under five different pressures and attack angles (θ) (**Figure 5.17**). Because the model is downscaled, the particle was set to travel at a lower velocity than the actual speed with respect to the orientation of the

fibre; for example, perpendicular to the fibre under N-O and parallel to the fibre under P-O. The boundary of the composite model was set to ENCASTRE (fix) at the bottom and sides (**Figure 5.18**).

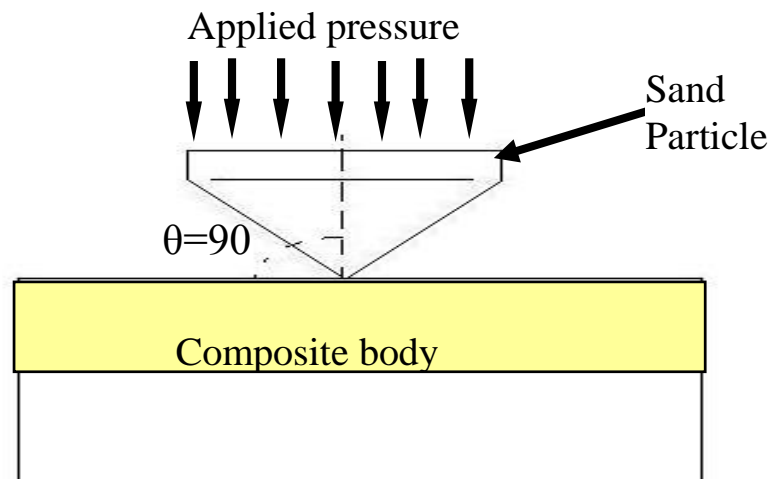


Figure 5.17 Attack angle θ of sand particle

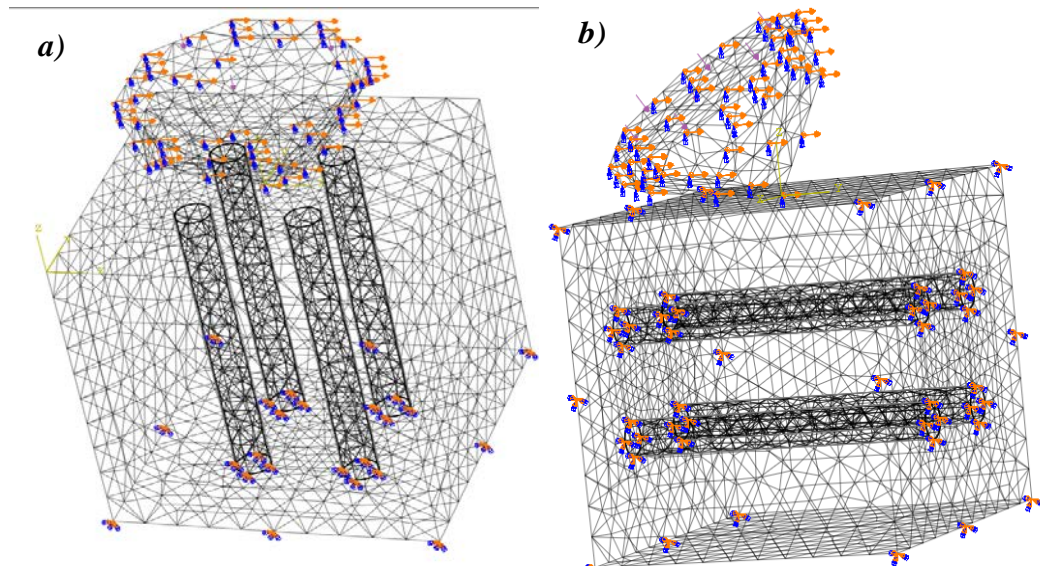


Figure 5.18 Boundary conditions for *a*) N-O and *b*) P-O

In the material properties input, the materials assumed to have elastic behaviour with isotropic characteristics. At the young's modulus and Poisson's ratio, yield strength and plastic strain used as input for the fibre, matrix and the sand particle. Contact between the fibre and the matrix was controlled by the interaction technique and properties in the Abaqus software, in which surface to surface option was used. Under this assumption, the master surface is the matrix since the matrix is fixed in the boundary conditions. Meanwhile, the slave surface is the outer layer of the fibre. With regards to the mesh generation for each part, different mesh was obtained by the software. For the matrix, the approximate global size was 0.05 mm and curvature controlled at maximum deviation factor of 0.1. For the fibres, the size was much smaller to about 0.005 and the maximum deviation factor was 0.01; similar to this the mesh for the particle was developed.

Setting the appropriate boundary condition for this model is important to generate an accurate approximation. In order to simplify the analysis, whereby an infinite of direction can be randomly travelled by the sand particle, and only three orientations were considered in this analysis. For the parallel orientation and antiparallel orientation, which declared in the finite element analysis, it is difference from the actual experiment. In the finite element analysis, each orientation declared is referring to the direction travel by the particle with respect to the fiber orientation.

The sand particle is set to travel normal to the fiber orientation. For the parallel orientation, the sand particle set to travel parallel to the orientation of the fiber and antiparallel to the orientation of the fiber for the antiparallel orientation. The assumptions made in the analysis are as follows

- The model particle is isolated from the rest
- The particle moves at 1 m/s across the surface
- The model particle only has a degree of freedom at the direction at which it travels
- Model composite is isolated from the rest of the composite
- Poisson effect is ignored for maximum effect of the analysis.
- Interfacial between the fiber and the matrix is frictionless in order to obtain worse situation.

5.5.1 Results of the Simulation

Different geometries of composites subjected to sand particles at different attack angles were developed to investigate the influence of the fibre orientation, pressure and attack angle on the 3B-A damage behaviour of the KFRE composite. For each of the geometries developed, the results of the stress were collected on both fibrous and resinous regions before failure (see **Appendix B**). The resistances of the composites to the stress induced by the particles were then determined.

For each geometry, each part was separated and the stress distribution and maximum value was determined. Samples of the results are presented in **Figure 5.19**, which shows the stress distribution on the composite surface in N-O and P-O, the fibres, the sand and the surface of the composites with the sand particles hidden. Different angles of attack by the sand and the stress subjected by the composite were selected and the required data were determined. A summary is presented in **Figure 5.20**, showing the influence of the attack angle and the stress induced by the sand for different KFRE orientations. This figure presents useful information on the maximum stress that the composite can be subjected to before failure. With regard to the effect of attack angle, the greater the angle, the lower the stress that the surface can carry. When the composite was oriented in either P-O or AP-O, there were no major differences since less stress could be carried by the surface at these orientations compared to N-O. At all selected attack angles and stress values, the composite in N-O was able to carry more stress than those in P-O and AP-O. These results strongly support the experimental results, which showed that the KFRE composites performed better when the fibres were oriented normally with respect to the counterface. A sample of the stress distribution on the composite surface oriented in N-O is given in **Figure 5.21**. Penetration of the sand particle is evident and can be found on the fibre ends, which generates a high stress region in the bonding area (**Figures 5.14 b** and **5.16 b**). Despite this, the deep bonding area still has a less stressed region in which the fibre was still well adhered, and there is no damage in the bonding region in the depth of the composites (**Figure 5.21 c** and **d**). In **Figure 5.21b**, maximum stress can be observed at the top ends of the fibres while the remaining portion of the fibre is still intact.

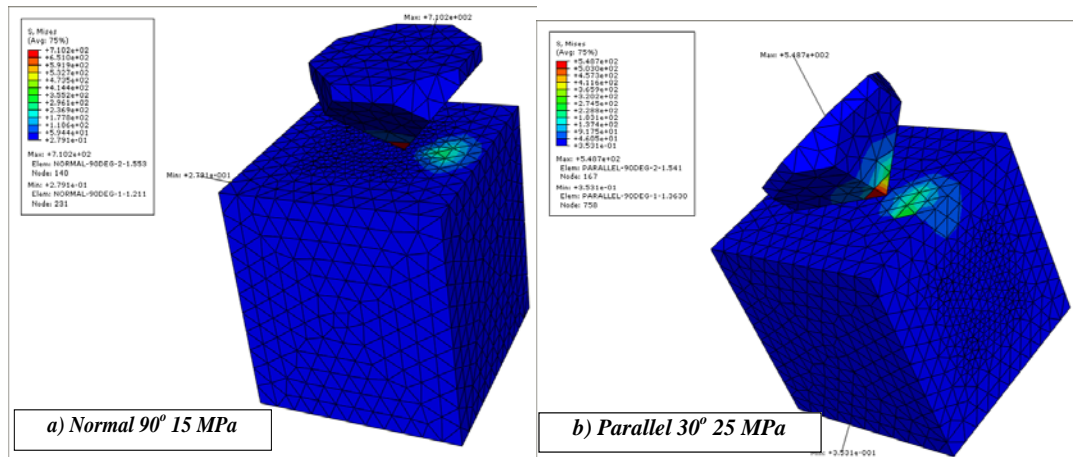


Fig. 5.19 continued

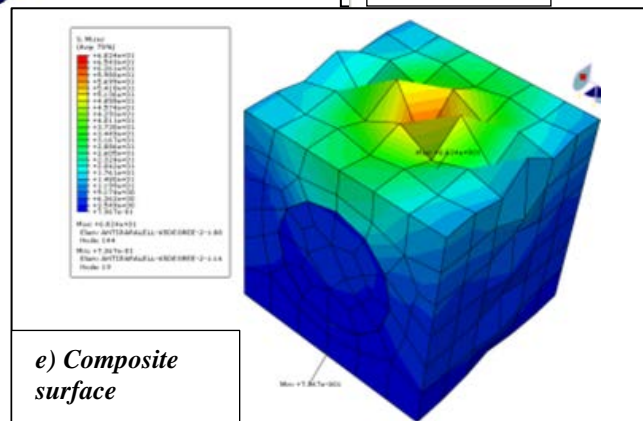
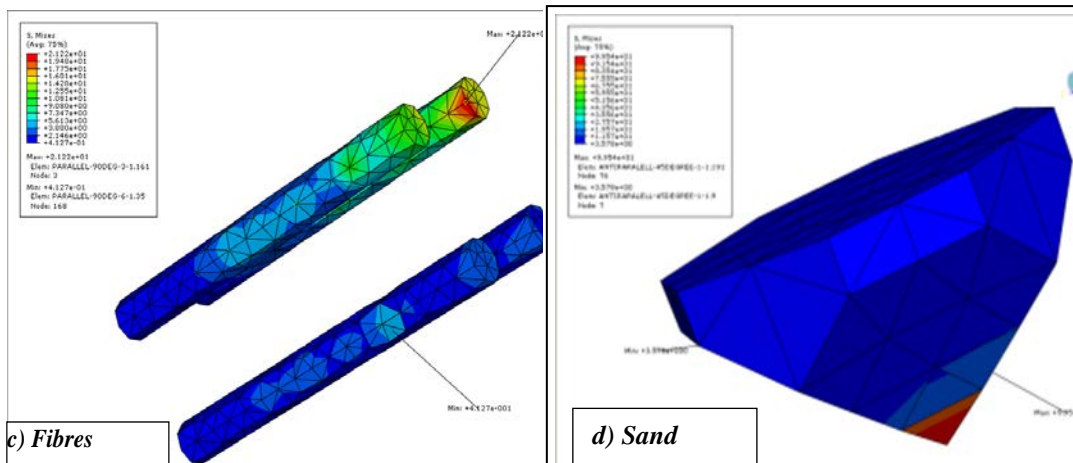


Figure 5.19 Stress distribution in the composites

From the simulation, it can be concluded that to obtain high wear resistance from fibre-polymer composites, it is highly recommended to orient the fibres normally with respect to the counterface. From the literature, composites in which the fibres were oriented either parallel or anti-parallel to the counterface e.g. carbon-epoxy and glass-epoxy composites (Suresha et al. 2007), and glass-vinyl ester composites (Suresha & Chandramohan 2008), suffered from high material removal from the surface due to the orientation of the fibre, i.e. weak bonding region and surface strength. The numerical results are in highly agreement with the experimental data given in **Figure 5.5**, in which oriented the fibre normally introduces better tribological performance to the epoxy composites compared to the others. **Fig. 5.20b** shows that the composites can be exposed to high stress at the 55 degrees since the stress can reached up to 275 MPa. This suggests that the composite in normal orientation performs better than the others which are in agreement with the experimental data in **Figure. 5.5**.

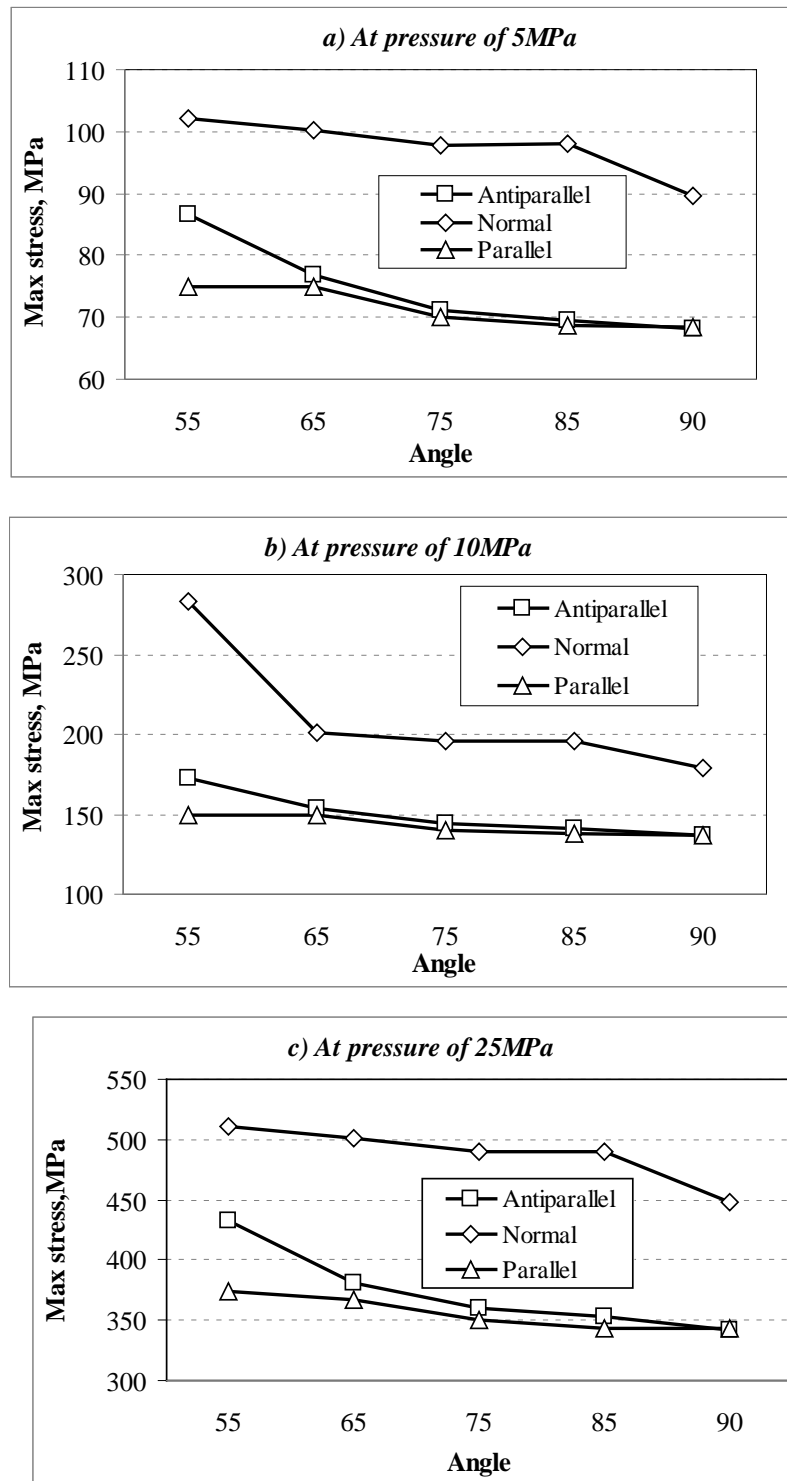


Figure 5.20 Maximum stress versus attack angle at different pressures and composite orientations

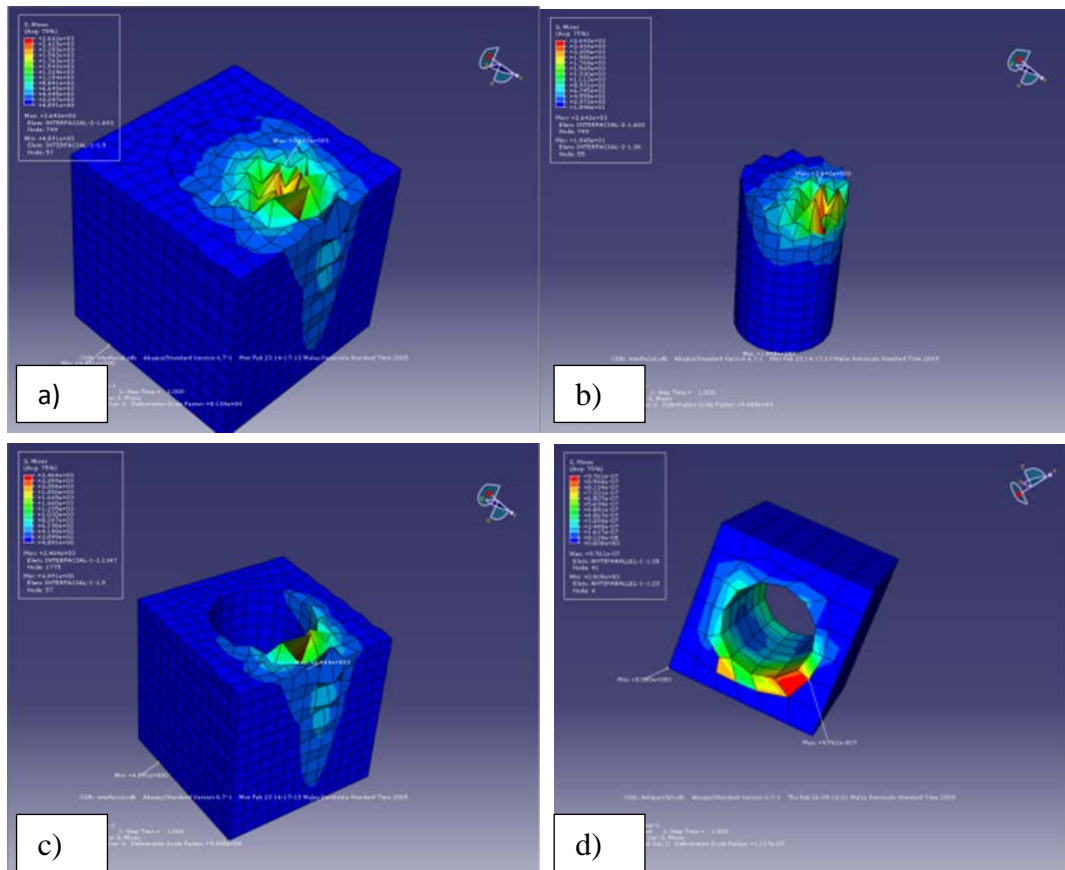


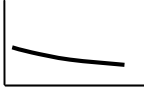
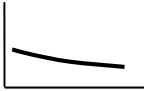
Figure 5.21 Stress distribution on the composite surface in N-O: fibre, bonding area and the resinous regions, a) the fibre embedded in the matrix, b) the fibre alone; c) the matrix without the fibre and d) inner surface of the matrix showing the stress distribution.

5.6 COMPARISON WITH PREVIOUS STUDIES

There is only one published study on high stress 3B-A of a polymeric composite based on natural fibres: that of Yousif and El-Tayeb (2008a) investigating a polyester composite based on treated/untreated oil palm fibres. **Table 5.1** summarises the range of the wear rates and their trends for the current study and that of Yousif and El-Tayeb (2008). The table indicates that kenaf fibre provide better support to the polymer matrix than the oil palm fibres; i.e., the KFRE composites are in the low

wear rate range. This is primarily due to the high interfacial adhesion of the kenaf fibres compared to that of the treated/untreated oil palm fibres. The latter showed high removal of materials during the rubbing process due to poor interfacial adhesion. Moreover, in that study, the oil palm fibres were randomly distributed within the matrix, another reason for the poor performance of the oil palm fibres compared to the kenaf fibres, which were normally oriented.

Table 5.1 3B-A wear results of KFRE (in N-O), untreated oil palm/polyester (UT-OPRP) and treated oil palm/polyester (T-OPRP) composites at 50 rpm rotational speed

Materials	3B-A wear rate range (mg/N) and its trend	Wear performance of the composite with respect to others
Kenaf (N-O)-Epoxy [current]	 0.5–0.22	Best
Treated oil palm-polyester (Yousif & El-Tayeb 2008a)	 4.2–2.25	Moderate
Untreated oil palm-polyester (Yousif & El-Tayeb 2008a)	 5–4.2	Poor

5.7 SUMMARY

- Fibre orientation has a significant influence on the 3BA wear and frictional behaviour of the KFRE composite. When the composite was tested in N-O, better wear and frictional performance were achieved. In N-O, the composite performs better than NE and the reduction in the wear rate was approximately 50–75 per cent. In contrast, the presence of the kenaf fibres in parallel and anti-parallel orientations worsened the wear and frictional performance of the epoxy under certain conditions.
- The predominant wear mechanisms were detachment and breakage of fibres and fracture and defragmentation in the epoxy regions when the composites was tested in P-O and AP-O. Meanwhile, micro-cracks at the ends of the fibres was the dominant wear mechanism in N-O.
- It is strongly recommended to assess the morphology of the particles after testing to determine whether high or low stress 3B-A has taken place. The current study showed both types. When small particles were used, low stress 3B-A occurred and there was no damage evident on the particles after the tests. On the other hand, tests with intermediate and large particles showed high stress 3B-A, since the particles were fractured after the tests.
- Numerical analysis using ABAQUS FEM software has enabled a better understanding of the wear mechanisms under high stress 3B-A. Both the particle attack angle and the applied pressure influence the damage features that occur on the composite surface. The most important factor affecting the wear behaviour of the composite is the fibre orientation, with normally-oriented fibres generating higher stress on the composite surface.

CHAPTER 6: CONCLUSIONS AND RECOMMENDATIONS

6.1 CONCLUSIONS

Epoxy composites based on natural kenaf fibres were developed in order to examine the possibility of using natural fibres as reinforcements for tribological applications. The mechanical properties and interfacial adhesion of the untreated and treated KFRE composites were evaluated. Adhesive wear tests were performed against a smooth stainless steel counterface under wet and dry contact conditions at different operating parameters and fibre orientations with respect to the sliding direction. Abrasive wear tests were carried out using the 3B-A technique against a steel counterface to simulate high stress 3B-A of the kenaf-epoxy composites. An ANN model was developed to predict the friction coefficient of the composites under adhesive dry contact conditions, with different operating parameters and fibre orientations as input data. ABAQUS software was used to assist with the analysis of the stress on the composites under high stress 3B-A. From these mechanical, adhesive and abrasive wear results, the following conclusions may be drawn:

1. *From the mechanical point of view*, treating the kenaf fibres with 6 per cent NaOH contributed to the high interfacial adhesion of the fibres with the matrix, resulting in a significant improvement in the mechanical properties of the epoxy composites.
2. *Under dry contact conditions*, the operating parameters had a relatively small influence on the wear and frictional performance of the composites. However, the orientation of the fibres strongly influenced the wear and frictional

behaviour of the KFRE composites. When oriented in N-O, kenaf fibres enhanced the wear performance of the epoxy by about 85 per cent. The wear mechanisms of the composite were predominated by micro-cracks (in N-O) and debonding (in P-O) in the fibrous regions and deformation in the resinous regions.

3. ***Under wet contact conditions***, the presence of water at the interface resulted in very low friction coefficients, in the range of 0.035–0.045. This is largely due to the removal of the debris at the interface and cooling of the contacted surfaces, which lowers the interaction between the asperities in contact. The SEM observations revealed the abrasive nature of the wear mechanism and peeling of fibres when the composites were tested in AP-O and P-O. Meanwhile, in N-O, the ends of the fibres resisted the sliding process and protected the resinous regions, which was the main reason underlying the better wear performance of the composite in this orientation.
4. ***From the ANN results***, it was shown that an ANN model can be developed with different training and learning functions to control the error and predictive performance of the model. In the current study, a log-sigmoid transfer function and the SCG learning rule with two hidden layers proved to give the optimum configuration to predict and obtain low error (<0.1) with an experimental data set of about 1,095 points.
5. ***Under 3B-A***, the fibre orientation and particle size determines the wear and the frictional behaviour of the KFRE composites. The presence of kenaf fibres in P-O and AP-O worsened the wear and frictional performance of the epoxy under certain operating parameters. Meanwhile, in N-O, better wear

and frictional performance were achieved, since a 50–75 per cent reduction in the wear rate was achieved compared to the NE as well as the composites in the other orientations.

6. *Under 3B-A*, surface observations revealed different wear mechanisms that were highly dependent on the fibre orientation and particle size. When the composite was tested in P-O and AP-O, the dominant wear mechanisms were detachment and breakage of fibres and fracture and defragmentation in the epoxy regions. Meanwhile, the most pronounced wear mechanism observed in the composite in N-O was micro-cracks at the ends of the fibres. The movements of the particles at the interface determine the type of damage to the surface. In the case of particle rolling, pitting and fracturing could be found in both the resinous and the fibrous regions. However, high levels of damage occurred with sliding movements, since detachment and breakage were observed in the fibrous regions along with ploughing in the resinous regions.
7. *Numerical analysis of the 3BA type* can aid in understanding the wear mechanisms occurring during high stress 3B-A. In this study, the attack angle and applied pressure influence the damage mechanisms on the composite surface. The numerical results were in strong agreement with the experimental findings, where the dominant factor affecting the wear behaviour of the composite was the fibre orientation. The N-O resulted in higher stress resistance on the composite surface compared to the other orientations, and is the main reason for the high wear resistance of the composite in N-O compared to those in P-O and AP-O.

6.2 RECOMMENDATIONS FOR FUTURE WORK

The areas deserve further investigation are listed below:

- Since kenaf fibres were found to be a good alternative candidate for synthetic fibres, and have better characteristics than other natural fibres, a better understanding of the degradation of these fibres is strongly recommended to assist the commercialisation process.
- Incorporation of solid lubricant additives may overcome the problem of the high adhesive friction coefficient of the KFRE under dry contact conditions, an important question that merits further investigation.
- In some applications, composites may be subjected to 3B-A and/or 2B-A loadings in the presence of liquids (such as water) at the interface; for example, water pumps in mining. Consequently, 3B-A and 2B-A under wet contact conditions should be studied to investigate the behaviour of KFRE composites under these conditions.

REFERENCES

- AKAIKE, H. 1974. Stochastic theory of minimal realization. *Automatic Control, IEEE Transactions on*, 19, 667-674.
- ALEKSENDRIĆ, D. 2010. Neural network prediction of brake friction materials wear. *Wear*, 268, 117-125.
- ALEKSENDRIĆ, D. & DUBOKA, C. 2006. Prediction of automotive friction material characteristics using artificial neural networks-cold performance. *Wear*, 261, 269-282.
- ALEKSENDRIĆ, D. & DUBOKA, C. 2007. Fade performance prediction of automotive friction materials by means of artificial neural networks. *Wear*, 262, 778-790.
- ALLSOPP, D., TREZONA, R. & HUTCHINGS, I. 1998. The effects of ball surface condition in the micro-scale abrasive wear test. *Tribology Letters*, 5, 259-264.
- ALSAEED, T., YOUSIF, B. F. & KU, H. 2013. The potential of using date palm fibres as reinforcement for polymeric composites. *Materials and Design*, 43, 177-184.
- AMEL, B. A., PARIDAH, M. T., SUDIN, R., ANWAR, U. M. K. & HUSSEIN, A. S. 2013. Effect of fiber extraction methods on some properties of kenaf bast fiber. *Industrial Crops and Products*, 46, 117-123.
- ARHAIM, Y., SHALWAN, A. & YOUSIF, B. 2013. Correlation between Frictional Force, Interface Temperature and Specific Wear Rate of Fibre-Polymer Composites. *Advanced Materials Research*, 685, 45-49.

- ASUMANI, O. M. L., REID, R. G. & PASKARAMOORTHY, R. 2012. The effects of alkali–silane treatment on the tensile and flexural properties of short fibre non-woven kenaf reinforced polypropylene composites. *Composites Part A: Applied Science and Manufacturing*, 43, 1431-1440.
- AZIZ, S. H. & ANSELL, M. P. 2004. The effect of alkalization and fibre alignment on the mechanical and thermal properties of kenaf and hemp bast fibre composites: Part 1 – polyester resin matrix. *Composites Science and Technology*, 64, 1219-1230.
- AZWA, Z. N., YOUSIF, B. F., MANALO, A. C. & KARUNASENA, W. 2013. A review on the degradability of polymeric composites based on natural fibres. *Materials & Design*, 47, 424-442.
- BASAVARAJAPPA, S. & ELLANGO VAN, S. 2012. Dry sliding wear characteristics of glass–epoxy composite filled with silicon carbide and graphite particles. *Wear*, 296, 491-496.
- BHUSHAN, B. 1999. *Principles and applications of tribology*, Wiley-Interscience.
- BIJWE, J., AWTADE, S. & GHOSH, A. 2006. Influence of orientation and volume fraction of Aramid fabric on abrasive wear performance of polyethersulfone composites. *Wear*, 260, 401-411.
- BIJWE, J. & RATTAN, R. 2007. Carbon fabric reinforced polyetherimide composites: Optimization of fabric content for best combination of strength and adhesive wear performance. *Wear*, 262, 749-758.
- BOISSONNET, L., DUFFAU, B. & MONTMITONNET, P. 2012. A wear particle-based model of friction in a polymer–metal high pressure contact. *Wear*, 286–287, 55-65.

- BORRUTO, A., CRIVELLONE, G. & MARANI, F. 1998. Influence of surface wettability on friction and wear tests. *Wear*, 222, 57-65.
- BRAHIM, S. B. & CHEIKH, R. B. 2007. Influence of fibre orientation and volume fraction on the tensile properties of unidirectional Alfa-polyester composite. *Composites Science and Technology*, 67, 140-147.
- BROSTOW, W., DEBORDE, J. L., JACLEWICZ, M. & OLSZYNSKI, P. 2003. Tribology with emphasis on polymers: friction, scratch resistance and wear. *Journal of Materials Education*, 25, 119-132.
- CANTERO, G., ARBELAIZ, A., LLANO-PONTE, R. & MONDRAGON, I. 2003. Effects of fibre treatment on wettability and mechanical behaviour of flax/polypropylene composites. *Composites Science and Technology*, 63, 1247-1254.
- CENNA, A. A., ALLEN, S., PAGE, N. W. & DASTOOR, P. 2001. A polyethylene-reinforced polymer composite abraded by bulk solids. *Wear*, 249, 663-671.
- CENNA, A. A., ALLEN, S., PAGE, N. W. & DASTOOR, P. 2003. Modelling the three-body abrasive wear of UHMWPE particle reinforced composites. *Wear*, 254, 581-588.
- CENNA, A. A., DOYLE, J., PAGE, N. W., BEEHAG, A. & DASTOOR, P. 2000. Wear mechanisms in polymer matrix composites abraded by bulk solids. *Wear*, 240, 207-214.
- CHAI, A. N. M., IBRAHIM, M., CHUAN, C. B. & YOUSIF, B. F. On the development of solar drying system. 2010. 469-473.

- CHAND, N. & DWIVEDI, U. 2006a. Effect of coupling agent on abrasive wear behaviour of chopped jute fibre-reinforced polypropylene composites. *Wear*, 261, 1057-1063.
- CHAND, NAVIN, AND U. K. DWIVEDI. "High stress abrasive wear study on bamboo." *Journal of materials processing technology* 183.2 (2007): 155-159.
- CHAND, N., NAIK, A. & NEOGI, S. 2000. Three-body abrasive wear of short glass fibre polyester composite. *Wear*, 242, 38-46.
- CHANG, L. & FRIEDRICH, K. 2010. Enhancement effect of nanoparticles on the sliding wear of short fiber-reinforced polymer composites: A critical discussion of wear mechanisms. *Tribology International*, 43, 2355-2364.
- CHANG, B.-P., MD. AKIL, H. & BT. MD. NASIR, R. 2013. Comparative study of micro- and nano-ZnO reinforced UHMWPE composites under dry sliding wear. *Wear*, 297, 1120-1127.
- CHAUHAN, S. R., KUMAR, A. & SINGH, I. 2010. Sliding friction and wear behaviour of vinylester and its composites under dry and water lubricated sliding conditions. *Materials and Design*, 31, 2745-2751.
- CHIN, C. W. & YOUSIF, B. F. 2009. Potential of kenaf fibres as reinforcement for tribological applications. *Wear*, 267, 1550-1557.
- DANAELAN, D. & YOUSIF, B. F. 2008. Adhesive wear performance of cfrp multilayered polyester composites under dry/wet contact conditions. *Surface Review and Letters*, 15, 919-925.
- DAVIM, J. P. 2013a. *Tribology of Nanocomposites*, Springer.
- DAVIM, J. P. 2013b. *Wear of advanced materials*, Wiley-ISTE.

- EDEEROZEY, A. M. M., AKIL, H. M., AZHAR, A. B. & ARIFFIN, M. I. Z. 2007. Chemical modification of kenaf fibres. *Materials Letters*, 61, 2023-2025.
- EL-SAYED, A. A., EL-SHERBINY, M. G., ABO-EL-EZZ, A. S. & AGGAG, G. A. 1995. Friction and wear properties of polymeric composite materials for bearing applications. *Wear*, 184, 45-53.
- EL-TAYEB, N. S. M. 2008. A study on the potential of sugarcane fibers/polyester composite for tribological applications. *Wear*, 265, 223-235.
- EL-TAYEB, N. S. M. 2009. Two-body abrasive behaviour of untreated SC and R-G fibres polyester composites. *Wear*, 266, 220-232.
- EL-TAYEB, N. S. M. & YOUSIF, B. F. Wear and friction behaviour of CGRP and WGRP composites subjected to dry sliding. 2005. 31-32.
- EL-TAYEB, N. S. M. & YOUSIF, B. F. 2007. Evaluation of glass fiber reinforced polyester composite for multi-pass abrasive wear applications. *Wear*, 262, 1140-1151.
- EL-TAYEB, N. S. M., YOUSIF, B. F. & YAP, T. C. 2006. Tribological studies of polyester reinforced with CSM 450-R-glass fiber sliding against smooth stainless steel counterface. *Wear*, 261, 443-452.
- FU, S.-Y. & LAUKE, B. 1996. Effects of fiber length and fiber orientation distributions on the tensile strength of short-fiber-reinforced polymers. *Composites Science and Technology*, 56, 1179-1190.
- GATES, J. 1998. Two-body and three-body abrasion: a critical discussion. *Wear*, 214, 139-146.

- GYUROVA, L. A. & FRIEDRICH, K. 2011. Artificial neural networks for predicting sliding friction and wear properties of polyphenylene sulfide composites. *Tribology International*, 44, 603-609.
- HAQUE, M. M., HASAN, M., ISLAM, M. S. & ALI, M. E. 2009. Physico-mechanical properties of chemically treated palm and coir fiber reinforced polypropylene composites. *Bioresource Technology*, 100, 4903-4906.
- HARSHA, A. P. 2011. An investigation on low stress abrasive wear characteristics of high performance engineering thermoplastic polymers. *Wear*, 271, 942-951.
- HARSHA, A. P. & TEWARI, U. S. 2002. Tribo performance of polyaryletherketone composites. *Polymer Testing*, 21, 697-709.
- HARSHA, A. P. & TEWARI, U. S. 2003. Two-body and three-body abrasive wear behaviour of polyaryletherketone composites. *Polymer Testing*, 22, 403-418.
- HARSHA, A. P., TEWARI, U. S. & VENKATRAMAN, B. 2003. Three-body abrasive wear behaviour of polyaryletherketone composites. *Wear*, 254, 680-692.
- HASHMI, S. A. R., DWIVEDI, U. K. & CHAND, N. 2007. Graphite modified cotton fibre reinforced polyester composites under sliding wear conditions. *Wear*, 262, 1426-1432.
- HEITZMANN, M. T., VEIDT, M., NG, C. T., LINDENBERGER, B., HOU, M., TRUSS, R. & LIEW, C. K. 2013. Single-Plant Biocomposite from Ricinus Communis: Preparation, Properties and Environmental Performance. *Journal of Polymers and the Environment*, 21, 366-374.

- HERRERA-FRANCO, P. J. & VALADEZ-GONZÁLEZ, A. 2004. Mechanical properties of continuous natural fibre-reinforced polymer composites. *Composites Part A: Applied Science and Manufacturing*, 35, 339-345.
- HOLMBERG, K., ANDERSSON, P. & ERDEMIR, A. 2012. Global energy consumption due to friction in passenger cars. *Tribology International*, 47, 221-234.
- ISLAM, M. N., RAHMAN, M. R., HAQUE, M. M. & HUQUE, M. M. 2010. Physico-mechanical properties of chemically treated coir reinforced polypropylene composites. *Composites Part A: Applied Science and Manufacturing*, 41, 192-198.
- JACOB, M., THOMAS, S. & VARUGHESE, K. T. 2004. Mechanical properties of sisal/oil palm hybrid fiber reinforced natural rubber composites. *Composites Science and Technology*, 64, 955-965.
- JAWAID, M. & ABDUL KHALIL, H. P. S. 2011. Cellulosic/synthetic fibre reinforced polymer hybrid composites: A review. *Carbohydrate Polymers*, 86, 1-18.
- JAWAID, M., ABDUL KHALIL, H. P. S. & ABU BAKAR, A. 2011. Woven hybrid composites: Tensile and flexural properties of oil palm-woven jute fibres based epoxy composites. *Materials Science and Engineering: A*, 528, 5190-5195.
- JAWAID, M., KHALIL, H. P. S. A., BAKAR, A. A. & KHANAM, P. N. 2011. Chemical resistance, void content and tensile properties of oil palm/jute fibre reinforced polymer hybrid composites. *Materials & Design*, 32, 1014-1019.

- JEAMTRAKULL, S., KOSITCHAIYONG, A., MARKPIN, T., ROSARPITAK, V. & SOMBATSOMPOP, N. 2012. Effects of wood constituents and content, and glass fiber reinforcement on wear behavior of wood/PVC composites. *Composites Part B: Engineering*, 43, 2721-2729.
- JIA, J., CHEN, J., ZHOU, H., HU, L. & CHEN, L. 2005. Comparative investigation on the wear and transfer behaviors of carbon fiber reinforced polymer composites under dry sliding and water lubrication. *Composites Science and Technology*, 65, 1139-1147.
- JIANG, Z., ZHANG, Z. & FRIEDRICH, K. 2007. Prediction on wear properties of polymer composites with artificial neural networks. *Composites Science and Technology*, 67, 168-176.
- KOOTTATHAPE, N., TAKAHASHI, H., IWASAKI, N., KANEHIRA, M. & FINGER, W. J. 2012. Two- and three-body wear of composite resins. *Dental Materials*, 28, 1261-1270.
- KU, H., WANG, H., PATTARACHAIYAKOOP, N. & TRADA, M. 2011. A review on the tensile properties of natural fiber reinforced polymer composites. *Composites Part B: Engineering*, 42, 856-873.
- LI, B. 2012. A review of tool wear estimation using theoretical analysis and numerical simulation technologies. *International Journal of Refractory Metals and Hard Materials*, 35, 143-151.
- LIU, C. Z., WU, J. Q., LI, J. Q., REN, L. Q., TONG, J. & ARNELL, A. D. 2006. Tribological behaviours of PA/UHMWPE blend under dry and lubricating condition. *Wear*, 260, 109-115.

- LIUJIE, X., DAVIM, J. P. & CARDOSO, R. 2007. Prediction on tribological behaviour of composite PEEK-CF30 using artificial neural networks. *Journal of Materials Processing Technology*, 189, 374-378.
- MARTÍNEZ, F. J., CANALES, M., IZQUIERDO, S., JIMÉNEZ, M. A. & MARTÍNEZ, M. A. 2012. Finite element implementation and validation of wear modelling in sliding polymer–metal contacts. *Wear*, 284–285, 52-64.
- MEON, M. S., OTHMAN, M. F., HUSAIN, H., REMELI, M. F. & SYAWAL, M. S. M. 2012. Improving Tensile Properties of Kenaf Fibers Treated with Sodium Hydroxide. *Procedia Engineering*, 41, 1587-1592.
- MERLINI, C., SOLDI, V. & BARRA, G. M. O. 2011. Influence of fiber surface treatment and length on physico-chemical properties of short random banana fiber-reinforced castor oil polyurethane composites. *Polymer Testing*, 30, 833-840.
- MISHRA, V. & BISWAS, S. 2013. Physical and Mechanical Properties of Bi-directional Jute Fiber Epoxy Composites. *Procedia Engineering*, 51, 561-566.
- MOLAZEMHOSSEINI, A., TOURANI, H., KHAVANDI, A. & EFTEKHARI YEKTA, B. 2013. Tribological performance of PEEK based hybrid composites reinforced with short carbon fibres and nano-silica. *Wear*, 303, 397-404.
- MYLSAMY, K. & RAJENDRAN, I. 2011. The mechanical properties, deformation and thermomechanical properties of alkali treated and untreated Agave continuous fibre reinforced epoxy composites. *Materials & Design*, 32, 3076-3084.

- MYSHKIN, N. K., PETROKOVETS, M. I. & KOVALEV, A. V. 2005. Tribology of polymers: Adhesion, friction, wear, and mass-transfer. *Tribology International*, 38, 910-921.
- NASIR, T., YOUSIF, B. F., MCWILLIAM, S., SALIH, N. D. & HUI, L. T. 2010. An artificial neural network for prediction of the friction coefficient of multi-layer polymeric composites in three different orientations. *Proceedings of the Institution of Mechanical Engineers, Part C: Journal of Mechanical Engineering Science*, 224, 419-429.
- NIRMAL, U., HASHIM, J., LAU, S. T. W., MY, Y. & YOUSIF, B. F. 2012. Betelnut fibres as an alternative to glass fibres to reinforce thermoset composites: A comparative study. *Textile Research Journal*, 82, 1107-1120.
- NIRMAL, U., YOUSIF, B. F., RILLING, D. & BREVERN, P. V. 2010a. Effect of betelnut fibres treatment and contact conditions on adhesive wear and frictional performance of polyester composites. *Wear*, 268, 1354-1370.
- NIRMAL, U., YOUSIF, B. F., RILLING, D. & BREVERN, P. V. 2010b. Effect of betelnut fibres treatment and contact conditions on adhesive wear and frictional performance of polyester composites. *Wear*, 268, 1354-1370.
- NISHIMURA, A., KATAYAMA, H., KAWAHARA, Y. & SUGIMURA, Y. 2012. Characterization of kenaf phloem fibers in relation to stem growth. *Industrial Crops and Products*, 37, 547-552.
- NISHINO, T., HIRAO, K., KOTERA, M., NAKAMAE, K. & INAGAKI, H. 2003. Kenaf reinforced biodegradable composite. *Composites Science and Technology*, 63, 1281-1286.

- NOSONOVSKY, M. & BHUSHAN, B. 2012. *Green Tribology: Biomimetics, Energy Conservation and Sustainability*, Springer.
- OCHI, S. 2008. Mechanical properties of kenaf fibers and kenaf/PLA composites. *Mechanics of Materials*, 40, 446-452.
- OSARA, K. & TIAINEN, T. 2001. Three-body impact wear study on conventional and new PM/ + HIPed wear resistant materials. *Wear*, 250-251, 785-794.
- PICKERING, K. L. 2008. *Properties and performance of natural-fibre composites*, CRC Press.
- PIGGOTT, M., XIONG, Y., SPRAGG, C. & DRZAL, L. Fiber, Matrix, and Interface Properties, ASTM STP 1290. 1996. American Society for Testing and Materials Philadelphia.
- QIU, M. & CHEN, L. 2010. Tribological characteristics of chromium steels in three various atmospheres under high-speed conditions. *Wear*, 268, 1342-1346.
- RASHED, F. S. & MAHMOUD, T. S. 2009. Prediction of wear behaviour of A356/SiCp MMCs using neural networks. *Tribology International*, 42, 642-648.
- RAY, S. & ROY CHOWDHURY, S. K. 2009. Prediction of contact temperature rise between rough sliding bodies: An artificial neural network approach. *Wear*, 266, 1029-1038.
- ROKBI, M., OSMANI, H., IMAD, A. & BENSEDDIQ, N. 2011. Effect of Chemical treatment on Flexure Properties of Natural Fiber-reinforced Polyester Composite. *Procedia Engineering*, 10, 2092-2097.
- ROSA, M. F., CHIOU, B.-S., MEDEIROS, E. S., WOOD, D. F., WILLIAMS, T. G., MATTOSO, L. H. C., ORTS, W. J. & IMAM, S. H. 2009. Effect of fiber

- treatments on tensile and thermal properties of starch/ethylene vinyl alcohol copolymers/coir biocomposites. *Bioresource Technology*, 100, 5196-5202.
- SABEEL AHMED, K., KHALID, S. S., MALLINATHA, V. & AMITH KUMAR, S. J. 2012. Dry sliding wear behavior of SiC/Al₂O₃ filled jute/epoxy composites. *Materials and Design*, 36, 306-315.
- SAHA, P., MANNA, S., CHOWDHURY, S. R., SEN, R., ROY, D. & ADHIKARI, B. 2010. Enhancement of tensile strength of lignocellulosic jute fibers by alkali-steam treatment. *Bioresource Technology*, 101, 3182-3187.
- SAPUAN, S. M., LEENIE, A., HARIMI, M. & BENG, Y. K. 2006. Mechanical properties of woven banana fibre reinforced epoxy composites. *Materials & Design*, 27, 689-693.
- SAW, S. K., SARKHEL, G. & CHOUDHURY, A. 2011. Surface modification of coir fibre involving oxidation of lignins followed by reaction with furfuryl alcohol: Characterization and stability. *Applied Surface Science*, 257, 3763-3769.
- SENATORE, A., D'AGOSTINO, V., DI GIUDA, R. & PETRONE, V. 2011. Experimental investigation and neural network prediction of brakes and clutch material frictional behaviour considering the sliding acceleration influence. *Tribology International*, 44, 1199-1207.
- SHALWAN, A. & YOUSIF, B. F. 2013. In State of Art: Mechanical and tribological behaviour of polymeric composites based on natural fibres. *Materials & Design*, 48, 14-24.

- SHARMA, M. & BIJWE, J. 2011. Influence of fiber-matrix adhesion and operating parameters on sliding wear performance of carbon fabric polyethersulphone composites. *Wear*, 271, 2919-2927.
- SHARMA, M., BIJWE, J. & MITSCHANG, P. 2011. Wear performance of PEEK–carbon fabric composites with strengthened fiber–matrix interface. *Wear*, 271, 2261-2268.
- SHARMA, M., RAO, I. M. & BIJWE, J. 2009. Influence of orientation of long fibers in carbon fiber–polyetherimide composites on mechanical and tribological properties. *Wear*, 267, 839-845.
- SHEKAR, R. I., DAMODHARA RAO, P., PADAKI, V., KIM, N. H. & LEE, J. H. 2010. Fibre-Fibre Hybrid Composites For Aerospace Applications. *Advanced Materials Research*, 123, 1231-1234.
- SHIBATA, S., CAO, Y. & FUKUMOTO, I. 2006. Lightweight laminate composites made from kenaf and polypropylene fibres. *Polymer Testing*, 25, 142-148.
- SHIN, H. K., PYO JEUN, J., BIN KIM, H. & HYUN KANG, P. 2012. Isolation of cellulose fibers from kenaf using electron beam. *Radiation Physics and Chemistry*, 81, 936-940.
- SHINOJ, S., VISVANATHAN, R., PANIGRAHI, S. & KOCHUBABU, M. 2011. Oil palm fiber (OPF) and its composites: A review. *Industrial Crops and Products*, 33, 7-22.
- SHIPWAY, P. H. & HODGE, C. J. B. 2000. Microabrasion of glass – the critical role of ridge formation. *Wear*, 237, 90-97.
- SHIPWAY, P. H. & NGAO, N. K. 2003. Microscale abrasive wear of polymeric materials. *Wear*, 255, 742-750.

- SIDDHARTHA & GUPTA, K. 2012. Mechanical and abrasive wear characterization of bidirectional and chopped E-glass fiber reinforced composite materials. *Materials and Design*, 35, 467-479.
- SINGH, N., YOUSIF, B. & RILLING, D. 2011. Tribological Characteristics of Sustainable Fiber-Reinforced Thermoplastic Composites under Wet Adhesive Wear. *Tribology Transactions*, 54, 736-748.
- SOLAR, M., MEYER, H., GAUTHIER, C., BENZERARA, O., SCHIRRER, R. & BASCHNAGEL, J. 2011. Molecular dynamics simulations of the scratch test on linear amorphous polymer surfaces: A study of the local friction coefficient. *Wear*, 271, 2751-2758.
- STRICKLAND, M. A., DRESSLER, M. R. & TAYLOR, M. 2012. Predicting implant UHMWPE wear in-silico: A robust, adaptable computational–numerical framework for future theoretical models. *Wear*, 274–275, 100-108.
- SURESH, A., HARSHA, A. P. & GHOSH, M. K. 2009. Solid particle erosion studies on polyphenylene sulfide composites and prediction on erosion data using artificial neural networks. *Wear*, 266, 184-193.
- SURESHA, B. & CHANDRAMOHAN, G. 2008. Three-body abrasive wear behaviour of particulate-filled glass–vinyl ester composites. *Journal of Materials Processing Technology*, 200, 306-311.
- SURESHA, B., CHANDRAMOHAN, G., SIDDARAMAIAH, SAMAPTHKUMARAN, P. & SEETHARAMU, S. 2007. Three-body abrasive wear behaviour of carbon and glass fiber reinforced epoxy composites. *Materials Science and Engineering: A*, 443, 285-291.

- SURESHA, B., DEVARAJAIAH, R. M., PASANG, T. & RANGANATHAIAH, C. 2013. Investigation of organo-modified montmorillonite loading effect on the abrasion resistance of hybrid composites. *Materials & Design*, 47, 750-758.
- SURESHA, B., SHIVA KUMAR, K., SEETHARAMU, S. & SAMPATH KUMARAN, P. 2010. Friction and dry sliding wear behavior of carbon and glass fabric reinforced vinyl ester composites. *Tribology International*, 43, 602-609.
- TIWARI, S., BIJWE, J. & PANIER, S. 2011. Gamma radiation treatment of carbon fabric to improve the fiber–matrix adhesion and tribo-performance of composites. *Wear*, 271, 2184-2192.
- TORRES, F. G. & CUBILLAS, M. L. 2005. Study of the interfacial properties of natural fibre reinforced polyethylene. *Polymer Testing*, 24, 694-698.
- TOWO, A. N. & ANSELL, M. P. 2008. Fatigue of sisal fibre reinforced composites: Constant-life diagrams and hysteresis loop capture. *Composites Science and Technology*, 68, 915-924.
- TRAN, L. Q. N., FUENTES, C. A., DUPONT-GILLAIN, C., VAN VUURE, A. W. & VERPOEST, I. 2011. Wetting analysis and surface characterisation of coir fibres used as reinforcement for composites. *Colloids and Surfaces A: Physicochemical and Engineering Aspects*, 377, 251-260.
- TREZONA, R. I. & HUTCHINGS, I. M. 1999. Three-body abrasive wear testing of soft materials. *Wear*, 233–235, 209-221.
- TUNGJITPORNKULL, S. & SOMBATSOMPOP, N. 2009. Processing technique and fiber orientation angle affecting the mechanical properties of E-glass

- fiber reinforced wood/PVC composites. *Journal of Materials Processing Technology*, 209, 3079-3088.
- UNAL, H., MIMAROGLU, A. & ARDA, T. 2006. Friction and wear performance of some thermoplastic polymers and polymer composites against unsaturated polyester. *Applied Surface Science*, 252, 8139-8146.
- VALLEJOS, M. E., CURVELO, A. A. S., TEIXEIRA, E. M., MENDES, F. M., CARVALHO, A. J. F., FELISSIA, F. E. & AREA, M. C. 2011. Composite materials of thermoplastic starch and fibers from the ethanol-water fractionation of bagasse. *Industrial Crops and Products*, 33, 739-746.
- VELMURUGAN, R. & MANIKANDAN, V. 2007. Mechanical properties of palmyra/glass fiber hybrid composites. *Composites Part A: Applied Science and Manufacturing*, 38, 2216-2226.
- VILAY, V., MARIATTI, M., MAT TAIB, R. & TODO, M. 2008. Effect of fiber surface treatment and fiber loading on the properties of bagasse fiber-reinforced unsaturated polyester composites. *Composites Science and Technology*, 68, 631-638.
- WAN, Y. Z., CHEN, G. C., RAMAN, S., XIN, J. Y., LI, Q. Y., HUANG, Y., WANG, Y. L. & LUO, H. L. 2006. Friction and wear behavior of three-dimensional braided carbon fiber/epoxy composites under dry sliding conditions. *Wear*, 260, 933-941.
- WANG, A. & ESSNER, A. 2001. Three-body wear of UHMWPE acetabular cups by PMMA particles against CoCr, alumina and zirconia heads in a hip joint simulator. *Wear*, 250-251, 212-216.

- WU, J. & CHENG, X. H. 2006. The tribological properties of Kevlar pulp reinforced epoxy composites under dry sliding and water lubricated condition. *Wear*, 261, 1293-1297.
- XUE, Y., DU, Y., ELDER, S., WANG, K. & ZHANG, J. 2009. Temperature and loading rate effects on tensile properties of kenaf bast fiber bundles and composites. *Composites Part B: Engineering*, 40, 189-196.
- YAMAMOTO, Y. & HASHIMOTO, M. 2004. Friction and wear of water lubricated PEEK and PPS sliding contacts Part 2. Composites with carbon or glass fibre. *Wear*, 257, 181-189.
- YANG, Y.-S., CHOU, J.-H., HUANG, W., FU, T.-C. & LI, G.-W. 2013. An artificial neural network for predicting the friction coefficient of deposited Cr_{1-x}Al_xC films. *Applied Soft Computing*, 13, 109-115.
- YOUSIF, B. & EL-TAYEB, N. 2007a. The effect of oil palm fibers as reinforcement on tribological performance of polyester composite. *Surface Review and Letters*, 14, 1095-1102.
- YOUSIF, B. & EL-TAYEB, N. 2008a. High-stress three-body abrasive wear of treated and untreated oil palm fibre-reinforced polyester composites. *Proceedings of the Institution of Mechanical Engineers, Part J: Journal of Engineering Tribology*, 222, 637-646.
- YOUSIF, B. & EL-TAYEB, N. 2010a. Wet adhesive wear characteristics of untreated oil palm fibre reinforced polyester and treated oil palm fibre reinforced polyester composites using the pin-on-disc and block-on-ring techniques. *Proceedings of the Institution of Mechanical Engineers, Part J: Journal of Engineering Tribology*, 224, 123-131.

- YOUSIF, B. F. 2009. Frictional and wear performance of polyester composites based on coir fibres. *Proceedings of the Institution of Mechanical Engineers, Part J: Journal of Engineering Tribology*, 223, 51-59.
- YOUSIF, B. F. 2010. Effect of oil palm fibres volume fraction on mechanical properties of polyester composites. *International Journal of Modern Physics B*, 24, 4459-4470.
- YOUSIF, B. F. 2013a. Design of newly fabricated tribological machine for wear and frictional experiments under dry/wet condition. *Materials & Design*, 48, 2-13.
- YOUSIF, B. F. 2013b. Editorial for SI: Materials, design and tribology. *Materials and Design*.
- YOUSIF, B. F. & EL-TAYEB, N. S. M. 2007b. The effect of oil palm fibers as reinforcement on tribological performance of polyester composite. *Surface Review and Letters*, 14, 1095-1102.
- YOUSIF, B. F. & EL-TAYEB, N. S. M. 2007c. Effect of water as lubricant on friction and wear properties of CGRP composite evaluated by POD and BOR techniques. *Surface Review and Letters*, 14, 185-191.
- YOUSIF, B. F. & EL-TAYEB, N. S. M. 2007d. On the effect of woven glass fabric orientations on wear and friction properties of polyester composite. *Surface Review and Letters*, 14, 489-497.
- YOUSIF, B. F. & EL-TAYEB, N. S. M. 2007e. Tribological evaluations of polyester composites considering three orientations of CSM glass fibres using BOR machine. *Applied Composite Materials*, 14, 105-116.
- YOUSIF, B. F. & EL-TAYEB, N. S. M. 2008b. Adhesive wear performance of T-OPRP and UT-OPRP composites. *Tribology Letters*, 32, 199-208.

- YOUSIF, B. F. & EL-TAYEB, N. S. M. 2008c. High-stress three-body abrasive wear of treated and untreated oil palm fibre-reinforced polyester composites. *Proceedings of the Institution of Mechanical Engineers, Part J: Journal of Engineering Tribology*, 222, 637-646.
- YOUSIF, B. F. & EL-TAYEB, N. S. M. 2008d. Wear and friction characteristics of CGRP composite under wet contact condition using two different test techniques. *Wear*, 265, 856-864.
- YOUSIF, B. F. & EL-TAYEB, N. S. M. 2010b. Wear characteristics of thermoset composite under high stress three-body abrasive. *Tribology International*, 43, 2365-2371.
- YOUSIF, B. F. & EL-TAYEB, N. S. M. 2010c. Wet adhesive wear characteristics of untreated oil palm fibre reinforced polyester and treated oil palm fibre reinforced polyester composites using the pin-on-disc and block-on-ring techniques. *Proceedings of the Institution of Mechanical Engineers, Part J: Journal of Engineering Tribology*, 224, 123-131.
- YOUSIF, B. F., NIRMAL, U. & WONG, K. J. 2010. Three-body abrasion on wear and frictional performance of treated betelnut fibre reinforced epoxy (T-BFRE) composite. *Materials & Design*, 31, 4514-4521.
- ZHANG, Z. & FRIEDRICH, K. 2003. Artificial neural networks applied to polymer composites: a review. *Composites Science and Technology*, 63, 2029-2044.
- ZHANG, Z., FRIEDRICH, K. & VELTEN, K. 2002. Prediction on tribological properties of short fibre composites using artificial neural networks. *Wear*, 252, 668-675.

ZHOU, X. H., SUN, Y. S. & WANG, W. S. 2009. Influences of carbon fabric/epoxy composites fabrication process on its friction and wear properties. *Journal of Materials Processing Technology*, 209, 4553-4557.

APPENDIX A: ARTIFICIAL NEURAL NETWORKS DEVELOPMENT STEPS

A.1 MATLAB WORKSPACE AND TOOLBOX

A1.1 Input data

The captured frictional force against the sliding distance at different operating parameters for the KFRE composite at N-O were collected for three tests at each operating parameter. The average of the three readings after each 100m sliding distance was determined. Figure A.1 shows the arrangement of the frictional data for the KFRE at N-O before it was exported to the Matlab workspace.

In the Matlab workspace, the input and the target data were imported from the Excel file as can be seen in Figures A.2a and A.2b. This step was then followed by developing the ANN model. At this stage there are several ways of developing the ANN model; i.e., through the Simulink, toolbox or writing the script. In this study the toolbox and the script were used for developing the model. Two methods are available in the toolbox for developing the ANN. The basic method is by following the steps shown in Figure A.3. The steps for training the model are also given in Fig. A.3. Figure A.4 shows the detailed steps involved in training one of the developed models. The script of the ANN in Matlab is given in Section A.2.

	A	B	C	D	E	F	G	H	I	J	K	L	M	N	O	P	Q	R	S	T
1	Sliding velocity	2.8	2.8	2.8	2.8	2.8	2.8	2.8	2.8	2.8	2.8	2.8	2.8	2.8	2.8	2.8	2.8	2.8	2.8	2.8
2	Sliding distance	0.1	0.2	0.3	0.3	0.4	0.5	0.6	0.7	0.8	0.8	0.9	1.0	1.1	1.2	1.3	1.3	1.4	1.5	1.6
3	Applied load	30.0	30.0	30.0	30.0	30.0	30.0	30.0	30.0	30.0	30.0	30.0	30.0	30.0	30.0	30.0	30.0	30.0	30.0	30.0
4	Friction coefficient	0.9	0.9	0.8	0.8	0.8	0.7	0.8	0.7	0.7	0.7	0.7	0.7	0.6	0.6	0.6	0.6	0.6	0.6	0.6
5																				
6	Sliding velocity	2.8	2.8	2.8	2.8	2.8	2.8	2.8	2.8	2.8	2.8	2.8	2.8	2.8	2.8	2.8	2.8	2.8	2.8	2.8
7	Sliding distance	0.1	0.2	0.3	0.3	0.4	0.5	0.6	0.7	0.8	0.8	0.9	1.0	1.1	1.2	1.3	1.3	1.4	1.5	1.6
8	Applied load	50.0	50.0	50.0	50.0	50.0	50.0	50.0	50.0	50.0	50.0	50.0	50.0	50.0	50.0	50.0	50.0	50.0	50.0	50.0
9	Friction coefficient	0.9	0.9	0.9	0.8	0.8	0.8	0.8	0.8	0.8	0.7	0.7	0.7	0.7	0.7	0.7	0.7	0.7	0.7	0.7
10																				
11	Sliding velocity	2.8	2.8	2.8	2.8	2.8	2.8	2.8	2.8	2.8	2.8	2.8	2.8	2.8	2.8	2.8	2.8	2.8	2.8	2.8
12	Sliding distance	0.1	0.2	0.3	0.3	0.4	0.5	0.6	0.7	0.8	0.8	0.9	1.0	1.1	1.2	1.3	1.3	1.4	1.5	1.6
13	Applied load	70.0	70.0	70.0	70.0	70.0	70.0	70.0	70.0	70.0	70.0	70.0	70.0	70.0	70.0	70.0	70.0	70.0	70.0	70.0
14	Friction coefficient	0.9	0.8	0.8	0.8	0.8	0.8	0.8	0.8	0.8	0.8	0.8	0.8	0.8	0.8	0.8	0.8	0.8	0.7	0.7
15																				
16	Sliding velocity	2.8	2.8	2.8	2.8	2.8	2.8	2.8	2.8	2.8	2.8	2.8	2.8	2.8	2.8	2.8	2.8	2.8	2.8	2.8
17	Sliding distance	0.1	0.2	0.3	0.3	0.4	0.5	0.6	0.7	0.8	0.8	0.9	1.0	1.1	1.2	1.3	1.3	1.4	1.5	1.6
18	Applied load	100.0	100.0	100.0	100.0	100.0	100.0	100.0	100.0	100.0	100.0	100.0	100.0	100.0	100.0	100.0	100.0	100.0	100.0	100.0
19	Friction coefficient	1.0	0.9	0.9	0.9	0.9	0.8	0.8	0.8	0.8	0.8	0.8	0.8	0.8	0.8	0.8	0.8	0.7	0.7	0.7
20																				
21																				
22	Sliding velocity	1.1	1.1	1.1	1.1	1.1	1.1	1.1	1.1	1.1	1.1	1.1	1.1	1.1	1.1	1.1	1.1	1.1	1.1	1.1
23	Sliding distance	0.0	0.1	0.1	0.1	0.2	0.2	0.2	0.3	0.3	0.3	0.4	0.4	0.4	0.5	0.5	0.5	0.6	0.6	0.6
24	Applied load	50.0	50.0	50.0	50.0	50.0	50.0	50.0	50.0	50.0	50.0	50.0	50.0	50.0	50.0	50.0	50.0	50.0	50.0	50.0
25	Friction coefficient	1.0	0.9	0.9	0.8	0.8	0.8	0.8	0.9	0.8	0.8	0.8	0.8	0.8	0.8	0.8	0.7	0.7	0.8	0.8
26																				
27																				
28	Sliding velocity	3.1	3.1	3.1	3.1	3.1	3.1	3.1	3.1	3.1	3.1	3.1	3.1	3.1	3.1	3.1	3.1	3.1	3.1	3.1
29	Sliding distance	0.1	0.2	0.3	0.4	0.5	0.6	0.7	0.7	0.8	0.9	1.0	1.1	1.2	1.3	1.4	1.5	1.6	1.7	1.8
30	Applied load	50.0	50.0	50.0	50.0	50.0	50.0	50.0	50.0	50.0	50.0	50.0	50.0	50.0	50.0	50.0	50.0	50.0	50.0	50.0
31	Friction coefficient	0.9	0.9	0.8	0.8	0.8	0.8	0.8	0.8	0.8	0.7	0.7	0.7	0.7	0.7	0.7	0.7	0.7	0.7	0.7
32																				
33																				
34	Sliding velocity	3.5	3.5	3.5	3.5	3.5	3.5	3.5	3.5	3.5	3.5	3.5	3.5	3.5	3.5	3.5	3.5	3.5	3.5	3.5
35	Sliding distance	0.1	0.2	0.3	0.4	0.5	0.6	0.7	0.8	0.9	1.1	1.2	1.3	1.4	1.5	1.6	1.7	1.8	1.9	2.0
36	Applied load	50.0	50.0	50.0	50.0	50.0	50.0	50.0	50.0	50.0	50.0	50.0	50.0	50.0	50.0	50.0	50.0	50.0	50.0	50.0
37	Friction coefficient	0.9	0.9	0.9	0.8	0.8	0.8	0.8	0.8	0.8	0.7	0.7	0.7	0.7	0.7	0.7	0.7	0.7	0.7	0.7
38																				
39																				

Fig. A.1 Sample of the Excel Frictional Data

Variable Editor - Input(1,1)

Input(1,1) <3x365 double>

	1	2	3	4	5	6	7	8	9	10	11	12	13	14	15	16
1	2.8000	2.8000	2.8000	2.8000	2.8000	2.8000	2.8000	2.8000	2.8000	2.8000	2.8000	2.8000	2.8000	2.8000	2.8000	2.8000
2	0	0.0840	0.1680	0.2520	0.3360	0.4200	0.5040	0.5880	0.6720	0.7560	0.8400	0.9240	1.0080	1.0920	1.1760	1.2600
3	30	30	30	30	30	30	30	30	30	30	30	30	30	30	30	30

- a) Importing the input data, consisting of 3×365 values of the operating parameters, sliding velocity, sliding distance and the applied load.

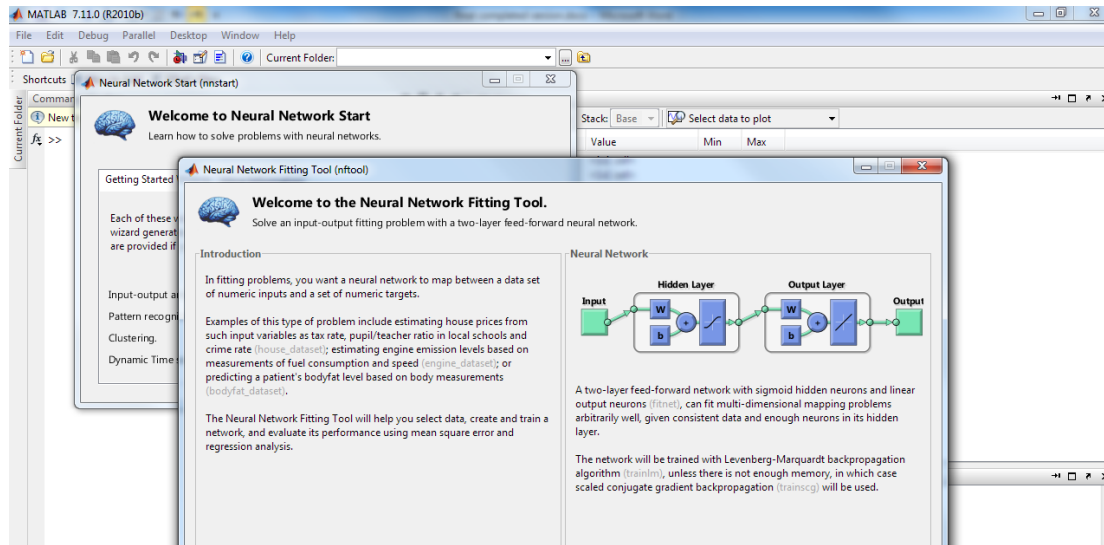
Variable Editor - Target(1,1)

Target(1,1) <1x365 double>

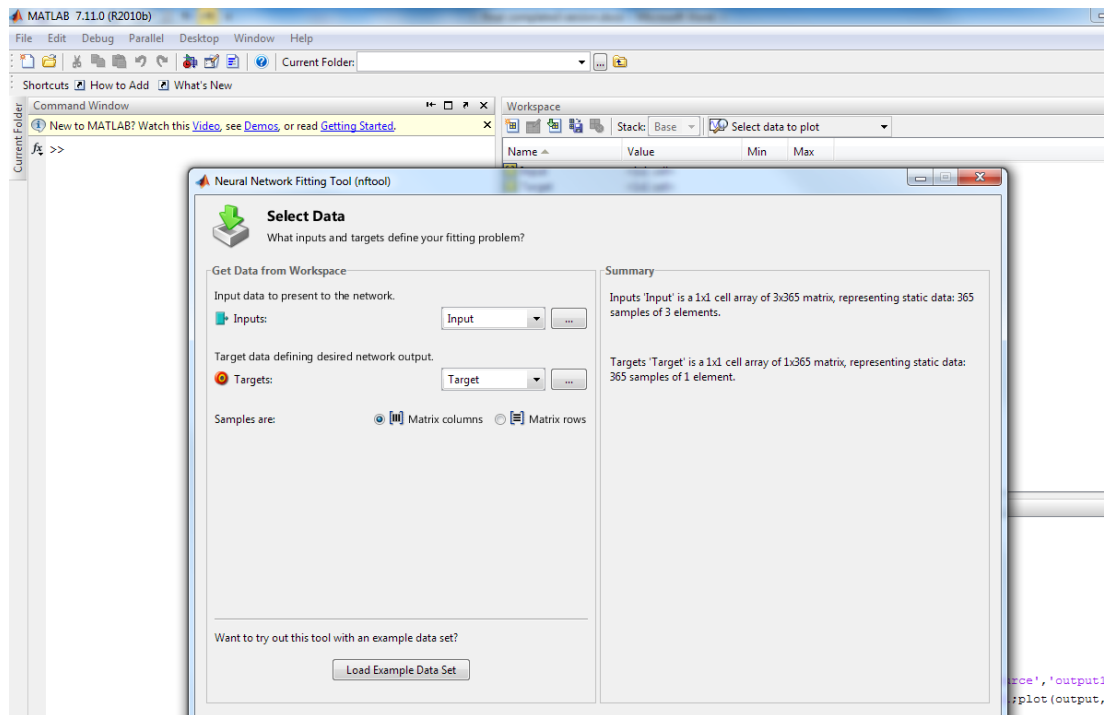
	1	2	3	4	5	6	7	8	9	10	11	12	13	14	15	16
1	0.9200	0.8500	0.8100	0.7800	0.7700	0.7400	0.7500	0.7200	0.7100	0.6700	0.6500	0.6700	0.6300	0.6100	0.6400	0.6000

- b) Importing the output data, consisting of 1×365 values of the friction coefficient at the operating parameters given in Part a) of this Figure.

Fig. A.2 Importing the Frictional Data to the Matlab Workspace

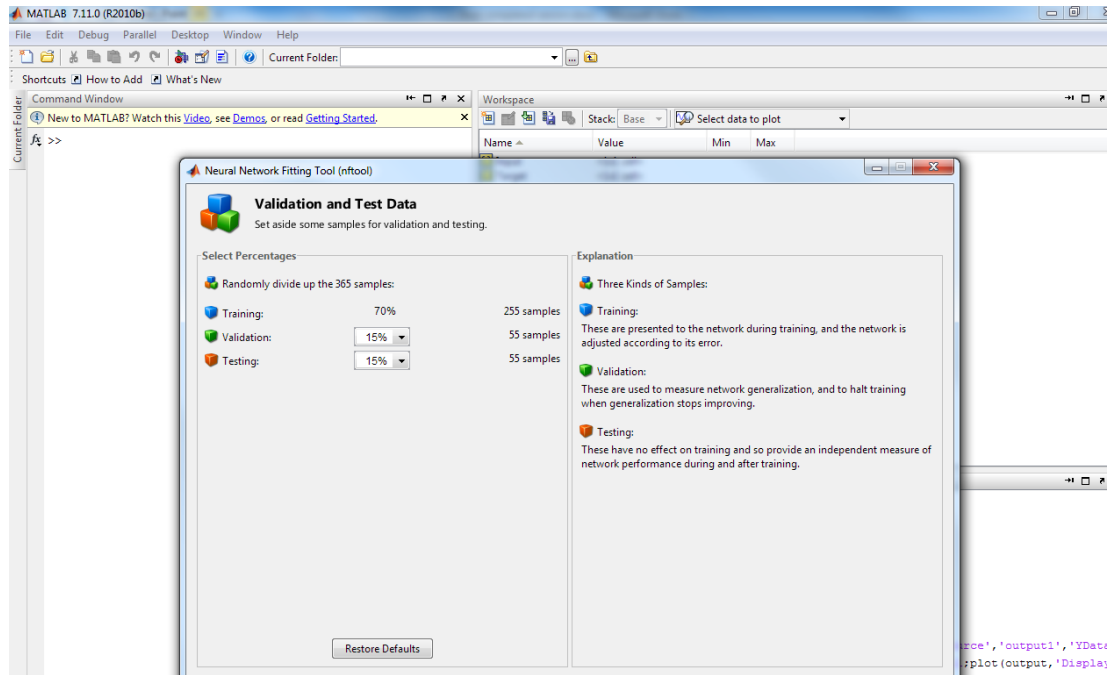


a) Selecting the ANN prediction method.

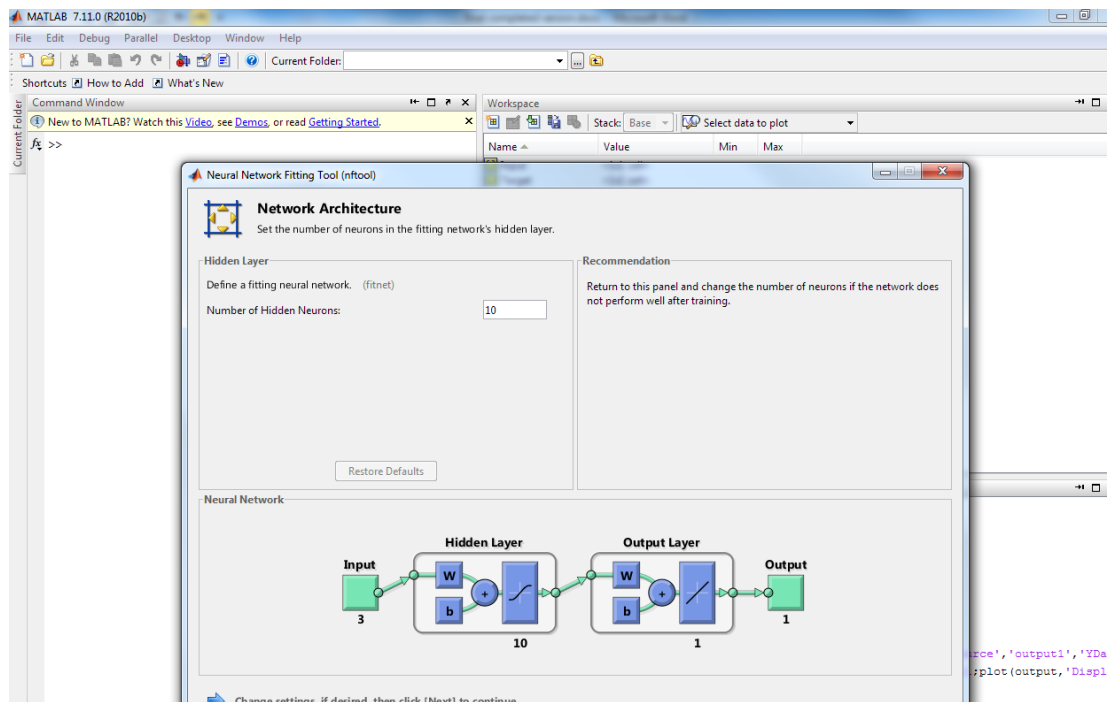


b) Selecting the input and target data.

Fig. A.3 continued

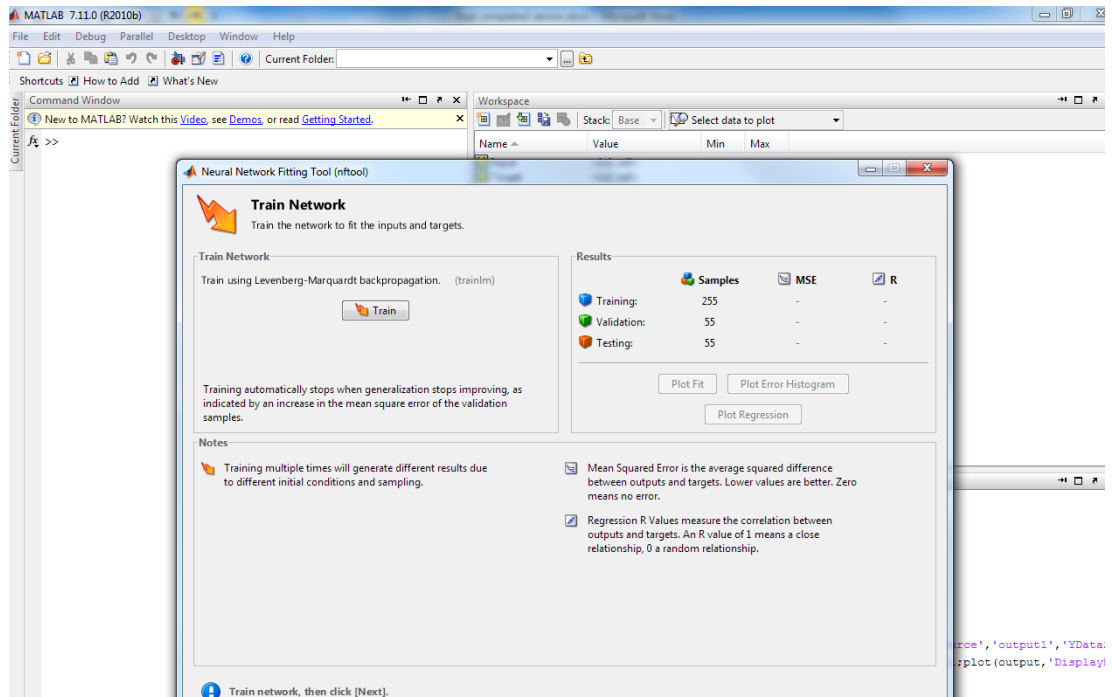


c) Selecting the percentage of training and verification data.

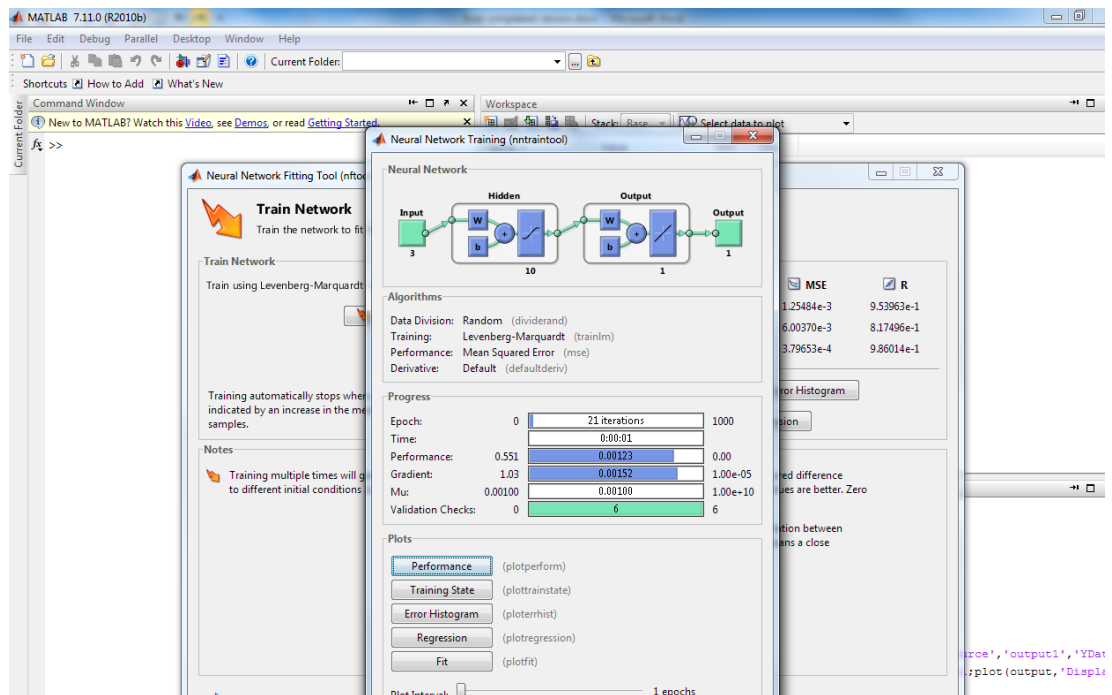


d) Selecting the number of neurons.

Fig. A.3 Steps for Developing the ANN Using the Matlab Toolbox

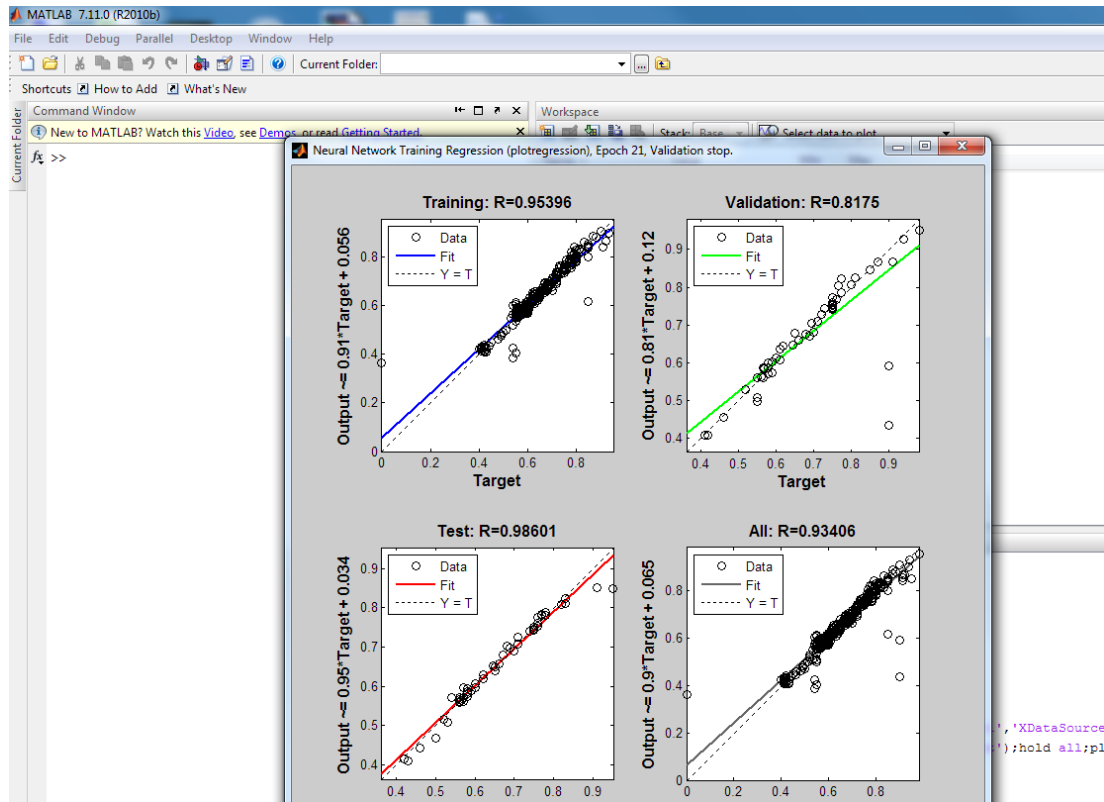


a) Training the data.



b) Checking the training performance and error.

Fig. A.4 continued



c) Checking the training performance and error.

Fig. A.4 Steps for Training the ANN and Obtaining the Performance Indication

A.2 MATLAB SCRIPT

```
% Solve an Input-Output Fitting problem with a Neural Network

% Script generated by NFTOOL

% Created Fri Jun 07 10:28:52 GMT+10:00 2013

%% This script assumes these variables are defined:

%% Input - input data.

% Target - target data.

inputs = Input;

targets = Target;

% Create a Fitting Network

hiddenLayerSize = 50;

net = fitnet(hiddenLayerSize);

% Choose Input and Output Pre/Post-Processing Functions

% For a list of all processing functions type: help nnprocess

net.inputs{1}.processFcns = {'removeconstantrows','mapminmax'};

net.outputs{2}.processFcns = {'removeconstantrows','mapminmax'};

% Setup Division of Data for Training, Validation, Testing

% For a list of all data division functions type: help nndivide

net.divideFcn = 'dividerand'; % Divide data randomly

net.divideMode = 'sample'; % Divide up every sample

net.divideParam.trainRatio = 70/100;

net.divideParam.valRatio = 15/100;

net.divideParam.testRatio = 15/100;

% For help on training function 'trainlm' type: help trainlm

% For a list of all training functions type: help nntrain
```

```
net.trainFcn = 'trainlm'; % Levenberg-Marquardt

% Choose a Performance Function

% For a list of all performance functions type: help nnperformance

net.performFcn = 'mse'; % Mean squared error

% Choose Plot Functions

% For a list of all plot functions type: help nnplot

net.plotFcns = {'plotperform','plottrainstate','ploterrhist', ...
'plotregression', 'plotfit'};

% Train the Network

[net,tr] = train(net,inputs,targets);

% Test the Network

outputs = net(inputs);

errors = gsubtract(targets,outputs);

performance = perform(net,targets,outputs)

% Recalculate Training, Validation and Test Performance

trainTargets = targets .* tr.trainMask{1};

valTargets = targets .* tr.valMask{1};

testTargets = targets .* tr.testMask{1};

trainPerformance = perform(net,trainTargets,outputs)

valPerformance = perform(net,valTargets,outputs)

testPerformance = perform(net,testTargets,outputs)

% View the Network

view(net)

% Plots

% Uncomment these lines to enable various plots.
```

`%figure, plotperform(tr)`

`%figure, plottrainstate(tr)`

`%figure, plotfit(net,inputs,targets)`

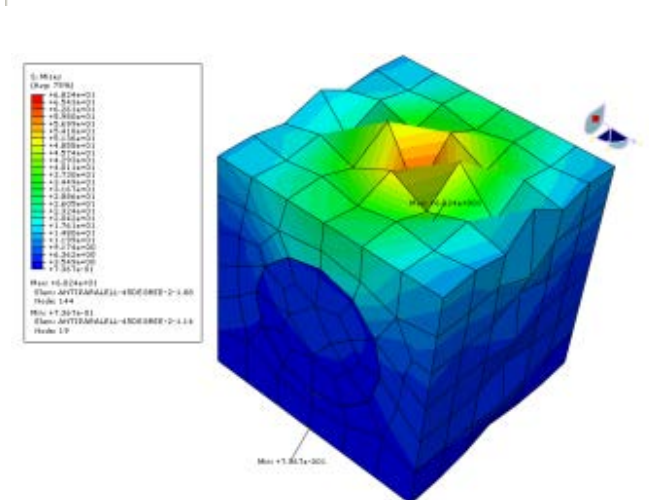
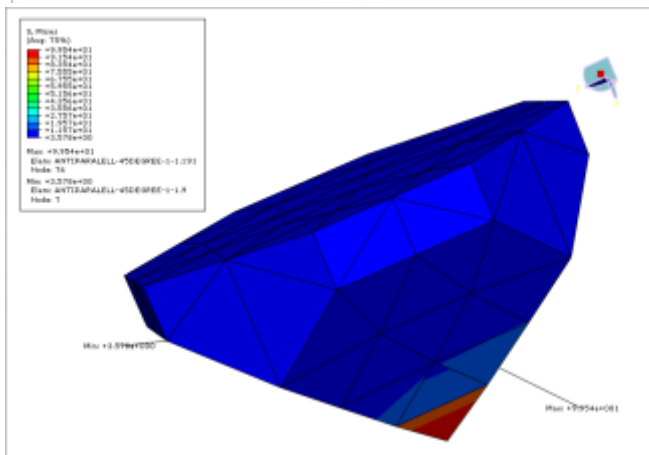
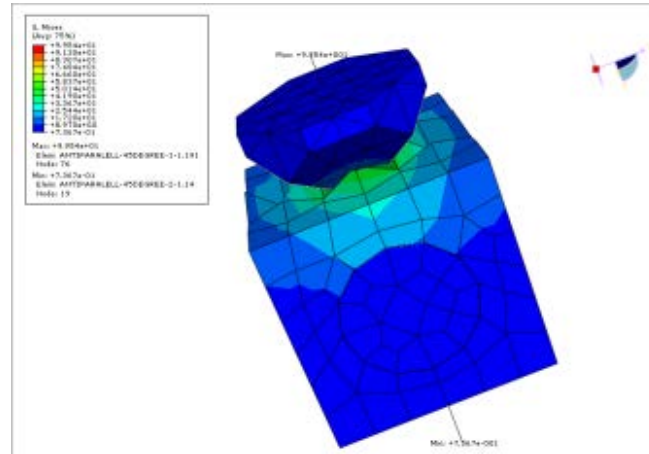
`%figure, plotregression(targets,outputs)`

`%figure, ploterrhist(errors)`

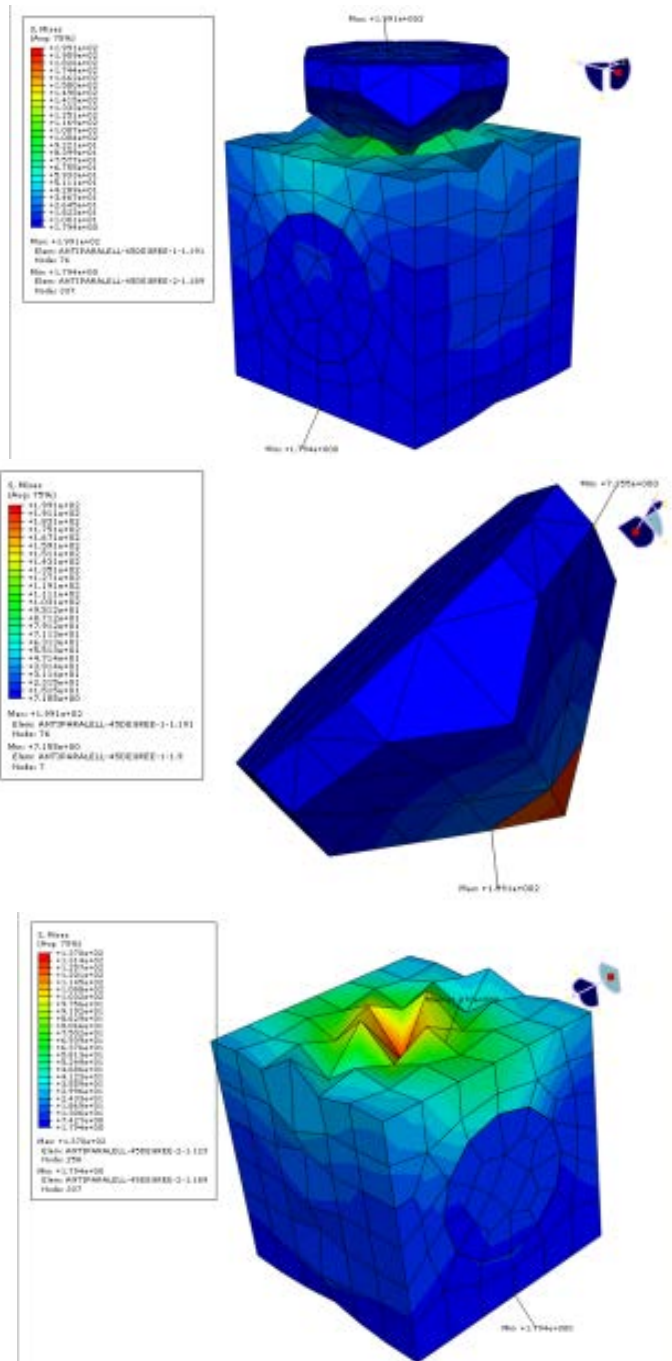
APPENDIX B : SAMPLE OF ABAQUS SIMULATION RESULTS

B.1 KFRE IN THE ANTI-PARALLEL ORIENTATION

- 90 degree under 5 Pa

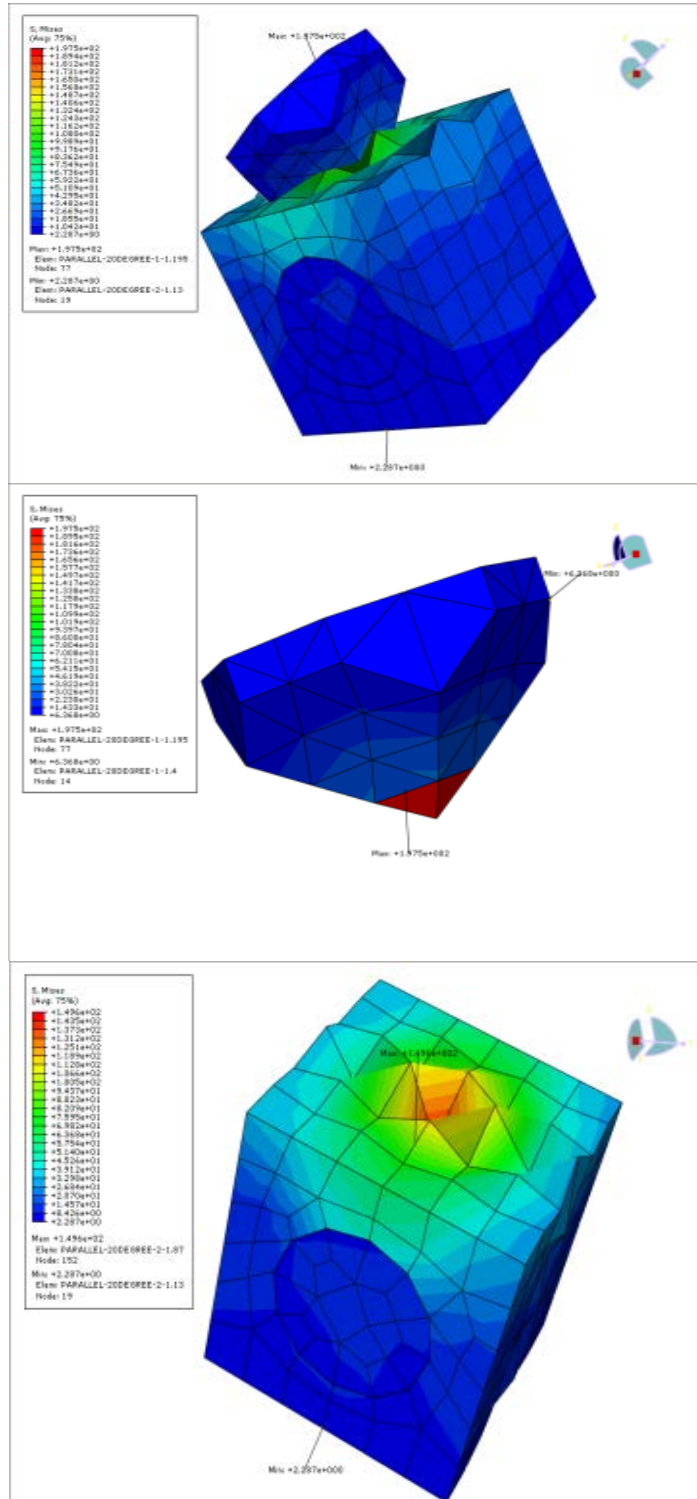


- 90 degree under 10 Pa



B.2 KFRE IN THE PARALLEL ORIENTATION

- 65 degree under 10 Pa



- 65 degree under 20 Pa

